Master Thesis

Functional Rydberg Complexes in the PXP-Model

Simon Stastny

February 24, 2023

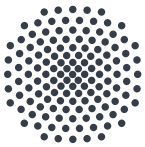

University of Stuttgart
Germany

Institute for Theoretical Physics III

Supervisor and Corrector:
Prof. Dr. Hans Peter Büchler

Secondary Corrector:
Prof. Dr. Maria Daghofer

Declaration

I hereby declare, that i have written the presented thesis independently and on my own, and that all used external sources and materials are properly declared in the text. This master thesis has not been examined or published before. I assure, that the submitted electronic version of this thesis is identical to the printed version.

Stuttgart, February 24, 2023 Simon Stastny

Abstract

String nets containing long range entanglement, and their associated models have promising applications like fault tolerant quantum computation, but are notoriously hard to realize. This thesis investigates an approach to realize these string nets on lattices with Rydberg atoms on their edges. A local perturbation is implemented on the lattice to enforce constraints on its vertices. These constraints energetically punish vertices that do violate the defined structure of the sting net. A realization of these constraints is a complex of Rydberg atoms. The atoms in these are in a dipole blockade (*Rydberg blockade*) with each other. The blockade can be used to realize logical languages like a `NOT` logic. This is because two detuned Rydberg atoms want to be excited, but due to the blockade, only one can be. Such a approach is already used, to realize a dimer model on the Kagome lattice, which hosts a interesting quantum many-body phase.[1] These complexes can realize more logical languages though, like the `NOR`-gate. Because of this and the functional completeness of the `NOR`-logic, all logical languages found in a classical Boolean algebra can be realized with these complexes. A very precise formalism on how to archive this has been constructed.[2] The Hamiltonian for these complexes is a effective Ising model and the (possibly) degenerate gapped ground state manifold of these complexes correspond to logical correlations between some labelled atoms of the complex (called ports), that represent the words of the realized language. However, constructing arbitrary languages by realizing the gates as complexes and construct a proper Boolean circuit with them, leads to very large complexes, impractical for implementation. In the second part of this thesis possible minimal realizations of complexes realizing all elementary Boolean gates in the PXP model are being constructed, and are proven to be minimal. Furthermore, the provably minimal string net complexes used to construct the surface code and Fibonacci anyons and presented. In the subsequent chapter, the mechanisms used to proof the minimal sizes of the complexes, are presented. In the last chapter, the PXP approximation is being investigated, by looking at how valid the constructed complexes are in hindsight of Van der Waals interaction. A quantity is introduced, that measures if, and how valid these complexes are, when considering changing blockade radii due to the Van der Walls interaction. We optimize the complexes numerically for this quantity.

Zusammenfassung

Das Konzept der Quanteninformation wird medial und wirtschaftlich immer relevanter. Quantencomputer nutzten Eigenschaften der Quantenmechanik, um Berechnungen schneller durchzuführen als herkömmliche Computer. Dabei werden sogenannte Qubits genutzt, das sind quantenmechanische Zwei-Niveau-Systeme, um das Konzept des Bits zu verallgemeinern. Ein Beispiel eines solchen Systems ist ein Rydberg Atom. Dieses kann entweder angeregt sein oder nicht. Manche Berechnungen, wie die Faktorisierung großer Zahlen, können damit deutlich schneller durchgeführt werden. Das bedeutet z.B. konkret, dass ein Algorithmen, welcher Shor's Algorithmus heißt, diese Faktorisierung in polynomialer Laufzeit erreicht,[3] während herkömmliche Algorithmen auf klassischen Computern (sub-)exponentielle Laufzeiten haben.[3] Da viele kryptografische Prozesse auf diesem Prinzip beruhen, d.h. dass große Zahlen eben nicht in polynomialer Laufzeit faktorisiert werden können, hätte ein funktionierenden Quantencomputer großen Einfluss auf die Gesellschaft. Jedoch sind alle bisherigen Quantencomputer sehr fehleranfällig bezüglich Störungen. Diese können sowohl lokal sein, wie eine falsche Konfiguration der Qubits, als auch 'global', wie dissipative, also z.B. thermische Störungen. Dies führt zu einer geringen Fidelität der Quantenzustände, und damit zu Fehlern der Berechnungen. Eine Möglichkeit, lokale Fehler zu unterbinden ist es, Quantencomputer mit sogenannten String Netzen zu realisieren. In diesen Vielteilchen-Systemen werden auf die Kanten eines Gitters Rydberg Atome platziert. Angeregte Kanten (Kanten deren Atome angeregt sind) können Muster bilden. Durch Regeln, wie viele angeregte Kanten an jeden Gitter-Knoten (engl. vertex) angrenzen dürfen, entstehen z.B. Dimer Modelle, oder geschlossene Schleifen von angeregten Kanten, wie z.B. beim 'Toric Code', einem Modell, welches abelsche Anyonen als Quasi-Teilchen in angeregten Zuständen besitzt. Das Verletzen dieser Regeln erfordert Energie, daher sind die (entarteten) energetischen Grundzustände der String Netze durch Überlagerungen all solcher Schleifen Konfigurationen gegeben.
In dieser Arbeit wird eine Möglichkeit gesucht, diese String Netze auf einem Gitter zu realisieren, indem man jedem Knoten energetische Constraints vorgibt. Diese bestrafen das Verletzen dieser Regeln energetisch und sorgen so für die Erhaltung des durch diese Regeln definierten String Netzes an diesem Knoten. Diese Constraints basieren auf Anordnungen von Rydberg Atomen. Zwei Rydberg Atome unterliegen einer gegenseitigen Van der Waals Wechselwirkung. In dieser Arbeit wird diese Wechselwirkung durch ein PXP Model approximiert. In diesem ist die Wechselwirkung unendlich, wenn zwei angeregte Atome einen bestimmten Blockade-Abstand r_B unterschreiten, ansonsten ist sie Null. Mittels solcher Anordnungen können logische Relationen zwischen diesen Atomen gebildet werden. Sind z.B. zwei Atome näher zusammen als r_B, kann nur eines von beiden angeregt sein, sonst wäre die Energie des Systems unendlich. Dies entspricht einer `NOT` Relation zwischen den Zuständen beider Atome. Eine Anordnung von Rydberg Atomen, welche eine derartige logische Relation zwischen einer Auswahl ihrer Atome aufweist, heißt (funktionaler) Rydberg Komplex.[2] Da auch alle anderen Logiken elementarer Bauteile mit Rydberg Komplexen realisiert werden können, kann man eine Vorschrift herleiten und beweisen, wie man aus kleineren Komplexen, größere Schaltkreise zusammenbaut.[2] Diese Mechanik bildet den Startpunkt dieser Arbeit. Diese Schaltungen bestehen aus dutzenden Atomen. Dies ist sehr fehleranfällig. Daher werden im zweiten Kapitel kleinstmögliche Komplexe angegeben, welche alle logischen Gatter und ein 'Crossing', also das planare Kreuzen zweier Leitungen' realisieren. Alle Komplexe der logischen Gatter haben maximal sieben Atome (das Crossing hat zehn), sodass eine 'brute-force' Computersuche durchgeführt wurde um diese zu finden. Es wird auch die Nichteindeutigkeit dieser Komplexe gezeigt. Anschließend werden Gitter konstruiert, welche energetisch die String Netze erfüllen. Die Konstruktionen basieren auf der 'Kachelung' minimaler Komplexe, welche die gewünschen String Netz Regeln auf jedem Knoten des Gitters gewährleisten. Die angegebenen Konstruktionen werden dabei sowohl auf Quadrat- also auch auf Hexaonal- ('honeycomb-') Gittern durchgeführt, wobei aus dem zweiten Fall der erste folgt. Auch hier werden meherere Optionen gezeigt. Im vierten Kapitel wird ein allgemeines analytisches Verfahren gezeigt, mit welchem man kleinstmögliche Komplexe (oder eine Untergrenze für die Atomanzahl dieser) findet. Des Weiteren werden Eingenschaften logischer Sprachen und deren Einfluss auf realisierende Komplexe angegeben. Es wird die Miminalität aller angegebener Komplexe gezeigt. Im letzten Abschnitt wird der Übergang zur Van der Waals Wechselwirkung untersucht, indem die Komplexe optimiert werden, sodass Atome, welche im PXP Modell miteinander interagieren, möglichst nah sind und alle anderen möglichst fern. Abschließend werden kurz Komplexe komplett im Van der Waals Model betrachtet.

Contents

Chapter 1

Basic Theory

1.1 Topological Phases

1.1.1 Topological Phases as an Extension of the Landau Paradigm

The Landau paradigm introduces an approach to deal with classical and quantum phases, by classifying the occurring phases with a local ordering parameter. This parameter, or its derivatives are not continuous at the phase transition. An example of this phenomenon would be the phase transition between a ferromagnetic and a paramagnetic phase in a traverse Ising model. The order parameter is a given by local correlations between close spins. Either these are aligned in one defined direction, which is the ferromagnetic phase, or they are unoriented in this direction, which defines the paramagnetic phase. So the symmetry of the system defines its phase. The magnetic phase transition can also be approached classically. Note, that this approach to phases is valid with or without spontaneous symmetry breaking. For more details on local order parameters and the mentioned models, see section 6.1.

However the Landau paradigm breaks down, when the intrinsic non locality of quantum mechanics comes into play - *entanglement*. Taking that into account, the definition of a phase needs to be modified, because entanglement patterns can occur. These patterns may evolve around the topology of the sample (lattice) they live on, or around other topological properties like chirality, or winding numbers, which only change at phase transitions. So new phases can occur, which are resistant against local perturbations as these do not affect the (global) topology. Such phases are thus called *topological* phases.[4] These topological invariants only change at phase transitions, thus the phases of these models are now classified by these parameters.

Famous topological phases like the quantum hall effect or the Haldane model introduce such topological invariants like the chern number, (that is based on the topological concept of holonomy). However the phases only show short range entanglement patterns, they do not realize long range entanglement patterns. Examples for phases that do show such long range patterns are the fractional quantum hall effect, or $\mathbb{Z}_2$ topological order. Some of these phases can contain excited states that show abelian (fractional) or non-abelian anyonic statistics. Examples of such phases are the toric code, or Fibonacci anyons, which are discussed in the following sections sections 1.2, 1.2.2 and 1.3. A toy model for topological order is the toric code, that realizes a $\mathbb{Z}_2$ gauge theory.

1.2 Toric Code

In this section, we give a brief overview of the toric code mode, its ground state properties, and its anyonic excitations.

1.2.1 Basic Construction of the Model and the Protected Subspace

A key example, and the toy model for quantum stabilizer codes and topological quantum computing is the toric code introduced by Kitaev.[5] The following two sections will closely follow his paper to sketch the basic properties of it. This section uses the notation of.[4]

Consider a $k \times k$ Lattice on a torus with spins (or Rydberg atoms i.e. a two level system) on its edges. An example is depicted in fig. 1.1. One can use a planar lattice with periodic boundary conditions instead of a torus. In this case, models like the toric code are also called a *surface code*.[6] So there are (in the square case) $2k^2$ spins. The star operator A_s of a star s and the plaquette operator B_p of a plaquette p are defined as:

$$A_s = \prod_{j \in s} \sigma_j^x \,, \;\; B_p = \prod_{j \in p} \sigma_j^z \,. \tag{1.1}$$

These operators, which are also called stabilizers, thus act on all spins of a star s or plaquette p such as the ones shown in fig. 1.1. All of the star and plaquette operators commute with each other because a star and a plaquette share either zero or two edges, so in the two subspaces $\{\sigma^x, \sigma^z\} = 0$ gives a (-1) and the two minuses cancel (trivially, two star (or plaquette) operators commute because on shared edges the Pauli matrix commutes with itself). Further, because $\sigma^i \sigma^i = 1$ it follows that

$$\prod_s A_s = \prod_p B_p = 1 \,. \tag{1.2}$$

The Hilbert space of the system on which the operators act is $\mathbb{H} = \mathbb{C}^{2^{\otimes 2k^2}}$. The protected or invariant subspace $PS \subset \mathbb{H}$ is defined as:

$$PS = \{ |\xi\rangle \in \mathbb{H} \,|\, A_s \,|\xi\rangle = |\xi\rangle \,, B_p \,|\xi\rangle = |\xi\rangle \;\forall s, p \} \,. \tag{1.3}$$

The goal is to encode qubits in this subspace, so at first we calculate the dimension of PS. Looking at eq. (1.2), we see that there are $m = 2k^2 - 2$ linear independent Operators that create the space $\mathscr{G}$ of Operators, that commute with all A_s and B_p. Possible generators of $\mathscr{G}$ are the string operators

$$Z[C] = \prod_{j \in C} \sigma^z, \;\; X[C'] = \prod_{j \in C'} \sigma^x \,, \tag{1.4}$$

Where C and C' are the contractible closed loops (dual loops) on the lattice (dual lattice) depicted in fig. 1.2. These operators do commute with the stabilizers, because they are products of them. A (dual-) loops is being created by sequencing (stars) plaquettes and using that $(\sigma^x)^2 = (\sigma^z)^2 = 1$. If these operators do not act on a loop rather than a open string S, they do not commute with the stabilizers, because a string has two endpoints, depicted in fig. fig. 1.2 (grey square markings). On these endpoints, a star (plaquette) has only one edge in common with the corresponding string. So we only have one site where a σ^x and a σ^z acts, and because they anticommute, the open string operators anticommute with the stabilizers. This implies, that

$$A_s \prod_{j \in S} \sigma^z \,|\xi\rangle = -\prod_{j \in S} \sigma^z A_s \,|\xi\rangle = -\prod_{j \in S} \sigma^z \,|\xi\rangle \tag{1.5}$$

and for the dual strings the same holds . So the open strings leave PS, and thus are not in $\mathscr{G}$, and not in the algebra $\mathbf{L}(PS) \simeq \mathscr{G}/I$ of linear operators from PS into itself.
However for closed loops, there is another class of (dual-) loops due to the fundamental group of the torus T (at any point p) being $\pi_1(T, p) = \mathbb{Z} \times \mathbb{Z}$. The non contractible (dual-) loops commute only with the (plaquette) star operator. So they are not in $\mathscr{G}$. However they span the Algebra $\mathbf{L}(PS)$, because they are the only nontrivial operators left commuting with the stabilizers (the open strings leave the protected subspace) and the stabilizers act trivially on PS and are divided out. There are four different non contractible loop operators on this space, we call them

$$Z[C'_z] = Z_1, \;\; Z[C_z] = Z_2, \;\; X[C_x] = X_1 \;\; X[C'_x] = X_2 \,. \tag{1.6}$$

Because the two X operators share no lattice atom, and a non parallel loop/ dual loop pair share one (red atom in fig. 1.2), they obey the Pauli Algebra

$$[Z_i, Z_j] = [X_i, X_j] = [X_i, Z_j] = 0, \;\; \{X_i, Z_i\} = 0 \,. \tag{1.7}$$

This implies that $\mathbf{L}(PS) \simeq \{\sigma_1^x, \sigma_2^x, \sigma_1^z, \sigma_2^z\}$ and PS is 4-dimensional and $PS \simeq \mathbb{C}^2 \otimes \mathbb{C}^2$, the space of two qubits. As stated above, the non contractible (dual-) loops commute with either a (plaquette) star and with the other non contractible loop of the same type. So they have

a common eigenbasis in which they can be diagonalized. Labelling these eigenstates by their eigenvalues of the Z operators, which are ± 1 because they consist of Pauli matrices, one gets a representation of PS which is:

$$PS = \{|\nu_1, \nu_2\rangle \mid \nu_1, \nu_2 \in \{-1, +1\}\}\,. \tag{1.8}$$

Due to the Pauli-Algebra, it holds

$$Z_j\,|\nu_1, \nu_2\rangle = \nu_j\,|\nu_1, \nu_2\rangle\,,\ X_1\,|\nu_1, \nu_2\rangle = |-\nu_1, \nu_2\rangle\,,\ X_2\,|\nu_1, \nu_2\rangle = |\nu_1, -\nu_2\rangle\ , \tag{1.9}$$

which again is the same as σ^x and σ^z acting on two spin-$\frac{1}{2}$ particles. So the non trivial X (X') and Z (Z') loop operators can realize quantum gates on these qubits namely σ^x and σ^z.

All the calculations above are not restricted to a square lattice, but can be done with arbitrary lattices as long as topological boundaries can be chosen properly i.e. the lattice forms a fundamental polygon of a topological space with a genus. With the calculations above the role of the genus becomes clear. there are (up to winding numbers) two ways to form non contractible loops around a torus and because all compact connected (orientable) closed surfaces are classified by their genus, they are all multiple tori glued together and for each hole we can find four loops to construct a Pauli Algebra thus getting 2 qubits or 4 dimensions per hole. For example the kagome lattice can be used to enforce boundary conditions to form a double torus, so $\dim PS = 4^2 = 8$, so 4 qubits can be stored.

In the last step, one can construct a Hamiltonian of the system, which has exactly PS as a subspace and the open strings as excitations. It is:

$$H = -J_A \sum_{s \in \mathbb{S}} A_s - J_B \sum_{p \in \mathbb{P}} B_p\,, \tag{1.10}$$

where S (P) is the set of ll stars (plaquettes) and $J_A, J_B > 0$. Notice that due to the periodic boundary conditions, two parallel loops can be created with a product of plaquette- (star-) operators. The 4 degenerate ground states of this Hamiltonian are equal weight superpositions of all closed (contractible) loop configurations with either none or one X-type (i.e. X or X') or a $Z-$ type non contractible loop. Note, that for each configuration of contractible loops (dual loops), an even number of atoms on each plaquette (star) are excited. This is called *Gauss's law* on a $\mathbb{Z}_2$ gauge-theory on a charge free background.

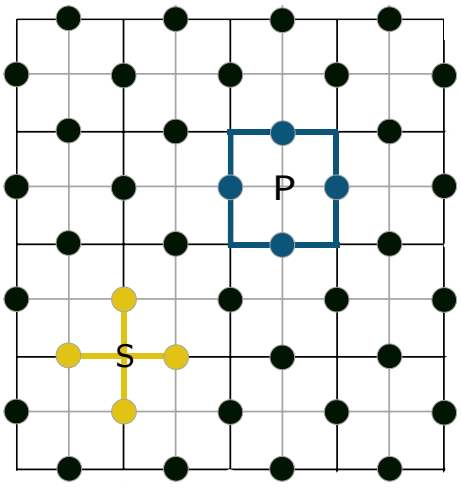

Figure 1.1: A 5×5 square lattice. A plaquette (blue) and a star (yellow) are depicted. The star is a plaquette on the dual lattice and vice versa.

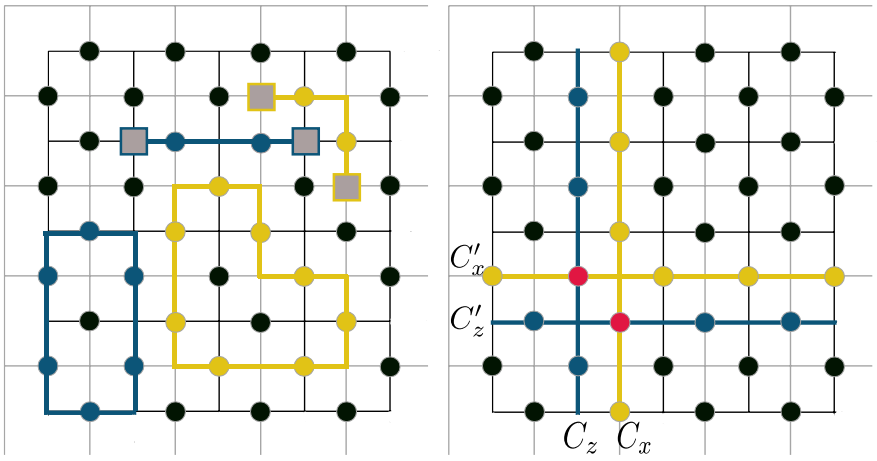

Figure 1.2: *A piece of a square lattice hosting a toric code model.* Trivial closed contractible loops and quasi particle excitations (left) and closed non contractible loops of the other homotopy class (right). For each loop (dual loop), an even number of atoms on each plaquette (star) are excited.

Before we look at the excitations of this gapped Hamiltonian, we observe, that the system is stable under local perturbations. These are of the form

$$V = -\mathbf{h}\sum_j \sigma_\mathbf{j} - \sum_{j<p} J_{jp}(\sigma_\mathbf{j}, \sigma_\mathbf{p})\,. \tag{1.11}$$

where only a small number (two) of local σ are contributing to the each term. Using time independent perturbation theory of the gapped system one gets that the perturbation is proportional to $\langle\xi|\, V^m\, |\eta\rangle$ or $\langle\xi|\, V^m\, |\xi\rangle - \langle\eta|\, V^m\, |\eta\rangle$ for $|\xi\rangle\,,\ |\eta\rangle \in PS$. These vanish for closed loops (again $\sigma^2 = 1$) unless it is a non contractible loop. This happens first in order $\frac{k}{2}$. However the energy splitting in that order is $\propto \exp(-ak)$, where a is a positive constant. So the splitting is small compared to the system gap if the correct parameters are chosen. Notice, that this potential looks like the Hamiltonian in eq. (1.38), (where for our model, σ_i are exchanged with $n = |1\rangle\langle 1|_i$) and indeed, in section 2.4 we energetically enforce string nets with such perturbations.

1.2.2 Anyonic Excitations

The ground states of the Hamiltonian in eq. (1.10) are the ones in PS, their energy is $-\sum_s J_A - \sum_p J_B$. Low excitations however are the open strings. In them at minimum only 2 signs are flipped, so the gap of the Hamiltonian's spectrum is $\min\{2J_A, 2J_B\} > 0$. These elementary low excitations crated by

$$S^z(S) = \prod_{j\in S}\sigma^z,\ \ S^x(S') = \prod_{j\in S'}\sigma^x \tag{1.12}$$

as stated in eq. 1.5. The endpoints of a $S^z(S)$ live on the vertices of the lattice and are called electric charges e, the endpoints of the dual strings $S^x(S')$ live inside the plaquettes (on the vertices of the dual lattice) and are called magnetic vertices m. Because these low energy excitations are exactly these open strings, it becomes clear that each of these quasi particles can only be generated in pairs of 2 (two e or two m particles). Lets look at these states, i.e $|\psi_m(S')\rangle = S^x(S')\,|\xi\rangle$ and $|\psi_e(S)\rangle = S^z(S)\,|\xi\rangle$. What happens if one exchanges two of those quasi particles with each other? Start with a m particle and create a e particle $|\psi\rangle = S^z(S)\,|\psi_x(S')\rangle$. Then loop the m particle around the e particle, one gets

$$|\psi_\text{final}\rangle = S^x(S')S^z(S)\,|\psi_m(S')\rangle = -S^z(S)S^x(S')\,|\psi_m(S')\rangle = -S^z(S)\,|\psi_m(S')\rangle = |\psi_\text{initial}\rangle \tag{1.13}$$

where we used $S^x(S')^2 = 1$ because the same Pauli matrix acts on the each state twice. So the two quasi particles are not interchangeable, the system gets a -1 when two quasi particles

of different types are exchanged i.e. moved around each other. This means, they are abelian anyons. Pairs of e or m particles however can be exchanged. These particles also are their own antiparticles as $(\sigma^z)^2 = (\sigma^x)^2 = 1$ (if one traces one particle back to the other or one creates a loop doing so, one leaves a A or B type pattern i.e. a closed loop). So their fusion rules become:

$$e \times e = 1\,,\ m \times m = 1\,, \tag{1.14}$$

$$\tag{1.15}$$

$$e \times m = m \times e = \epsilon\,, \tag{1.16}$$

where ϵ is the quasi particle that gets created when a m type particle occupies a plaquette while in the corner of this plaquette a e type particle occupies the lattice site. Its fusion rules can be derived from them of the other two:

$$m \times \epsilon = e\,,\ e \times \epsilon = m\,, \tag{1.17}$$

$$\tag{1.18}$$

$$f \times f = 1\,,\ f \in \{e, m\} \tag{1.19}$$

These rules again show that the anyons are abelian. These quasi particles are deeply connected to the topology of the model and thus to the structure of the ground state manifold. In fact the degeneracy of the ground state manifold due to the topology follows from the existence of these anyons: Lets create a pair of e type particles. One can move them around the lattice with local perturbations i.e. apply the Pauli matrices or string operators of the same kind to the endpoints of this string. So the following can be done: Start from a ground state $|\xi\rangle$ in PS. Create a pair of e particles. Move one around the torus with Z (or Z', where the starting point of the particle is removed from the product) and then annihilate the pair The resulting state is $Z\,|\xi\rangle$ ($Z'\,|\xi\rangle$), which is again a ground state in PS, as no particle excitations are present. So the operations of the Z and X type operators on PS can be explained by operations on these anyons. If a pair of e and a pair of m particles is generated, one can apply the following operator to the resulting state:

$$\prod_{\substack{j\in C_z\\ j\neq i}} \sigma_j^z \prod_{\substack{j\in C'_x\\ j\neq i'}} \sigma_j^x \prod_{\substack{j\in C_z\\ j\neq i}} \sigma_j^z \prod_{\substack{j\in C'_x\\ j\neq i'}} \sigma_j^x\, |e'_i, e'_k, m_i, m_k\rangle \tag{1.20}$$

where i and i' (k and k') denote the endpoints of the string operators i.e. the lattice sites adjacent to the vertex/plaquette of the particle. This operator propagates the e type particle around the torus along C_x, then the m type particle along C'_z, then it traces the e type particle back (moving it the same way backwards) and finally the m type particle is being traced back. Using the commutation relations of the Pauli matrices again it holds

$$\prod_{\substack{j\in C'_z\\ j\neq i}} \sigma_j^z \prod_{\substack{j\in C_x\\ j\neq i'}} \sigma_j^x \prod_{\substack{j\in C'_z\\ j\neq i}} \sigma_j^z \prod_{\substack{j\in C_x\\ j\neq i'}} \sigma_j^x\, |e'_i, e'_k, m_i, m_k\rangle = -\,|e'_i, e'_k, m_i, m_k\rangle \tag{1.21}$$

on the other hand it holds:

$$\prod_{\substack{j\in C'_z\\ j\neq i}} \sigma_j^z \prod_{\substack{j\in C_x\\ j\neq i'}} \sigma_j^x \prod_{\substack{j\in C'_z\\ j\neq i}} \sigma_j^z \prod_{\substack{j\in C_x\\ j\neq i'}} \sigma_j^x\, |e'_i, e'_k, m_i, m_k\rangle \tag{1.22}$$

$$= Z_1^{-1} X_1^{-1} Z_1 X_1\, |e'_i, e'_k, m_i, m_k\rangle = Z_1 X_1 Z_1 X_1\, |e'_i, e'_k, m_i, m_k\rangle \tag{1.23}$$

As $Z^{-1} = Z$ and $X^{-1} = X$ because $(\sigma^i)^2 = 1$. The same can be done for X_2 and Z_2, while nothing happens for mixed combinations. Thus the commutation relations of those operators and the structure of ground state manifold follow from the existence of anyons. As mentioned above, the these operations can be viewed as quantum gates acting on qubits. However abelian anyons can not be used for universal quantum computing so the model needs to be generalized to non abelian anyons.

1.3 Fibonacci Model

This section follows section IV and VI of Levin's paper.[7] The Fibonacci anyons are usually mentioned in the context of chern insulators. However a string-net condensate hosting Fibonacci

anyons on a lattice like the toric code can be constructed, in fact it generalizes this model of a $\mathbb{Z}_2$ gauge theory.

While the toric code is defined on a square lattice, the Fibonacci anyons are constructed on the honeycomb lattice, where again the atoms (spins) sit on the edges of the lattice. This thesis follows this approach although neither the Fibonacci model, nor the constructions of the surface codes in this thesis are bound to one lattice type. The model consists of two particle types, the trivial particle (i.e. the vacuum) 1 and the τ type particle, called a tauon. The fusion rules are[8]

$$1 \times \tau = \tau \times 1 = \tau, \tag{1.24}$$

$$\tag{1.25}$$

$$\tau \times \tau = 1 \oplus \tau. \tag{1.26}$$

This implies, that the anyons are non abelian. To describe the string net, and its excitations, we thus need the F-symbols and quantum dimensions d of the tauons.
It is $F_d^{abc} = 1$ if one index is 1. Solving the pentagon equations, so it follows that only one F-symbol is nontrivial, which is[8]

$$F_\tau^{\tau\tau\tau} = (F_\tau^{\tau\tau\tau})^\dagger = \begin{pmatrix} \varphi^{-1} & \varphi^{-\frac{1}{2}} \\ \varphi^{-\frac{1}{2}} & \varphi^{-1} \end{pmatrix}, \tag{1.27}$$

where $\varphi = (1+\sqrt{5})/2$, the golden ratio. It is also worth mentioning, that the ground state manifold of a system with n separated tauons *in the plane* is F_n fold degenerate, where $F_{n+1} = F_n + F_{n-1}$ with $F_0 = 0$ and $F_1 = 1$. These numbers can be written as

$$F_n = \frac{\varphi^n - (-\varphi)^{-n}}{\sqrt{5}}., \tag{1.28}$$

and are called the Fibonacci sequence, which gives these anyons their name. Thus the degeneracy can be written in terms of the golden ratio as well (also note that $\lim_{n\to} \frac{F_{n+1}}{F_n} = \varphi$).

The quantum dimension d of the tauons is φ, so the to get a tauon after two tauons fusing is $p = \frac{1}{d} = \frac{1}{\varphi}$. The probability to get 1 is thus $1 - p = \frac{1}{\varphi^2}$.[8]

In the following we change the notation of the indices of the F_d^{abc} symbols, such that $i \in \{0,1\}$ for every index i. The map is

$$\begin{cases} 1 \mapsto 0 \\ \tau \mapsto 1 \end{cases}. \tag{1.29}$$

Again, one can define star and plaquette operators acting on stars and plaquettes which are depicted in fig. 1.4.

The star operator is defined as

$$A_s = \delta_{ijk}, \tag{1.30}$$

where $\delta_{ijk} = 1$ if the configuration of the edges is allowed (that is the spins on either none, two or three edges are excited, and $\delta_{ijk} = 0$ otherwise. So this operator is diagonal. This is similar to the toric code where the star operator also is diagonal and acts as 1 on a allowed configuration. However due to the fusion rules, more states are allowed, strings can now fuse at the star, i.e. three lines can meet.

As fig. 1.4 shows, the plaquette operators change. They act on the plaquette as well es the edges adjacent to it. It is now not just a product of Pauli matrices which act as ± 1 on a plaquette. Now it is defined with the F- symbols. As it does not change the states at $a, .., f$ from fig. 1.4, this $2^12 \times 2^12$ matrix can be block diagonalized with 2^6 blocks of size $2^6 \times 2^6$. Let $|a,b,c,d,e,f;g,h,i,j,k,l\rangle$ denote the plaquette. Then the B_p operator is given as $a_0 B_p^0 + a_1 B_p^1$ with

$$B_p^s \,|a,b,c,d,e,f;g,h,i,j,k,l\rangle = \sum_{g',h',i',j',k',l'} B_{pg,h,i,j,k,l}^{sg',h',i',j',k',l'}(abcdef)\,|a,b,c,d,e,f;g',h',i',j',k',l'\rangle\,, \tag{1.31}$$

where $s \in \{0,1\}$ and

$$B_{pg,h,i,j,k,l}^{g',h',i',j',k',l'} = F_{sg'l'}^{alg} F_{sh'g'}^{bgh} F_{si'h'}^{chi} F_{sj'i'}^{dij} F_{sk'j'}^{ejk} F_{sl'k'}^{fkl}\,. \tag{1.32}$$

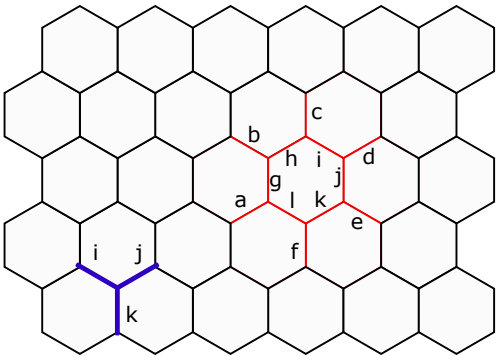

Figure 1.3: The edges of a star (blue) and a plaquette (red) act on. The edges are labelled with variables, which are 0 if the edge is not excited and 1 if it is (The spins (or Rydberg atoms) sitting on the edges are omitted here). The key difference is the plaquette which now includes edges adjacent to the original honeycomb plaquette and the plaquette operators don't change these spins, but their action on the remaining ones depend on these spins.

It is $a_0 = 1 + \varphi$ and $a_1 = (1 + \varphi)/\varphi$. With these operators at hand, on can again write down the Hamiltonian similar to eq. (1.10):

$$H = -\sum_s A_s - \sum_p B_p. \tag{1.33}$$

Again the ground state is a spin liquid consistent of a now weighted superposition of closed loops as the operators A_s and B_P commute with the Hamiltonian. These loops can however fuse now.

The excited states are again open strings as depicted in fig. 1.4, however these strings can fuse again. The properties of the ground state manifold again follow from the properties of the anyons. The degeneracy of the string nets the honeycomb lattice with PBC is $(1 + \varphi^2)^M + (1 + \varphi^{-2})^M$ where M is the number of unit cells.[9,10] Adding quantum fluctuations to them by applying the plaquette operators theoretically realizes the Fibonacci anyons.

This model hosts non abelian anyons, thus here the actions on states in the ground state manifold can describe universal quantum computing. The quasi particles are given by the endpoints of open weighted strings, see fig. 1.4.

As we have seen in the last two sections, these phases and their anyonic behavior are closely related to the loop structure at the vertices of the lattice (and co-lattice). For the toric code only an even number of spins of a star can be excited, and for the Fibonacci anyons also three edges can be excited to allow for fusion.

In the following sections, we explain, how Rydberg atoms can be arranged, to enforce constrains on a lattice, that may be able to realize such string nets.

1.4 The Rydberg Blockade and the PXP Model

Rydberg atoms can be modeled as a two level system, with the excited state $|1\rangle$ and the ground state $|0\rangle$.[11] Due to the strong dipole moment of the excited state (it goes with n^2), a system of two close non overlapping Rydberg atoms can be modeled by the Hamiltonian:[12,13]

$$H = \frac{\Omega}{2}(\sigma_1^x + \sigma_2^x) + \frac{C_6}{r^6} n_1 n_2 \tag{1.34}$$

Here σ_i^x is the x-Pauli matrix on the i-th Atom and $n_i = (|1\rangle\langle 1|)_i$. The first part is a Rabi oscillation with two non interacting Rydberg atoms. Ω is the corresponding Rabi-Frequency. The second term is a Van der Waals potential, which has its source in the polarization of the

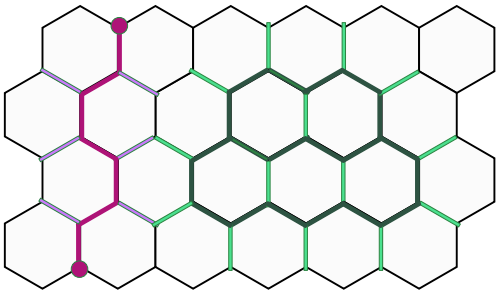

Figure 1.4: A closed loop created by a product of weighted B_p operators and a general string created by a generalized string operator. One can see that now the closed loops can fuse like the quasiparticles (i.e. the open strings). The lighter marked edges are also acted upon. Their states remain unchanged but the action of the operators on the other edges depend upon them.

charged cloud, which is the excited Rydberg atom. So the atoms are decoupled Rabi Oscillators unless they are in the state $|1\rangle \otimes |1\rangle$. Two Regimes arise. The weak interacting regime is given by $\frac{|C_6|}{R^6} << \Omega$. Here the perturbation is small and the Rabi Oscillations are hardly modified. In the strong interacting regime it is $\frac{|C_6|}{R^6} >> \Omega$. The system is perturbed and the $|1\rangle \otimes |1\rangle$ is out of resonance. It can not be reached by the Rabi oscillation, and dependent of the distance, the offset can be arbitrarily large, so it can be decoupled from the dynamics. This situation called 'Rydberg blockade'.

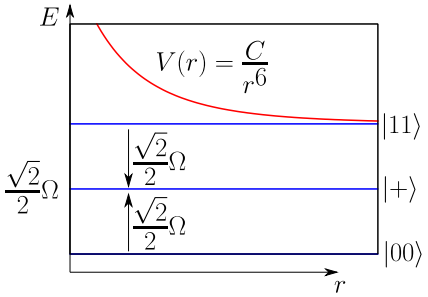

Figure 1.5: Dynamics of the Rydberg blockade. The Hamiltonian ineq. (1.34) without the Van der Waals potential describes a three level system, where $H|gg\rangle = H|rr\rangle = \frac{\sqrt{2}}{2}\Omega|+\rangle$. However due to the blockade the system is asymmetric and $H|rr\rangle$ gets shifted by a $\propto \frac{1}{r^6}$ potential. At some r_B the Rabi frequency equals the van der Waals interaction, where we leave the non interacting regime and the Van der Waals interactions dominates i.e. the blockade kicks in.

Due to the strong decrease of the Van der Waals interaction with $\frac{1}{r^6}$, a simplification to the described model can be achieved by replacing this potential with the infinite Wall potential

$$V_{\mathrm{PXP}}(r) = \begin{cases} 0 & r \leq r_B \\ \infty & r \geq r_B \end{cases} \tag{1.35}$$

where r_B is called the *blockade radius*. This is the *PXP model*. So if now two neighboring atoms are excited, the energy is infinite (relative to the allowed sates where no two atoms are in blockade). One says, they violate the blockade. If many Rydberg atoms in blockade with each other are driven by Rabi Oscillations Ω, interesting many-body quantum phases with long range topological order can occur.[1] This motivates a structured approach to the problem of creating distinguished Rydberg arrays, which have interesting low energy correlations between their atoms.

1.5 Functional Completeness of Rydberg Complexes

In the following section, we define, how Rydberg atoms can be arranged, to realize logical structures. Such Rydberg arrays have already been used for geometric programming.[14] In this section, and the remaining thesis, we use them, to realize structures which can realize string nets, that can potentially host topological quantum phases like the toric code. This section follows closely the first six chapters of the paper, to which this thesis contributes the other chapters.[2]

1.5.1 The physical Setup

Consider a planar arrangement of N Rydberg atoms. Each atom is assigned an index $i \in V = \{1, ..., N\}$, and is placed at the position $\mathbf{r}_i \in \mathbb{R}^2$. Each atom is a two level system $|n_i\rangle$, where $|0\rangle$ is the ground state, whereas $|1\rangle$ is the excited Rydberg state. Each atom is coupled to external lasers, with site dependent Rabi frequency Ω_i and detunings Δ_i. The Configuration of this arrangement of Rydberg atoms thus is $\mathcal{C} = \{\mathbf{r}_i, \Delta_i, \Omega_i\}_{i\in V}$, which we call a *(Rydberg) structure*. The position data $\{\mathbf{r}_i\}_{i\in V}$ is called the *geometry* of the structure $\mathcal{C}$. The Hamiltonian describing this arrangement is given by

$$H[C] = \sum_i (\frac{\Omega}{2}\sigma_i^x - \Delta_i n_i) + \sum_{i<j} V(|\mathbf{r}_i - \mathbf{r}_j|) n_i n_j \,. \tag{1.36}$$

Here $n_i = |1\rangle\langle 1|_i$. The Hilbert space of the system is $\mathbb{H} = (\mathbb{C}^2)^{\otimes N}$. In the general case, the interaction between the atoms is the Van der Waals interaction $V(|\mathbf{r}_i - \mathbf{r}_j|) = \frac{C}{r^6}$. However in the remainder of this thesis (except the last chapter), the interaction is being described with the PXP-model, that is given by eq. (1.35) so all states that violate the Rydberg blockade can be projected out. A state violates the (Rydberg blockade), when there are (at least) two atoms at positions r_i and r_j such that $|r_i - r_j| < r_B$, and $n_i = n_j = 1$, so both are excited. Then $V(|\mathbf{r}_i - \mathbf{r}_j|) = \infty$ due to eq. (1.35).

Instead of writing the Hamiltonian in the form of eq. (1.36), one can use the projector P, that projects onto the low energy subspace (the subspace of states, that do not violate the blockade), to write it as:

$$H[C] = P \sum_i (\frac{\Omega}{2}\sigma_i^x - \Delta_i n_i) P. \tag{1.37}$$

If one restricts the states the Hamiltonian is applied to, to the projected low energy subspace, the P become relevant only in the first term, which is $P\sigma_i^x P$. The the quantum fluctuations can perturb the system out of the low energy subspace, so P needs to be applied. Here the name of the model originates.

For the remaining thesis we look at the limit $\Omega \to 0$, so there are no quantum fluctuations present and a structure is given only by $\mathcal{C} = \{\mathbf{r}_i, \Delta_i\}_{i\in V}$. The Hamiltonian then simplifies to

$$H[C] = -\sum_i \Delta_i n_i + \sum_{i<j} V_{\mathrm{PXP}}(|\mathbf{r}_i - \mathbf{r}_j|) n_i n_j \,. \tag{1.38}$$

which after projecting out the high energy states (which violate the blockade), becomes diagonal. The prerequisites to realize such structures are already in place.[15] In the PXP model the interaction can be approximated by a kinematic constraint, which is completely encoded by a *blockade graph* $B = (V, E)$, whose vertices are the atoms, and its edges $\{i, j\}$ between atoms i and j indicate, that the two atoms are in blockade with each other, that is $|r_i - r_j| < r_B$. An abstract graph that realizes this, is called a *unit disk graph*,[16] where here r_B is the 'unit'. Obviously not every graph has this property. If there exists a geometry $G_{\mathcal{C}}$, that realizes $\mathcal{C}$ as blockade graph, this geometry is a *unit disk embedding* of this blockade graph (with the 'unit' r_B).

1.5.2 Definition of the Problem

In the next sections, a lot of consecutive definitions will be made, which will seem very technical. In fig. 1.7 a graphical overview of the general problem is shown, and how these definitions are

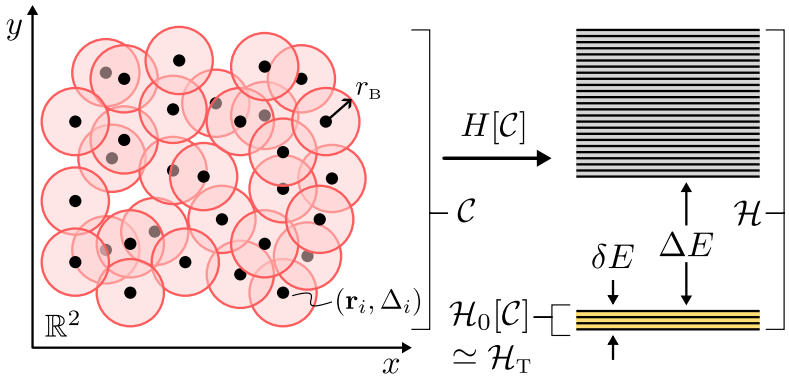

Figure 1.6: *Setting & Objective.*[2] A structure $\mathcal{C} = (\mathbf{r}_i, \Delta_i)_{i\in V}$ of atoms at positions $r_i \in \mathbb{R}^2$ and site dependent detunings Δ_i. The system is described by a Hamiltonian $H(\mathcal{C})$. with the PXP potential. The blockade radius is r_B. The spectrum of the Hamiltonian gives rise to a low energy eigenspace $\mathbb{H}_0 < \mathbb{H}$ of energy width δE which is gapped out from the high energy states by a gap ΔE. Finding small structures $\mathcal{C}$ so that $\mathbb{H}_0 \simeq \mathbb{H}_T$ for a given target Hilbert space is the main objective of this thesis.

related to it. The spectrum of the Hamiltonian defined in eq. (1.38) splits $\mathbb{H}$ into a low energy eigenspace $\mathbb{H}_0 < \mathbb{H}$ of energy width δE, which is energetically separated by the energy gap ΔE from the excited states. The main goal of this thesis is to find structures $\mathcal{C}$ such that their low energy eigenspace $\mathbb{H}_0$ is isomorphic to a certain target Hilbert space $\mathbb{H}_T$, whose properties are defined in the next part of this section.

Formal languages. A *word* $(x_1x_2...x_n) = x_1x_2...x_n \in \mathbb{F}_{22}^*$ of length n is a finite string of letters $x_i \in \mathbb{F}_{22}$ ($\mathbb{F}_{22}^*$ is the space of all such words). A *language* is a set of words. If all words have the same length, the language is called *uniform*. We will only look at uniform languages in this thesis. Examples of uniform languages are the class of languages generated by Boolean functions $\omega : \mathbb{F}_2^{n-1} \to \mathbb{F}_2$. The language then is $L[\omega] := \{x_1...x_{n-1}y \,|\, y = \omega(x_1...x_{n-1}) \in \mathbb{F}_2\} \in \mathbb{F}_2^*$. Such a language has $n-1$ words of length n. For $n = 2$, these languages thus have 4 words of length 3. They are exactly the truth tables of the logic gates, depicted in fig. 2.1.

A important class of languages we investigate in section 2.4, are *tessellated languages* on a lattice. The concept is not restricted to a lattice type but in the following a finite square lattice $\mathcal{L}$ with periodic boundary conditions is used as an example, to illustrate the construction of such a language. The setup is depicted in fig. 1.8. Place K qubits on each edge $e \in E(\mathcal{L})$. A bit configuration $x \in \mathbb{X}_\mathcal{L} \subset \mathbb{F}_2^{K|E(\mathcal{L})|} \subset \mathbb{F}_2^*$ assigns every bit on the lattice a Boolean value x_e^i ($i \in \{1, ..., K\}$). These configurations can be arbitrary generated by all the qubits on the lattice. However we want to look at a language that is characterized by local properties (like the string nets in section 2.4). For each site $s \in V(\mathcal{L})$ let the *bit-projector* $\mathfrak{u}_s(x) = (x_{e_1}^1...x_{e_4}^K)$ be the function that singles out the (ordered) set of the $g = 4K$ bits of the four edges e_i adjacent to s. Let $f : \mathbb{F}_2^g \to \mathbb{F}_2$ be an arbitrary Boolean function on g qubits. This language is called the *(local) check function*. With this, a language on every qubit on the lattice can be built. The tessellated language of bit patterns on $\mathcal{L}$ is generated by f and is defined as

$$L_\mathcal{L}[f] := \{x \in \mathbb{X}_\mathcal{L} \,|\, \forall s \in V(\mathcal{L}) : f(\mathfrak{u}_s(x)) = 1\}\,. \tag{1.39}$$

$L_\mathcal{L}[f]$ is thus the language that contains bit pattern on $\mathcal{L}$, that satisfy local constraints imposed on them by f.

Target Hilbert spaces. With the formal definition of languages at hand , we can now define the properties of the target Hilbert spaces $\mathbb{H}_T$. Every formal uniform language naturally gives rise to a linear subspace of n qubits. It is defined as

$$\mathbb{H}(L) = \mathrm{span}(\{|x\rangle \,|\, x \in L\}) \subset (\mathbb{C}^2)^{\otimes n}\,. \tag{1.40}$$

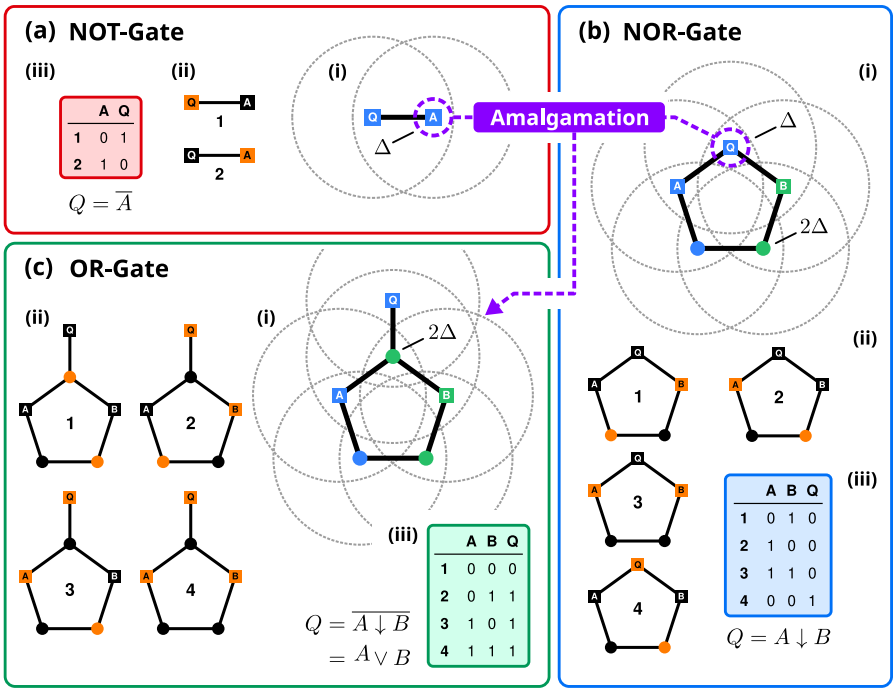

Figure 1.7: *Complete set of logic primitives.*[2] (a) (i) A Rydberg complex. Each port has a label. Every atoms has a detuning Δ. Some atoms are within a blockade radius (grey circles) of each other. They are then in blockade with each other (black line). (ii) The ground state manifold is given by states, where some atoms are excited (on). In these states the ports satisfy certain logical relations. In this example the relation is $Q = \bar{A}$, the NOT logic (iii). This 'logics' are given by languages, whose words describe the states of the ports i.e. the word 10 corresponds to the state where A is excited, and B is not. (b) Another example of a Rydberg complex (i). This complex requires two ancillas which have no label (but detunings). It realizes the NOR language (ii). given by a truth table (iii), which can be defined with a Boolean function $Q = f(A, B)$. (c) Complexes can be amalgamated. Here NOT complex gets amalgamated with a OR complex, by identifying the output of the NOR complex with one of the ports of the NOT complex. The resulting ground state manifold (ii) realizes the language of the OR logic given by $Q = f(A, B)$ (iii). The old port is a ancilla in the new complex.

For example consider the 'copy' language: $L_{\text{CPY}} = \{000, 111\}$. The associated Hilbert space is $\mathbb{H}(L_{\text{CPY}}) = \text{span}\{|000\rangle, |111\rangle\}$. A target Hilbert space is then a Hilbert space defined by eq. (1.40) with a target language f_T, so $\mathbb{H}_T := \mathbb{H}(L_{\text{T}})$, where f_T contains a logical structure (to be realized with a structure $\mathcal{C}$). If the language is a tessellated one, the tessellated target Hilbert space is defined by the check function as

$$\mathbb{H}_T = \mathbb{H}_{\mathcal{L}}(f_T) := \mathbb{H}(L_{\mathcal{L}}[f_T])\,. \tag{1.41}$$

The tessellated language has a spatial structure (bits on the edges of $\mathcal{L}$). The tessellated target Hilbert space inherits that structure as this Hilbert space is the space of the system of $K((\,E\mathcal{L}))$ qubits, where K qubits sit on every edge on $\mathcal{L}$. As an example look at the $\mathbb{H}_{|}|\mathbb{Z}_2$ of the even $\mathbb{Z}_2$ gauge theory, which will become important in section 2.4. It is the subspace of a Hilbert space on a square lattice ($K = 1$, $g = 4$). $\mathbb{H}_{\mathbb{Z}_2}$ is spanned by the product states in which the qubits in the state $|1\rangle$ form closed loops. This space can be realized as a tessellated target Hilbert space with the check function

$$f_{\mathbb{Z}_2}(x_1, x_2, x_3, x_4) = 1 \oplus x_1 \oplus x_2 \oplus x_3 \oplus x_4\,, \tag{1.42}$$

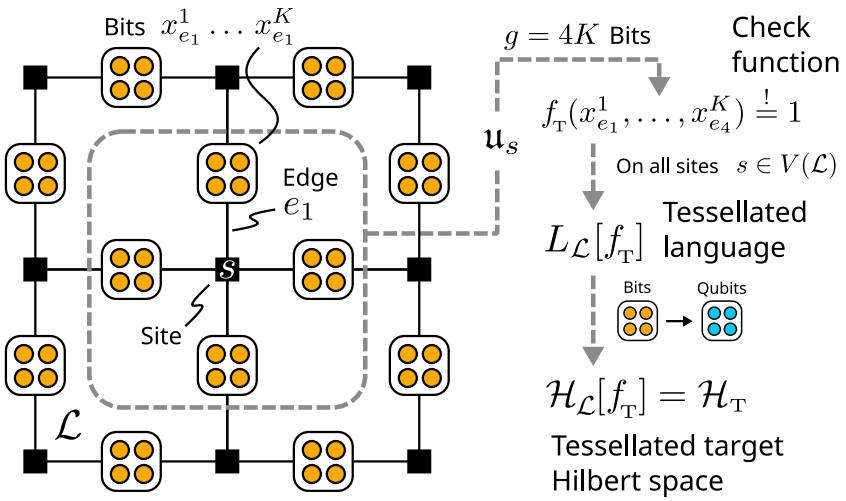

Figure 1.8: *Tessellated language & target Hilbert space.*[2] Emanating from a lattice site s of a lattice $\mathcal{L}$ are edges e_i (4 on a square lattice). On each edge K bits sit. The bit projector $\mathfrak{u}_s$ selects the $g = 4K$ bits adjacent to the site s, on which a check function $f_T : \mathbb{F}_2^g \to \mathbb{F}_2$ can be applied. If the bits are replaced by qubits, the tessellated Hilbert space is the subspace of the Hilbert space of those K bits, which is spanned by product states $|x\rangle$ whose qubits form patterns encoded by words $x \in L_{\mathcal{L}}[f_T]$. The tessellated target Hilbert space $\mathbb{H}_T = \mathbb{H}_{f_T}$ is the subspace of qubits, whose patterns locally satisfy the constraints imposed by the Boolean check function f_T.

where $\oplus$ denotes the addition in $\mathbb{Z}_2$ (addition modulo 2). The bit-projector is given as

$$\mathfrak{u}_s \left(\begin{array}{c} x^1_{e_1} \\ x^1_{e_2} \cdots s \cdots \\ x^1_{e_3} \quad x^1_{e_4} \end{array} \right) = (x^1_{e_1}, x^1_{e_2}, x^1_{e_3}, x^1_{e_4})\,.^2 \tag{1.43}$$

The check function in eq. (1.42) can be viewed as Gauss' law over a charge free background, because strings of $|1\rangle$ bits can not end or emerge from a site s. This is exactly the string net emerging at the toric code. More general string nets (like the one discussed in section 1.3) can be realized as tessellated target spaces as well.

1.5.3 Rydberg Complexes

In this section the connection between structure of Rydberg atoms and the concept of Languages and check functions is established. This is done by introducing Rydberg complexes, which generalize the concept of Rydberg structures. First realize that not all target Hilbert spaces with languages of length n can be realized as ground state manifolds of structures with n atoms. For example the `CPY` language $L_{\texttt{CPY}} = \{000, 111\}$, whose target Hilbert space is $\mathbb{H}_T = \mathrm{span}\{|000\rangle, |111\rangle\}$ can not be realized with a 3 atoms structure $\mathcal{C}_{\mathrm{CPY}}$ because the state $|111\rangle \in H_0[\mathcal{C}_{\mathrm{CPY}}]$. This implies, that no atoms are in blockade with each other, so $|111\rangle$ and $|000\rangle$ can not be the only two states in $H_0[\mathcal{C}_{\mathrm{CPY}}]$. This fact is true for many languages. One needs a larger structures with $N > n$ to realize this check function. We formalize this concept. Let $\mathcal{C}$ be a structure of N Rydberg atoms and let $L \subset \mathbb{F}_2^n$ be a uniform language of length n. Let $\mathfrak{L} = \{\mathrm{A}, \mathrm{B}, \dots\}$ be a set of N labels, where each label is associated with a fixed letter position of the words in L (if the words of L are written as rows of a table, the labels are the column headers). These labels are now assigned to n atoms with a injective function $l : \mathfrak{L} \to V$. These n atoms are called *ports*. The other $N - n$ atoms are called *ancillas*. A structure combined with a distinguished set of ports defined by l is called a *(Rydberg) complex* $\mathcal{C}_L$ if $\mathbb{H}_0(\mathcal{C})$ can be identified by the port configurations alone, that is

$$\mathbb{H}_0[C_L] := H_0[\mathcal{C}] = \mathrm{span}\{|x, a(x)\rangle \in \mathbb{H} \,|\, x \in L\}\,. \tag{1.44}$$

The states $|x, a(x)\rangle$ are bit configurations , where the first n bits are defined by bit configurations of x, the remaining ones by the ancilla configuration, defined by a function $a : L \to \mathbb{F}_2^{N-n}$. The ground state $\mathbb{H}_0(C_L)$ is called *L-ground state-manifold*. If the language is clear, the L is omitted. Note, that the ancillas do not contribute degrees of freedom for this space, they are merely there to realize states with the Rydberg blockade, which otherwise would not be energetically degenerate (with width δE) or in the low energy space at all. We say, a complex $\mathcal{C}_T = \mathcal{C}_{L_T}$ realizes a target Hilbert space, iff

$$(\mathbb{C}^2)^{\otimes N} \supseteq \mathbb{H}_0[\mathcal{C}_T] \simeq \mathbb{H}_T = \mathbb{H}(L_T) \subseteq (\mathbb{C}^2)^{\otimes n} \tag{1.45}$$

with the isomorphism $\simeq$ given by $|x, a(x)\rangle \leftrightarrow |x\rangle$. A complex realizes a language L, if the target Hilbert space $\mathbb{H}_T = \mathbb{H}(L)$ is defined by this language L.

As a example look at the Language of the logical gate `XOR`, which is generated by the check function $\omega_{\texttt{NOR}}(x_1, x_2) = x_1 \otimes x_2$. So the language is $L_{\texttt{NOR}} = L[\omega_{\texttt{NOR}}] = \{001, 100, 010, 110\}$. The ground state manifold of a Rydberg complex $\mathcal{C}_{\texttt{NOR}}$ thus must be

$$H_0[\mathcal{C}_{\texttt{NOR}}] = \text{span}\{|001, a(001)\rangle, |100, a(100)\rangle, |010, a(010)\rangle, |110, a(110)\rangle\}. \tag{1.46}$$

where the port configuration determines the ancilla configuration a. It is shown in section 3.1 that we need at least 2 ancillas to realize this complex. Complexes that realize languages generated by check functions that are logical gates are also called *gates*. The ports , that are assigned a input of the gate by l are also called *input (ports)*, and the *output (port)* is the port, that the output of the gate is assigned to. This is extended to logical circuits that have more than two (one) input (output). However there is no dynamic involved, so no information flows into and out of complexes.

Finally note two things:

1. The same structure $\mathcal{C}$ can be interpreted as different complexes depending on the labelling function l.
2. A given structure $\mathcal{C}$ with a $|L|$ fold degenerate ground state manifold does not have to allow for a labelling l that realizes a certain language L.

So the general construction of these complexes is not trivial. And one can imagine, that these complexes get really large and non trivial for a general check function of a large circuit. This makes a reducible approach reasonable, where like in electronics, large circuits are built by small and few primitives. This is defined in the next section.

1.5.4 Amalgamation

Combining two complexes to a larger one is called amalgamation. Let L_1 and L_2 be two uniform languages of length n_1 and n_2. Let $\gamma \subseteq \{(p_1, p_2) \,|\, p_i \in \{1, \ldots, n_i\}\}$ be a set of disjoint pairs of letter positions. Disjoint means $(x_1, y_1) \neq ((x_2, y_r))$ if $x_1 \neq x_2$ and $y_1 \neq y_2$. Let $\gamma_i := \{p_i \,|\, p \in \gamma\}$, and for a word $x \in L$, x^{γ_i} is the word with all letters at positions γ_i deleted. With that, the *γ-intersection of* $\mathcal{L}_1$ and $\mathcal{L}_2$ is defined as

$$L_1 \overset{\gamma}{\cap} L_2 := \left\{x\, y^{\gamma_2} \,|\, x \in L_1, y \in L_2, \forall_{(a,b)\in\gamma}\, x_a = y_b\right\}$$

which is the Language of concatenations of words from L_1 and L_2, where the letters at the positions defined by γ coincide and the second copy of these letters is deleted. It is a uniform language with words of length $n_1 + n_2 - |\gamma|$. One can now define the *reduced γ-intersection*

$$L_1 \overset{\gamma}{\cap} L_2 := \left\{x^{\gamma_1}\, y^{\gamma_2} \,|\, x \in L_1, y \in L_2, \forall_{(a,b)\in\gamma}\, x_a = y_b\right\},$$

which is almost the same definition as above, only now both copies of the letters in γ are deleted. The words are now of length $n_1 + n_2 - 2|\gamma|$.

As an example look at the `NOR` language $L_{\texttt{NOR}} = \{001, 100, 010, 110\}$ again. To copy the output of the `NOR` gate one can amalgamate the output port of this gate (letter 3) with the input port of a `CPY` gate (letter 1), where the `CPY` language is $L_{\texttt{CPY}} = \{000, 111\}$. So $\gamma = \{(3, 1)\}$. The γ-intersection then is the language

$$L_{\texttt{NOR}} \overset{\gamma}{\underline{\cap}} L_{\texttt{CPY}} = \{00\underline{0}00, 01\underline{1}11, 10\underline{1}11, 11\underline{0}00\} \tag{1.47}$$

where the underscore denotes the letters, which come from both languages, i.e. they are the letter 3 in the NOR language and letter 1 in the CPY language, and where one copy is deleted. The words are of length $3+3-1=5$. The reduced intersection the given by

$$L_{\texttt{NOR}} \overset{\gamma}{\cap} L_{\texttt{CPY}} = \{0000, 0111, 1011, 1100\} \ . \tag{1.48}$$

The words are of length $3+3-2=4$.

With these concepts at hand we can define the *amalgamation of complexes*. Given two complexes $\mathcal{C}_{L_1}$ and $\mathcal{C}_{L_2}$ that realize languages L_1 and L_2 consisting of N_1 and N_2 atoms. To amalgamate them, fix γ so that $L' := L_1 \overset{\gamma}{\underline{\cap}} L_2 \neq \emptyset$. Then combine the two complexes to one by identifying the pairs of atoms in γ with each other:

$$\mathcal{C}_{L'} = \mathcal{C}_{L_1} \overset{\gamma}{\otimes} \mathcal{C}_{L_2} :=$$

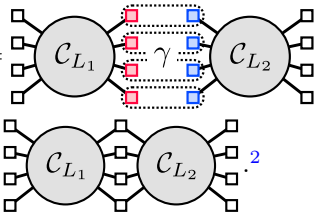

$$= \mathcal{C}_{L_1} \quad \mathcal{C}_{L_2} \ .^{2} \tag{1.49}$$

The new complex realizes the language L'. It has $N_1 + N_2 - |\gamma|$ atoms. It is possible to arrange complexes such that the ports are 'on the boundary' of the complex (see section 1.5.5). The Hamiltonian of the new complex is given by

$$H[\mathcal{C}_{L'}] = \left(H[\mathcal{C}_{L_1}] + H[\mathcal{C}_{L_2}] + \delta H\right)/\gamma \tag{1.50}$$

where $\bullet/\gamma$ denotes that pairs in γ that are identified with each other. The residual part $\delta\mathbb{H}$ denotes additional interactions between the atoms of the complexes. However in the PXP model, they vanish. In the Van der Waals model they do not, however they decay quickly. The Hamiltonian thus consists of all terms of the old ones. However if $(i,j) \in \gamma$ these atoms get identified. So $(-\Delta_i n_i - \Delta_)/\gamma = -(\Delta_1 + \Delta_2) n_i$, because both identified atoms are in the same state. The new complex realized the new language L', which can be shown easily. Weather $n' = 0$ or $n' = 1$, the ground state energy of the new complex is lower bounded by the configurations of the summands $\mathbb{H}_0(L_i)$. This are just the words in L'. If $|L_1 \overset{\gamma}{\underline{\cap}} L_2| = |L_1 \overset{\gamma}{\cap} L_2|$ the state of the atoms in γ provide no new information about the ground state manifold, thus the new identified atoms can be made an ancilla. Then $L' = L_1 \overset{\gamma}{\cap} L_2$.

At last what happens if one wants to amalgamate complexes generated by a check function, for example logical gates? Let $f(x_1, x_2)$ and $f'(x_1', x_2')$ be two Boolean functions of two gates. These gates get concatenated into a circuit with three inputs $\tilde{f}(x_1', x_1, x_2) := f'(x_1', f(x_1, x_2))$. So the two last ports go into the gate described by f, and its output is an input of f' together with x_1'. It is then $L[\tilde{w}] = L[w] \overset{\gamma}{\cap} L[w']$ with $\gamma = \{(3,2)\}$. Here 3 denotes $y = f(x_1, x_2)$ and 2 denotes x_2'. Note that Boolean circuits without redundancies fulfil $|L[w] \overset{\gamma}{\underline{\cap}} L[w']| = |L[w] \overset{\gamma}{\cap} L[w']|$ because the input bits define all words. In the following we only look at Languages without redundancies. So one can built large circuits with small Rydberg complexes. This is done in the next section.

1.5.5 Functional Completeness

In this section, a proof for the following theorem is given:

Theorem 1 (Functional completeness)**.** *For every tessellated target Hilbert space $\mathbb{H}_T = \mathbb{H}_{\mathcal{L}}[f_T]$ on some lattice $\mathcal{L}$ that is generated by a check function f_T, there exists a structure $\mathcal{C}_T$ in the PXP model such that*

$$\mathbb{H}_T \overset{loc}{\simeq} \mathbb{H}_0[\mathcal{C}_T] \,, \tag{1.51}$$

with finite gap $\Delta E > 0$ and perfect degeneracy $\delta E = 0$.

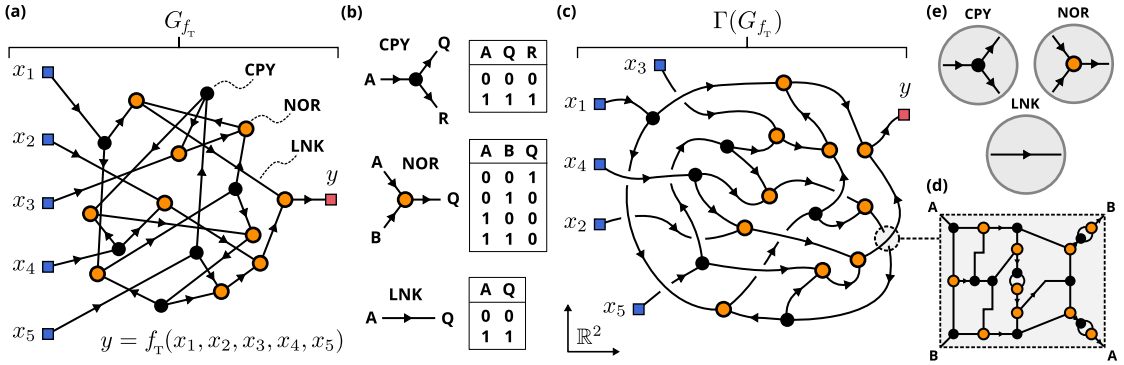

Figure 1.9: *Decomposition of Boolean functions.*[2] (a) A oriented trivalent graph G_{f_T} that has 6 ports at open links on its boundary. 5 ports are inputs $x_1, ...x_5$, and one is the output $y = f_T(x_1, ...x_5)$. There are two types of vertices depending on the number of in- and outgoing edges. The embedding is not planar. (b) The vertices are either a LNK complex or a NOR complex. The oriented edges are LNK complexes. (c) By using a planar embedding for a crossing complex, the embedding of the graph $\Gamma(G_{f_T})$ can be made planar. Also, if any ports are not on its boundary, one can add additional wiring (links) that may cross other links in the embedding $\Gamma(G_{f_T})$. Replacing these with the planar crossing keeps the embedding planar. (d) A logical circuit for a crossing (CRS) circuit built from NOR gates.[17] This gives a planar embedding for a CRS complex consisting of the three primitives LNK, CPY and NOR.

Here $\overset{\text{loc}}{\simeq}$ denotes, that the formal isomorphism between those Hilbert spaces conserves local structures. The local structure of $\mathbb{H}_0(\mathcal{C}_\text{T})$ is the underlying structure of the Rydberg atoms and their excitation patterns. The local structures of $\mathbb{H}_T = \mathbb{H}_\mathcal{L}[f_T]$ comes from the lattice $\mathcal{L}$ and is imposed by the check function f that defines the tessellated language $L_\mathcal{L}[f_T]$. So these local structures define $\mathbb{H}_T$. This will become relevant in section 2.4.

Proof. The proof is constructive and completed in 5 steps. Steps 1 to 4 construct a complex $\mathcal{C}_{f_T=1}$ that implements a check function. Step 5 amalgamates copies of that complex to construct $\mathcal{C}_\text{T}$.

Step 1: Decomposition of f_T. At first we use the fact, that logical circuits are complete, that is there exists a universal gate from which every circuit can be constructed. Here the universal NOR gate

$$A \downarrow B := \overline{A \vee B}\,. \tag{1.52}$$

is chosen as building block to decompose f. We can thus write

$$f_T(x_1, \ldots, x_g) = (\ldots(x_i \downarrow x_j)\ldots(x_k \downarrow x_l)\ldots)\,. \tag{1.53}$$

Note that the same variable can occur at multiple places in this decomposition (due to copying bits). So the logic of the check function can be transformed into a trivalent graph G_{f_T}, see fig. 1.9a. This graph has $g+1$ open vertices which is where the input bits $(x_1, \ldots, x_g)$ enter the logic, and one where the result $f_T(x_1, \ldots, x_g)$ is given out. G_{f_T} is trivalent, because bits can be copied ('splitting a wire in a circuit'), directed and contains two sorts of vertices. The direction of the edges displays the direction of information flow. They can be interpreted as the wires of the circuit, and thus follow a 'link' language (denoted as L_LNK, see fig. 1.10). The vertices are then distinguished by the number of edges that go into and come out of a vertex. A vertex is a NOR, if two edges enter, and one comes out. A vertex is a CPY if one edge enters and two come out. If the vertices are assigned with the truth tables of fig. 1.10b, the output bit of the graph is exactly $f_T(x_1, \ldots, x_g)$. Without redundancies there are 2^g configurations for a circuit with g inputs.

Step 2: Embedding of G_{f_T}. To realize G_{f_T} as a Rydberg complex, it needs to be embedded in $\mathbb{R}^2$. For this, there has to be a planar embedding $\Gamma(G_{f_T})$. For graphs of our topology, there

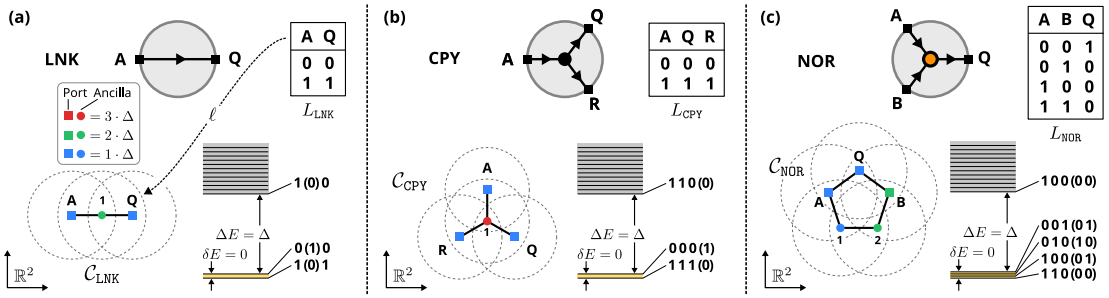

Figure 1.10: *Complete set of logic primitives.*[2] (a) The (elementary) LNK-complex $\mathcal{C}_{\texttt{LNK}}$ that realizes the $L_{\texttt{LNK}}$ language can be realized with three atoms, which are two links amalgamated. The ports are labelled A and Q by the labelling function l. Both have detuning $\Delta_A = \Delta_Q = \Delta$ The Ancilla has a detuning $\Delta_1 = 2\Delta$. The spectrum has a the desired ground state manifold $\mathbb{H}_0[\mathcal{C}_{\texttt{LNK}}]$ with width $= 0$ and gap $\Delta E = \Delta$. The Atoms in blockade are connected with a black line (A and Q are not in blockade). (b) The CPY-complex $\mathcal{C}_{\texttt{CPY}}$ consists of three NOT amalgamated to a single ancilla. The ports A, R and Q have detuning Δ. The ancilla has detuning 3Δ. $\mathbb{H}_0[\mathcal{C}_{\texttt{CPY}}]$ is degenerate and a gap of width Δ to the remaining spectrum. The ancilla is needed to connect the ports as they must not be connected to realize a ground state manifold that contains $|111\rangle$. (c) The NOR-complex $\mathcal{C}_{\texttt{NOR}}$ can be realized with two ancillas (blue and green circles). The blockade graph is a ring where both ports A and B are blocked with Q. Again the spectrum is gapped (which is why the ancillas are needed. Otherwise the the ports with the given blockades) between them would be sufficient) with gap $= \Delta$, and degenerate.

always exists an embedding, however it does not have to be planar. It can be made planar however, if one can resolve wire crossings. This can be done in electronics as a there exists a planar circuit consisting of NOR gates (and CPYs), that can replace two crossing wires without changing the circuit, see fig. 1.9d. This circuit will be further discussed in section 2.3. So a graph with the same properties as G_{f_T} can be constructed for that crossing circuit. One can thus replace any crossings in $\Gamma(G_{f_T})$ with a embedding of the crossing graph. Given that NOR, LNK and LNK can be realized planar, the resulting embedding $\Gamma(G_{f_T})$ is a planar embedding. In the next step, these three planar embeddings are constructed. They are depicted in fig. 1.10.

Step 3a: Constructing the LNK complex. Unlike electrical circuits, which we used as a blueprint for $\Gamma(G_{f_T})$, our Complex has no wires. So one needs to construct a counterpart to wires, which is the LNK complex. The most primitive logic to be realized as a complex is the NOT. The NOT language is $L_{\texttt{NOT}} = \{01, 10\}$. It is a single bit gate with the check function $f(x) = \bar{x}$. It realizes the core mechanics of the Rydberg blockade as it can be built as a complex by just putting two atoms in blockade with each other. The Hamiltonian in the PXP model is

$$H_{\texttt{NOT}} = -\Delta(n_A + n_Q) + V_{\text{PXP}} n_A n_Q \tag{1.54}$$

where $|\mathbf{r}_A - \mathbf{r}_Q| < r_B$. The labels are given by the labelling function l, where $A, B, ...$ are inputs and $Q, R, ...$ are outputs. The ground state manifold is $\mathbb{H}_0[\mathcal{C}_{\texttt{NOT}}] = \text{span}\{|01\rangle, |10\rangle\}$ with degeneracy $\delta E_{\texttt{NOT}} = 0$ and gap $\Delta E_{\texttt{NOT}} = \Delta > 0$. The LNK complex is then just the amalgamation of two NOTs. The Hamiltonian is

$$H_{\texttt{LNK}} = -\Delta n_A - 2\Delta \tilde{n}_1 - \Delta n_Q + V_{\text{PXP}} n_A n_1 + V_{\text{PXP}} n_1 n_Q \,, \tag{1.55}$$

For the rest of the thesis we label ancilla with numbered indices and tildes. Again one finds $\delta E_{\texttt{LNK}} = 0$ and gap $\Delta E_{\texttt{LNK}} = \Delta > 0$. The LNK ground state manifold is given by

$$\mathbb{H}_0[\mathcal{C}_{\texttt{LNK}}] = \text{span}\{|0(1)0\rangle, |1(0)1\rangle\} \,. \tag{1.56}$$

The LNK complex is depicted in fig. 1.10a. For the remainder of this thesis, ancillas are written in parenthesis. Arbitrary links can be built by amalgamating LNK complexes.

Step 3b: Constructing the CPY complex. Classical bits can be copied by splitting a wire. In the Rydberg formalism a complex is needed, that does this. The copy language is $L_{\texttt{CPY}} = \{000, 111\}$. The CPY complex can not be built with 3 atoms, see section 3.1. However it can be realized with 4, see fig. 1.10b. One ancilla $\tilde{n}_1$ is in blockade with all three ports, which are not in blockade with each other so $|111\rangle$ can be realized. The complex can be viewed as three NOT amalgamated to a single ancilla. (Just three unconnected ports would result in three uncorrelated atoms). The Hamiltonian is

$$H_{\texttt{CPY}} = -\Delta(n_A + n_Q + n_R) - 3\Delta\,\tilde{n}_1 + V_{\mathrm{PXP}}\tilde{n}_1 n_Q + V_{\mathrm{PXP}}\tilde{n}_1 n_Q + V_{\mathrm{PXP}}\tilde{n}_1 n_R\,. \tag{1.57}$$

Its ground state manifold is

$$\mathbb{H}_0[\mathcal{C}_{\texttt{CPY}}] = \mathrm{span}\,\{\,|000(1)\rangle\,, |111(0)\rangle\,\}\,. \tag{1.58}$$

Again one finds $\delta E_{\texttt{CPY}} = 0$ and $\Delta E_{\texttt{CPY}} = \Delta > 0$.

Step 3c: Constructing the NOR complex. At last, the NOR gate must be realized with a Rydberg complex. The NOR language is $L_{\texttt{NOR}} = \{100, 100, 010, 110\}$. This language is not a intersection of copies of the NOT language, the complex can thus not be amalgamated from NOT complexes The NOR complex requires at least 5 atoms as proven in section 3.1 The complex is depicted in fig. 1.10c. The Hamiltonian is

$$H_{\texttt{NOR}} = -\Delta(n_A + n_Q + \tilde{n}_1) - 2\Delta(n_B + \tilde{n}_2) + V_{\mathrm{PXP}}\tilde{n}_1 n_2 + V_{\mathrm{PXP}}\tilde{n}_2 n_B + V_{\mathrm{PXP}} n_B n_Q + V_{\mathrm{PXP}} n_Q n_A + V_{\mathrm{PXP}}\tilde{n}_1 n_A. \tag{1.59}$$

Again one finds $\delta E_{\texttt{NOR}} = 0$ and $\Delta E_{\texttt{NOR}} = \Delta > 0$. The ground state manifold is

$$\mathbb{H}_0[\mathcal{C}_{\texttt{NOR}}] = \mathrm{span}\left\{ \begin{array}{l} |001(01)\rangle\,, |010(10)\rangle\,, \\ |100(01)\rangle\,, |110(00)\rangle \end{array} \right\}. \tag{1.60}$$

In this complex the ancilla are only needed to energetically degenerate the states 010 and 100 with 110. This NOR complex is not unique. There exist other NOR complexes with $N = 5$ atoms. However from all complexes realizing logical gates, the NOR complexes is the smallest. This is due to the 'negating' nature of the Rydberg blockade. This is why this universal gate was chosen in this proof. At last note, that the graph $G_{\texttt{NOR}}$ is planar.

Step 4: Constructing the f_T-complex. To construct the f_T-complex one simply builds the planar embedding $\Gamma(G_{f_T})$, by placing LNK complexes where links are (as described above, they can be adjusted in length, by amalgamating several LNK), CPY complexes on the CPY type vertices and NOR complexes on the NOR type vertices. By separating everything with enough links, there are no additional blockades in the PXP model so the resulting complex is a f_T complex with $g = 4K$ designated input ports (labelled by a labelling function l) and a output port $y = f_T(x^1_{e_1}, ...)$ on a output. These ports are on the boundary of the complex (one can place them there because additional crossings that are created through the additional 'wiring' can be made planar). It follows $\delta_{f_T} E = 0$, so its ground state manifold is degenerate and it is gapped by Δ_{f_T}. The situation thus looks like this:[2]

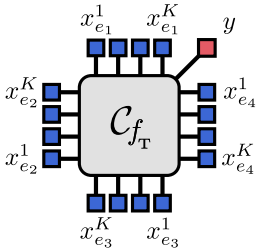

(1.61)

Now it is proven, that one can build all Boolean gates as a Rydberg complex. To realise a check function and make this construction useful for amalgamation, on needs to enforce the condition $f_T(x^1_{e_1}, ...) = 1$. This can be achieved by adding a local detuning of order ΔE to the output y

and make it an ancilla:[2]

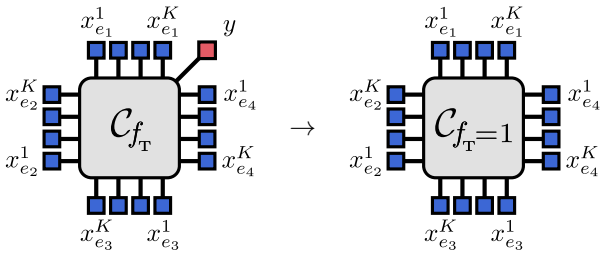

(1.62)

The (degenerate and gapped) ground state manifold now consists of all the states that satisfy the constraint imposed by the check function $f_T(x^1_{e_1}, ...) = 1$.

Step 5: Constructing $\mathcal{C}_T$. To construct the tessellated complex $\mathcal{C}_T$, one places copies of $\mathcal{C}_{f_T=1}$ on every site s of the lattice $\mathcal{L}$, and amalgamate adjacent complexes by their correct ports (if necessary, add links to avoid unwanted blockades):[2]

$\mathcal{C}_T :=$

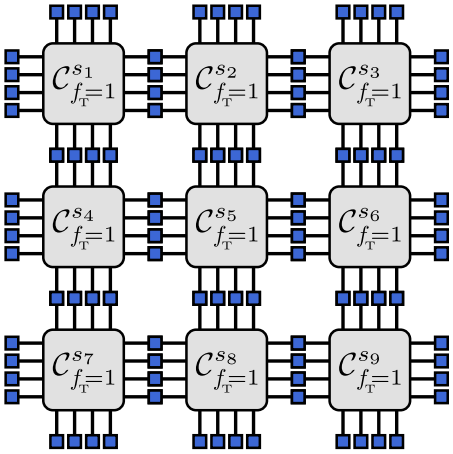

(1.63)

The ground states of this resulting complex are in one to one correspondence with the words in $x \in L_{\mathcal{L}}[f_T]$ (using the blue squares as ports). And the resulting map maps excitation patterns of the bits and the ancilla at the local site s (local unitaries of $\mathbb{H}_0[\mathcal{C}_T]$) to word patterns imposed by the check function (and the bit-projector), the local unitaries of $\mathbb{H}_T$. Note, that for the second one, the ancillas play no role i.e. they add no degrees of freedom to these isomorphic subspaces. In conclusion we showed $\mathbb{H}_T \overset{\text{loc}}{\simeq} \mathbb{H}_0[\mathcal{C}_T]$. □

Two remarks need to be made:

- In eq. (1.62) the output port was given an additional ancilla and was then demoted to an ancilla. However, if there are no blockades between inputs and this output, one can instead simply delete it along with all ancillas in blockade with it, and get the same result.
- If $f_T(x_{e_1}, ...) = 1$, it can be rewritten as $f_1(x^1_{e_1}, \dots, x^1_{e_2}, \dots) \overset{!}{=} f_2(x^1_{e_3}, \dots, x^1_{e_4}, \dots)$, with Boolean functions f_1 and f_2 that take $2K$ inputs each, then $\mathcal{C}_{f_T=1} = \mathcal{C}_{f_1} \overset{\gamma}{\otimes} \mathcal{C}_{f_2}$, so the two sub-complexes $\mathcal{C}_{f_1}$ and $\mathcal{C}_{f_1}$ can be amalgamated along their output ports to realize the resulting complex $\mathcal{C}_f$:[2]

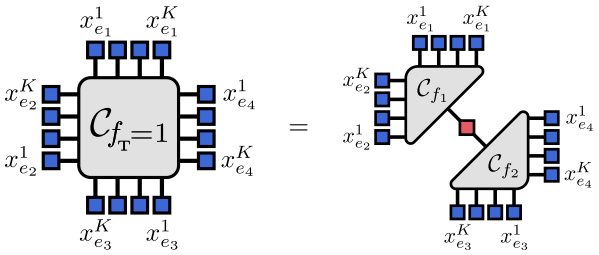

(1.64)

This is used in this thesis for the some spin liquids in section 2.4, which have this property.

So every (tessellated) Language (without redundancies) can be realized by a Rydberg complex. However these complexes can get really large (see section 2.3), and easily require more than 100 atoms, which are not suitable, especially for tessellation. So they are an upper bound for the size of the complexes. The main question and the topic for the next two chapters is, how small a complex, realizing a certain language, can get.

Chapter 2

Minimal Complexes

The main goal of this thesis is to find Rydberg complexes, for different languages / check functions. In principle, this can be achieved with the recipe given in section 1.5.5. However, the resulting complexes are large, which makes error free experimental realisations of those nearly impossible, especially when one wants to build a tessellated complex. So the question is, given an arbitrary target Hilbert space $\mathbb{H}_T = \mathbb{H}(L_\mathrm{T})$, what is a lower bound for N, the number of atoms to realize a complex $\mathcal{C}_\mathrm{T}$ with ground state manifold $\mathbb{H}_0[\mathcal{C}_\mathrm{T}]$. We want to find the minimal complexes for given languages.

2.1 Preliminaries

To find complexes for given languages, we need to address some preliminaries first.

2.1.1 Blockade Graphs and Maximal Independent Sets

As we've proven in section 1.5.5, the local structure f $\mathbb{H}_T$ can be translated to excitation patterns of Rydberg states in the resulting complex $\mathcal{C}_\mathrm{T}$, see fig. 1.7. The approach to find small (minimal) complexes for given languages is graph theory. More precisely, we look at the blockade graph $B = (V, E)$ of the complex. Because all languages of interest for the remaining thesis can be realized as Boolean check functions, no irreducible language or a language with the properties 1 or 2 of section 2.1.3 occur. We assume this from now on unless otherwise stated. W.l.o.g. we can thus assume, that the graph is connected. If it is not, the states of both subgraphs are completely uncorrelated, so the realizing language is reducible. As we concluded in section 1.5.5, $\mathbb{H}_0[\mathcal{C}_\mathrm{T}]$ is perfectly degenerate. We can also conclude, that all atoms in the complex have positive integer detunings. It follows, that $\Delta E \in \mathbb{N}_+ = \{1, 2, ...\}$, and $\delta E = 0$.

Due to this, the ground states (their excitation pattern) is given by a *weighted Maximal independent set* MIS^* of the unit disc blockade graph (see fig. 1.7 and **??**). A MIS^* is a subset of vertices, such that no vertices in the subset are connected by vertices, and no vertices can be added without violating this condition. *Maximum independent sets* MIS are the largest MIS^* (w.r.t. the number of selected vertices). Because the detunings determine the ground state energy, the MIS^* we look at are weighted, i.e. in addition to satisfying the condition to be a MIS^*, they maximize the sum of the vertex labels (the detunings). So we focus on finding graphs with MIS^*, which, create the desired pattern of excited ports to realize a language. Then the detunings are used to balance these. This implies detunings of order $\Delta E \approx 1$.

2.1.2 Finding Complexes

Finding a Rydberg complex $\mathcal{C}_\mathrm{T}$ to realize a language L_T is NP hard. This is for two main reasons:

- Finding a MIS^* on a unit disc graph is NP hard[18] (finding all MIS^* in general is[19,20]), yet alone weighted MIS^*. The proof of section 1.5.5 shows this as well. The check function for three inputs has to satisfy $f(x_1, x_2, x_3) = 1$ in the ground state. Finding this circuit is the NP-hard 3sat-problem. As this is equivalent to finding the weighted MIS^* in a Rydberg complex this problem reduces to 3sat (so if we could find a Rydberg complex with the desired properties in P, 3sat would be in P as well).

- Finding unit disc embeddings is also NP hard.[21]

In addition there are many degrees of freedom given by the detunings $\Delta_i,\ i \in V$ and the the labelling function l. So to find the small complexes, we realize a potential blockade graph as a adjacency matrix M, with $M_{ii} = -\Delta_i$

$$M_{ij} = \begin{cases} V, & \{i,j\} \in E \\ 0, & \text{otherwise} \end{cases} , \tag{2.1}$$

were $V = 100$ is large compared to the $\Delta_i \approx 1$, and approximates $V_{\text{PXP}} = \infty$. With this the energy of a state of a complex with N atoms can be written as a QUBO[22] problem:

$$E = -\mathbf{n}^T M \mathbf{n} \tag{2.2}$$

where $\mathbf{n} \in \mathbb{F}_2^N$, and $\mathbf{n}_i = 1$ denotes the atom i is excited, 0 denotes it is not. One can specify L_{T} and thus $\mathbb{H}_T$. Solving this NP hard minimization problem for several adjacency matrices leads to the ground state manifold. One needs to compare the port bits of the found states with the words in L_{T}. Doing this leads eventually to a complex $\mathcal{C}_{\text{T}}$. Note that one still has degrees of freedom from the labelling function l, to determine the realized language (so the algorithm might miss the right complex at first due to wrong labelling). Also not all infinite possible detuning combinations must theoretically be gone through. However, as explained in this subsection, only positive detunings of order Δ, only cases of detunings in order of $\Delta E \approx 1$ are relevant. We conducted a search with this approach with a program, and found all the complexes depicted in figs. 2.1 and 2.2. The source code is available at DaRUS.[23]

For larger complexes $N \approx 8, 9, ..$ this is not a good approach. However some spin liquids and the crossing require larger complexes (see section 3.2) which are not accessible with this numerical approach as such. Even very effective 'graph generators' implemented in mathematica failed at the task of finding complexes, as one still must find all (relevant) MIS^*. Instead an analytical 'clever' method is used to find lower boundaries N, for which a complex can be realized. which is described in chapter 3

2.1.3 Irreducible Languages

For the remaining thesis, we only look at *irreducible* languages. These are languages L whose words x are not concatenations of words a and b of two languages L_1 and L_2. This, by definition, excludes 'dummy' ports from the complexes realizing a language of interest. A 'dummy' port is a port p, which has two properties:

1. For every word $x \in L$, where $x_p = 1$ (i.e. p is excited), there exists a otherwise identical word x' only with $x'_p = 0$

2. The opposite is also true. For every word $x \in L$, where the letter assigned to $x_p = 0$ (i.e. p is not excited), there exists a otherwise identical word x' only with $x'_p = 1$.

Languages can only have property 1 or property 2. If this is the case, the languages can still be irreducible, like $L_r = \{000, 100, 011\}$, where the first letter has the first property, but L_r is not reducible. We will only look at languages, which do not have this structure. These constrictions come into play in the next section and in chapter 3 when we deal with `NOT` and `LNK` in a more general matter.

2.1.4 Detunings

As stated above, the detunings are of order Δ. The arbitrary real detunings Δ assigned to each atom in a complex, can be chosen to be in $\mathbb{N}$, where only the ports can have detuning $\Delta = 0$. If the realizing language does not have the property of 1 from section 2.1.3, all detunings in the complex can be chosen to be in $\mathbb{N}_+$.

Proof. Let $\mathcal{C}_{\text{T}}$ be a Rydberg complex with N atoms, realizing a language L_{T}. The ground state manifold is $\mathbb{H}_0[\mathcal{C}_{\text{T}}]$

Detunings are integers. First we show, that $\Delta_i \in \mathbb{Q}$. Let the gap of the spectrum be and $\mathbb{H}_0[\mathcal{C}_\mathrm{T}]$ has a width of so $\frac{\delta E}{\Delta E} \ll 1$. Let the complex have a irrational detuning. We want replace this detuning with a rational ones. To see that this is possible and $\mathbb{H}_0[\mathcal{C}_\mathrm{T}]$ remains gapped and still contains the same lowest energy states we use that $\mathbb{Q}$ is dense in $\mathbb{R}$. This implies that for the detuning $\Delta \in \mathbb{R} \setminus \mathbb{Q}$ a sequence $\{\Delta_n\}_{n\in\mathbb{N}}$ exists, such that the sequence converges towards Δ. But by definition this means that $\forall\epsilon > 0\ \exists n_0 \in \mathbb{N}\ \forall n \geq n_0\ |\Delta_n - \Delta| < \epsilon$. Choose ϵ such that $\frac{\delta E+\epsilon}{\Delta E-\epsilon} \ll 1$, The choice is motivated by the fact that $\delta E' = \delta E + \epsilon$ is the maximum possible energetic width of $\mathbb{H}_0[\mathcal{C}_\mathrm{T}]$, and the new gap is at minimum $\Delta E' = \Delta E - \epsilon$. This is just the condition $\frac{\delta E'}{\Delta E'} \ll 1$. Choose a Δ_n with $n > n_0(\epsilon)$, to replace Δ. The choice of ϵ ensures, that $\mathbb{H}_0[\mathcal{C}_\mathrm{T}]$ is still gapped, and contains the same states as before. By expanding all the rational detunings by the least common multiple $\mathrm{lcm}\{\Delta_i : i \text{ Lattice site}\}$, all the detunings become integers.

Detunings are positive. If a detuning is negative, all states that 'use' it will not be in $\mathbb{H}_0[\mathcal{C}_\mathrm{T}]$, because it is gapped by 1 from all the states that do not use it. But then one can remove it without changing the GSM. So the remaining complex realizes the same logic without negative detunings. Thus all detunings in a complex can be chosen to be positive Integers.

Ancillas also have nonzero detunings. Such an ancilla, lets call it $\tilde{n}$ can not play a role energetically, it can merely act as a bridge between adjacent atoms. There are two types of states in $\mathbb{H}_0[\mathcal{C}_\mathrm{T}]$. Some in which $\tilde{n}$ is excited and some in which $\tilde{n}$ is not. In the first case however one can put the detuning off as well, and the remaining unchanged bit configuration, (especially the ports are unchanged), has the same energy. So for every state $|\psi\rangle_1 \in \mathbb{H}_0[\mathcal{C}_\mathrm{T}]$ with the detuning excited, there is a state $|\psi\rangle_2 \in \mathbb{H}_0[\mathcal{C}_\mathrm{T}]$ which has the same energy and (other than the ancillas) the same bit configuration. So if a ancilla with $Delta_{\tilde{n}}$ exists, one can delete it and realize the same language. Note, that if this ancilla is the only connection between the two sub complexes, the language is already irreducible. For ports, the situation is differently. If a port p has zero detuning, the additional degeneracy of the states in $\mathbb{H}_0[\mathcal{C}_\mathrm{T}]$ as described now leads to new words in the realized language. This degeneracy realizes the property of L_r (see section 2.1.3). If the language to be realized by a complex does not have this structure, all ports have nonzero, thus positive detunings. □

2.2 The Logic Primitives

They key part of section 1.5.5 is the decomposition of large circuits into smaller gates. One can use the primitives to construct the other logical gates as Rydberg complexes. But even the other logical gates can get very large and convoluted. For example the `AND` gate $\wedge$ can be decomposed into `NOR` gates:

$$A \wedge B = (A \downarrow A) \downarrow (B \downarrow B)\,. \tag{2.3}$$

To satisfy this, two `CPY` and three `NOR` complexes are required, together with some `LNK`. So 20 atoms are required for a very simple gate. Thus the question arises, whether the important logic primitives of Boolean logic can be realizes in a smaller, more elementary way. The answer is positive. In addition to the common gates of Boolean algebra, `NOT` ($\neg$ or $\overline{\bullet}$), `AND` ($\wedge$), and `OR` ($\vee$), there are four Boolean gates, we realize as provably minimal Rydberg complexes:

$$\texttt{NOR:}\quad A \downarrow B\ = \overline{A} \wedge \overline{B} \tag{2.4a}$$

$$\texttt{NAND:}\quad A \uparrow B := \overline{A} \vee \overline{B} \tag{2.4b}$$

$$\texttt{XOR:}\quad A \oplus B := (A \wedge \overline{B}) \vee (\overline{A} \wedge B) \tag{2.4c}$$

$$\texttt{XNOR:}\quad A \odot B := (A \wedge B) \vee (\overline{A} \wedge \overline{B})\,. \tag{2.4d}$$

The complexes are depicted in fig. 2.1. Only `NOR` and `NAND` are universal gates. Some of these gates are inverted versions of others (as the N in their name suggests). The relations are:

$$A \wedge B = \overline{A \uparrow B} \tag{2.5a}$$

$$A \vee B = \overline{A \downarrow B} \tag{2.5b}$$

$$A \oplus B = \overline{A \odot B}\,. \tag{2.5c}$$

We already know minimal complexes for NOT (2 atoms), LNK (3 atoms), CPY (4 atoms) and NOR (5 atoms). We can immediately construct a small OR complex by using eq. (2.5b) and amalgamate a NOT to the output of the NOR complex given in section 1.5.5. Using eq. (2.5b), we can immediately construct an OR-complex with six atoms by amalgamation of a NOT-complex to the output port of a NOR-complex. It is however unclear, whether this graph is a minimal realization of a OR complex. In chapter 3, section 3.1 we proof that the complexes depicted in fig. 2.1, and thus the so constructed OR complex, are indeed minimal. The method used to do this, is generalized in chapter 3, section 3.2. It can not only find lower bounds for complexes, it can also, in principle, find them, and, if they are not unique, it can find all of them. In addition to the method described in chapter 3, a computer search for these small complexes has been conducted. The script found all the complexes depicted in this section, (together with all choices of detunings (we set $\max\{\Delta_i \,|\, i \in V(B)\} = 3$ in the code)). It is briefly discussed in section 2.1.2.

In fact, only the XNOR gate and the XOR gate are unique, i.e. their complexes have unique blockade graphs, see section 6.2. The other gates are not unique and all their realisations are depicted in fig. 2.2. Notice two things:

1. The AND gate can be realized from a NOR gate by amalgamating a NOT to one input and change the labelling.

2. The relations of eq. (2.5) are reflected by the minimal complexes. Indeed, if we amalgamate a NOT to the output of a minimal NOR complex, we get a minimal OR complex. The similar amalgamation leads to a NAND complex from an AND complex and a XOR complex from a XNOR complex. Looking at the relation between a NOT and a LNK, the NOT is the smaller one and they are related by the same amalgamation. In the Boolean algebra and its circuits on the other hand, a 'wire' i.e. the LNK is the smallest unit, and a NOT is a larger one. Our circuits are built from a intrinsic NOT logic, as it is the smallest operation the Rydberg blockade can perform, because it is its defining operation.

Due to these points, all complexes of the gates emerge from the topology of the three realisations of the NOR complexes, leading to the complexes in fig. 2.2. These are provably all minimal complexes of the gates (see section 3.1.2).

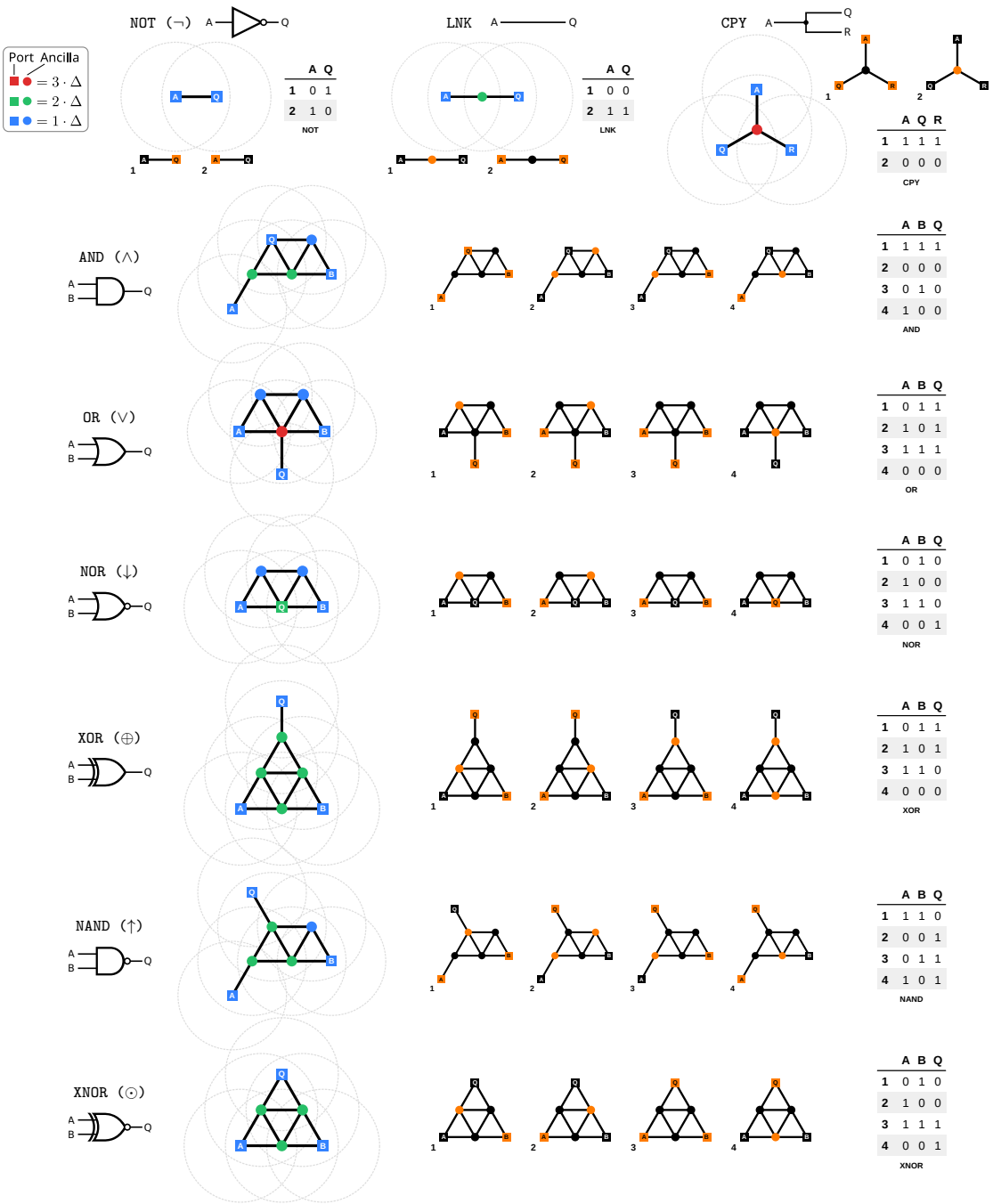

Figure 2.1: *Common logic primitives.*[2] Minimal Rydberg complexes for all the logical gates, which are the most common primitives for Boolean circuits. For the proof of their minimal size see section 3.1. Some of the depicted minimal complexes are not unique. All different minimal complexes of the non-unique gates are depicted in fig. 2.2. The depicted complexes consist of (1) their geometry with blockade radii (grey dashed circles, and black lines between two atoms, which in blockade with each other), (2) the ground state manifold (orange: $|1\rangle_i$, black: $|0\rangle_i$) and (3) the truth table of the ports (labelled atoms), of the states in the ground state manifold. The rows of these tables correspond to the configurations of the configurations of the ports in the realized ground states (where $A = 1$ represents $|1\rangle_A$ and $A = 0$ represents $|0\rangle_A$). Colors of ancillas and ports in the geometry encode the detunings (see key).

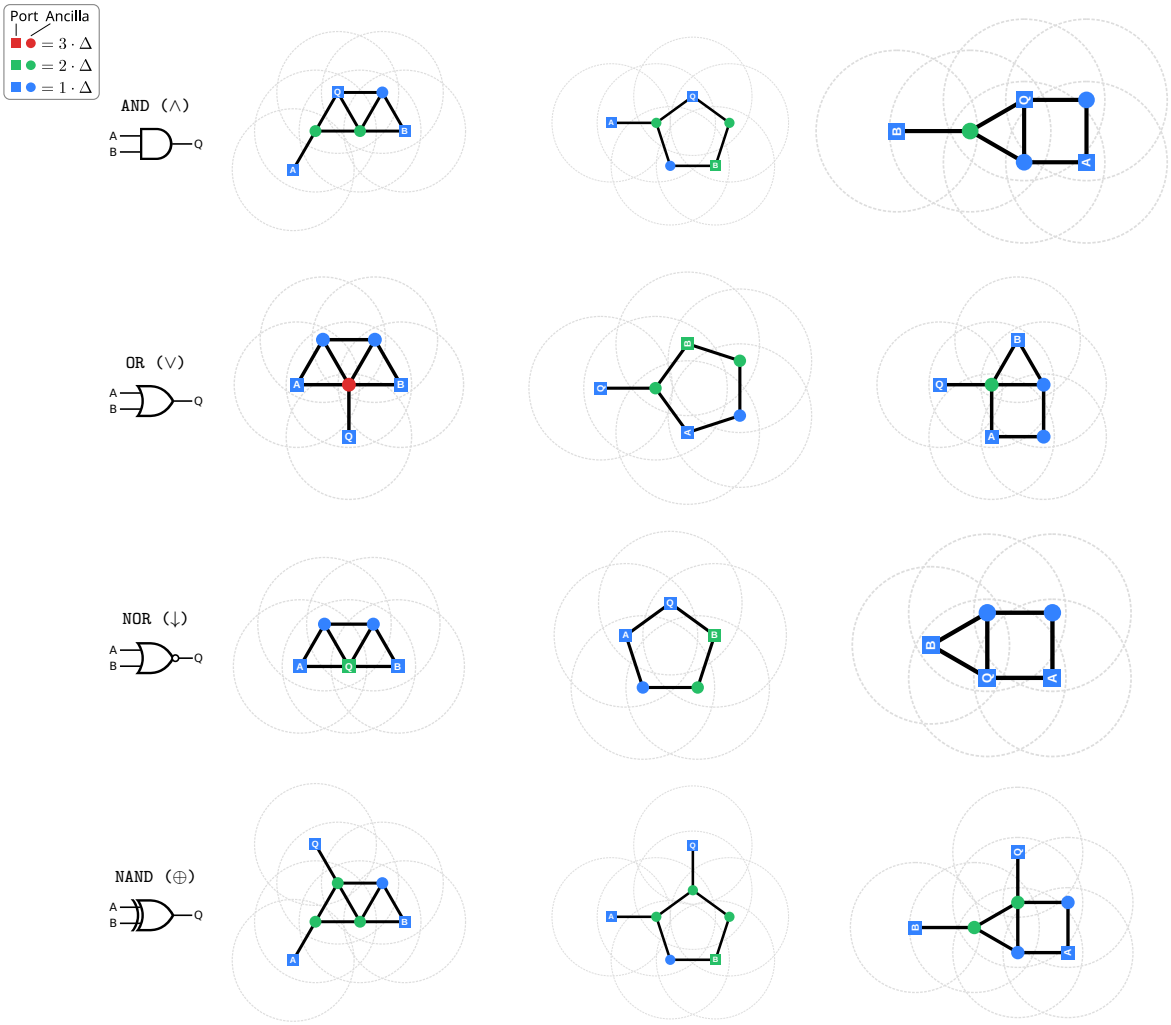

Figure 2.2: *All minimal Versions of the complexes of gates.* Except for the XNOR and the XOR, the gates have multiple minimal realisations. All of these are depicted. Notice, that all gates have three variations, which have the same basic structure. This is because the AND complex is the NOR complex with a additional NOT amalgamated to one input, and with different labelling. All gates and their 'negatives' (like NOR and OR) differ in size by one, and the additional atom of the larger gate is amalgamated to the output of the smaller.

2.3 Crossing

In circuits of electronics, crossing two wires can be achieved by simply placing them over each other. However a circuit built from NOR gates alone exists,[17] that realizes the same, see fig. 1.9d. This is a somewhat surprising feature, because it allows information to pass two channels of information around them self in a strict planar setting. This result is used in section 1.5.5 to ensure the existence of a planar embedding of the abstract blockade graph of a circuit. Constructing a crossing (CRS) complex by realizing such a circuit with Rydberg complexes as described in section 1.5.5 however leads to huge complexes with ≈ 27 atoms, see fig. 2.3a. Note that the depicted circuit uses XNOR gates a building blocks (which, in electronics are again build from NOR gates). The question again is, whether we find a smaller elementary complex that realizes a CRS logic.

We indeed find a smaller complex, that realizes a CRS complex. It is build from a complex

that realizes a ICRS. This is the inverted crossing, where both outputs are inverted after the crossing process. Again the inverted complex is smaller than the 'basic' one. The ICRS complex needs $N = 8$ atoms, and the CRS complex needs $N = 10$ atoms. The complexes are depicted in fig. 2.3b and fig. 2.3c. The ICRS complex has also been described in another paper,[14] where it is used to map non planar optimization problems to planar Rydberg structures. Again we show with the method described in section 3.2, that these complexes are minimal. We also show, that the ICRS is unique. The additional difficulty here is the topological constraint, see section 3.5.1. If one does not respect it, the method gives a $N = 7$ atom crossing, which however consists of two connected parallel LNK, which is not a crossing.

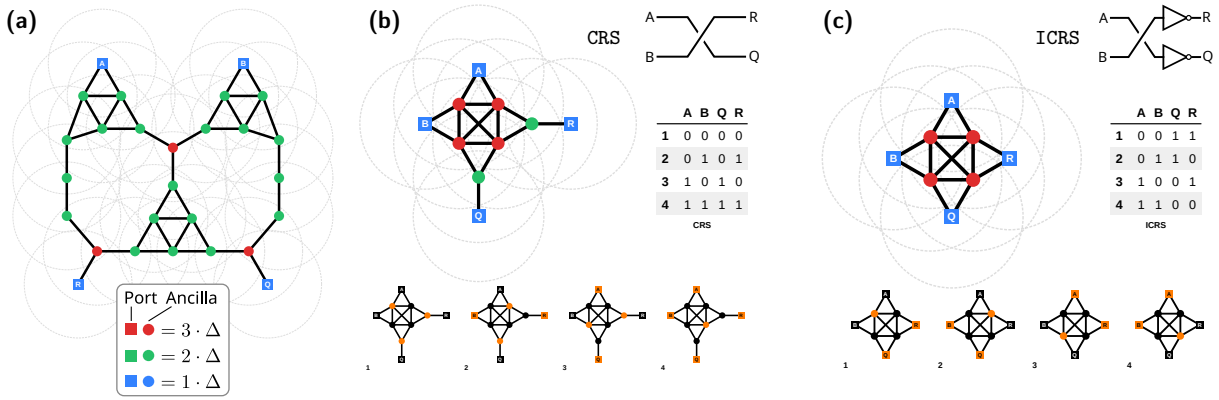

Figure 2.3: *Crossing.*[2] (a) The crossing (CRS) constructed from logic primitives as explained in section 1.5.5. Note, that instead of NOR gates, XOR gates are used. The gates are then amalgamated with CPY and LNK complexes to realize the 'crossing'-circuit. The ground state manifold of the complex (not shown) ensures $A = Q$ and $B = R$. The complex requires ≈ 27 atoms and is therefore too large to have practical relevance (as it realizes a very simple and common operation). Note, that the XOR gates are not universal, so construct them from universal NOR's, would require dozens of atoms as well for each of the three gates, requiring ≈ 100 atoms for the CRS complex. (b) A minimal CRS complex by contrast requires only $N = 10$ atoms. It is provably minimal, see section 3.5.2. The depicted data is explained in the caption of fig. 2.1. (c) The (unique) minimal inverted 'crossing' ICRS complex is again smaller than the CRS complex, and requires $N = 8$ atoms. For the proof of minimal size and uniqueness again see section 3.5.2. To construct a CRS from this complex, one needs to invert two adjacent ports by amalgamating a NOT to them. This is again due to the negating nature of the Rydberg blockade.

2.4 The Surface Code and Fibonacci Anyons

In this chapter, we construct the complexes, that motivated this thesis and the paper it contributes to,[2] namely ones that realize tessellated languages of string nets. The idea is, that dimer models can be based on Rydberg atoms on the edges of a lattice, that are in blockade with each other at the lattice sites. So only one edge adjacent to a site can have its atom excited. These models can carry topological order.[1] So by placing proper complexes at the lattice sites, on can create more complex string net models, like the toric code (or surface codes) and models that can carry Fibonacci anyons.[7]

2.4.1 Constructing the Surface Code

In this section, we look at a surface code model like the toric code on a lattice with periodic boundary conditions. Remember, that the ground states of the systems are based on equal weight superposition of all allowed loop configurations. We want to realize them using a tessellated language defined in section 1.5.2. A way to do this, is by using the property of the ground state(s)

$|G\rangle$ in these models:

$$B_p |G\rangle = A_s |G\rangle = |G\rangle \ , \tag{2.6}$$

for all star operators A_s and plaquette operators B_p (see section 1.2). As two plaquettes (stars) always act on an even number of sites the same time, one can trivially enforce the first condition by choosing the state $|\mathbf{0}\rangle$ with $\sigma_e^z |\mathbf{0}\rangle = |\mathbf{0}\rangle$ as $|G\rangle$. This corresponds to the state where all spins are aligned, or in our case, all Rydberg atoms are not excited. A_s does not act trivially on this state, as this operator flips spins (changes the states of the Rydberg atoms). To create a state that satisfies eq. (2.6), we modify the state: For the set of all stars $\mathbb{S}$ we define the multiplicative group $\mathcal{A} = \langle \{ A_s \,|\, s \in \mathbb{S} \} \rangle$.[2] The state

$$|G\rangle \propto \sum_{C \in \mathcal{A}} C \, |\mathbf{0}\rangle \ . \tag{2.7}$$

then satisfies eq. (2.6). This is because $\mathcal{A}$ is left-invariant under multiplications with B_p (because $[B_P, B_q] = 0$) and because $[A_s, B_p] = 0$. Each state $C\,|\mathbf{0}\rangle$ imprints a loop of flipped spins (excited Rydberg atoms) on the lattice of un-flipped spins (non-excited Rydberg atoms). So the state $|G\rangle$ is exactly the equal weight superposition of all closed loop configurations that forms the basis for the ground state manifold of the toric code, see section 1.2.

The toric code system would be realized by implementing the Hamiltonian eq. (1.10), then cooling the system to its ground state,[2] however each star (plaquette) consists of four atoms and these four-atom-interaction makes this very hard to do.
A different approach on the Rydberg platform is more promising: On constructs only the subspace

$$\begin{aligned} \mathcal{H}_{Loop} &:= \{ \, |\Psi\rangle \, | \, \forall \, \text{Sites } s : B_p \, |\Psi\rangle = |\Psi\rangle \, \} \\ &= \text{span} \, \{ \, |C\mathbf{0}\rangle \, | \, C \in \mathcal{A} \, \} \, . \end{aligned} \tag{2.8}$$

This space is thus spanned by all allowed loop configurations. It is the Hilbert space of a $\mathbb{Z}_2$-gauge theory on a charge free background,[2] and $B_p \, |\Psi\rangle = |\Psi\rangle$ is a gauge symmetry of it, called *Gauss's law*.[2] The A_s terms then are added perturbatively by ramping up the Rabi frequency Ω. This gives rise to quantum fluctuations and the string net condensed ground state(s), leading to interesting quantum phases,[1] like the toric code ground state manifold. The boundary conditions are important here, as the plane we construct here without them would only host a 'plane code', and as the genus of the plane is 0, the ground state would be one dimensional (and realize the equal weight superposition of loop configurations.) Due to Gauss's law, $\mathcal{H}_{Loop}$ motivates the construction of a complex $\mathcal{C}_{\text{loop}}$, with

$$\mathbb{H}_0[\mathcal{C}_{Loop}] \overset{\text{loc}}{\simeq} \mathbb{H}_T = \mathbb{H}_{Loop} = \text{span} \, \{ \, C \, |\mathbf{0}\rangle \, | \, C \in \mathcal{A} \, \} \ . \tag{2.9}$$

This Rydberg complex has ground states that one-to-one map to loop configurations on the (square) lattice. $\mathbb{H}_0[\mathcal{C}_{Loop}]$ has dimension $\propto 2^M$, where M is the number of unit cells of the square lattice.[2] Note that $\mathbb{H}_0[\mathcal{C}_{Loop}]$ cannot be decomposed into factors of local Hilbert spaces, like the full Hilbert space, which is $\mathbb{H} = (\mathbb{C}^2)^{\otimes 2M}$. Now we use the definitions from section 1.5, illustrated in fig. 1.8 and apply our model to it: We assign one bit x_e^1 to every edge, so $K = 1$ and $g = 4$. The language we want to realize is $L_{\mathcal{L}}[f_{Loop}]$ which contains all bit patterns, so that the edges assigned to the bits form the desired closed loop configurations. This implies, that the local check function realizes Gauss's law, so for each lattice site, an even number of adjacent edges (their atoms/bits) must be excited (see fig. 1.2 and section 1.2). In other words, the bit projector $\mathfrak{u}_s$ selects the four bits adjacent to the site s,

$$\mathfrak{u}_s \left(\begin{array}{c} \\ x^1_{e_2} \quad x^1_{e_1} \\ \cdots \quad s \quad \cdots \\ x^1_{e_3} \quad x^1_{e_4} \\ \\ \end{array} \right) = (x^1_{e_1}, x^1_{e_2}, x^1_{e_3}, x^1_{e_4}) \, ^2 \tag{2.10}$$

and the local check function is given by

$$f_{Loop}(x_1, x_2, x_3, x_4) = (x_1 \odot x_2) \odot (x_3 \odot x_4) \tag{2.11}$$

with the XNOR-gate $\odot$ defined in eq. (2.4d), that is, $A \odot B = 1$ iff $A = B$. One can thus use the XNOR complex from fig. 2.1, to build this complex, by amalgamating three of them in the following way:

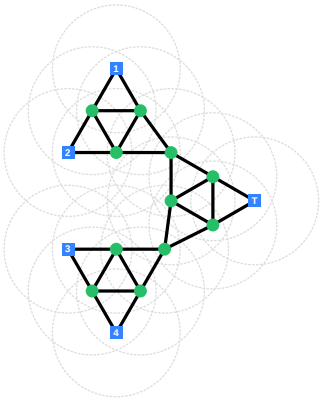

(2.12)

This complex uses $N = 16$ atoms to realize the vertex complex $\mathcal{C}_{\texttt{SCU}} \equiv \mathcal{C}_{f_{Loop}=1}$. The complex indeed realizes $f_{Loop}(x_1, x_2, x_3, x_4) = (x_1 \odot x_2) \odot (x_3 \odot x_4) = 1$. We can realize a smaller complex though. Because in ground states $f_{Loop}(x_1, x_2, x_3, x_4) = 1$, the check port T is always exited, so we use the modification introduced in step 4 in section 1.5.5, and remove it and all ancillas in blockade with it. The resulting complex has $N = 13$ atoms, and is depicted in fig. 2.6. Notice how this complex then realizes the surface code on the honeycomb lattice , as depicted in fig. 2.6 as well. This complex consists of two XOR gates amalgamated at their outputs. Because

$$f_{Loop} = 1 \quad \Leftrightarrow \quad x_1 \odot x_2 = x_3 \odot x_4\,, \tag{2.13}$$

we know from section 1.5.5, that the surface code complex $\mathcal{C}_{\texttt{SCU}}$ can be realized by two complexes, amalgamated at their ports. Further, For the square lattice, the LNK connecting both XNOR gates can be removed (i.e. its edge gets contracted), and the (not unique) minimal surface code vertex complex $\mathcal{C}_{\texttt{SCU}}$ is two XNOR gates amalgamated at their outputs. It consists of $N = 11$ atoms, and is depicted in fig. 2.4a. In fig. 2.4b the truth table of the vertex check function is depicted, and in fig. 2.4c the ground state configurations realizing this table are depicted. In fig. 2.4d, a sample of the square lattice formed by the ports of the tessellated $\mathcal{C}_{\texttt{SCU}}$ complexes is depicted. A sample of a string net on this lattice sample is depicted in fig. 2.5. The lattice has no PBC. So adding quantum fluctuations like in eq. (1.10) would lead to a single ground state $|G\rangle$ form eq. (2.7). For the toric code, ports (which have detuning 1) on the opposing boundaries must be identified, so they get detuning 2 as well. The depicted lattice on the torus would thus have uniform detunings. Note, that $\mathcal{C}_{\texttt{SCU}}$ is not unique. A different realization of it is $\mathcal{C}_{\texttt{SCUALT}}$ depicted in fig. 2.7, together with the ground state configurations and the lattice it creates. In this complex, one port has degree one, so the remaining $N = 10$ atoms realize $\bar{L}_S CU$ (see section 3.3).

The construction of removing a LNK is more general and is also used for the Fibonacci unit cell complex $\mathcal{C}_{\texttt{FMU}}$: The hexagonal unit cell complexes also form a square lattice, as tessellated unit cells form the lattice by definition. So they are also realisations of the square lattice check function. However the opposite is not true, as the minimal surface code vertex complex $\mathcal{C}_{\texttt{SCU}}$ depicted in fig. 2.4a can not realize the model on a honeycomb lattice, as the center atom, at which the two XNOR gates are amalgamated, can not act as a port for the additional lattice edge needed, if fact it is (by construction) inverted to such a atom.

In fig. 2.6 the unit cell complex for the hexagonal lattice $\mathcal{C}_{\texttt{SCUHX}}$ is depicted, together with a sample of the resulting lattice. Note, that it is geometrically a amalgamation of two XOR gates at their outputs, however this atom stays a port and does not get demoted to ancilla as it would be by a formal amalgamation. It is also minimal, as the vertex complexes building it are (they are XOR gates), and two ancillas can not be used by both vertices together as this would exclude needed states from the ground state manifold (see fig. 2.6c for the configurations).

The constructed complexes are then being tessellated, to realize the tessellated language. This is done by using step 5 of section 1.5.5, so the tessellated complexes are amalgamated at their ports (except the center one in the honeycomb case), as depicted in fig. 2.4d, fig. 2.6d and

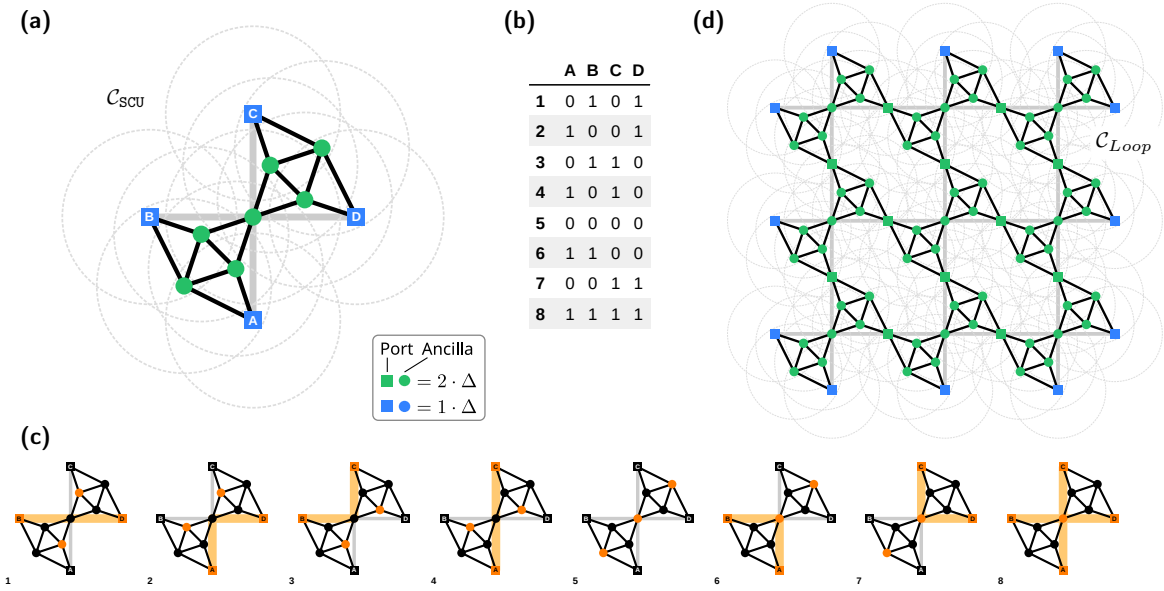

Figure 2.4: *Surface code on a square lattice.*[2] (a) A vertex complex $\mathcal{C}_{\texttt{SCU}}$ of the surface code for the square lattice. In this case, the vertex complex is also identical to the unit cell. The complex is originally a amalgamation of two `XOR` gates at their outputs (see fig. 2.6). The `XOR` is just a inverted `XNOR`, thus the output of a `XOR` is just in blockade with one ancilla, see fig. 2.1. So we can deform the vertex complex into the depicted amalgamation of two `XNOR` gates (see section 1.5.5). (b,c) Truth table and ground state manifold of the complex (the data is explained in fig. 2.1). The ground state manifold realizes all configurations in which an even number of ports is excited. This realizes Gauss's law of the $\mathbb{Z}_2$-gauge theory on the lattice site. It provides a local isomorphism between $\mathbb{H}_T = \mathbb{H}_{Loop}$ and $\mathbb{H}_0[\mathcal{C}_{Loop}]$, where local unitaries are mapped onto each other. (d) Periodic tessellation $\mathcal{C}_{Loop}$ of the vertex complex $\mathcal{C}_{\texttt{SCU}}$. The copies are amalgamated at the ports (which makes the detunings uniform in the bulk).

fig. 2.7d.
Finally note, that the process of finding these minimal complexes is reversed to the way presented. One starts by examining the states to satisfy the check function on a vertex of the honeycomb lattice. The `XOR` gate does it. Then one amalgamates, and simplifies it, to get the desired unit cell complexes (with or without a 'checking' port that is always on in the ground states).

2.4.2 Constructing the Fibonacci Model

In this section we realize lattices for potential Fibonacci string nets, that might host non abelian anyons. These anyons again derive their properties from the ground state manifold, the spin liquid, they live on (and vice versa). Because these model and its ground state(s) can be realizes as string nets (see section 1.3), we modify the complexes from the previous section to allow for string nets that allow for the fusion rules (thus the fusion of loops) as described in section 1.3 and by Levin.[7] The ground state in this model is no longer a equal weight superposition of all allowed loop configurations, instead it is a weighted one. The ground state thus is

$$|G\rangle = \sum_{\mathbf{S}} \Phi(\mathbf{S}) \; |\mathbf{S}\rangle \; , \tag{2.14}$$

where the sum goes over all string nets (all loop configurations) $\mathbf{S}$ of flipped spins $|1\rangle$ (excited Rydberg atoms) on the edges of the lattice, where no strings end at a vertex of the lattice. This means, that the string net also consists of loops, however two strings can fuse at vertices, so loops can have connecting lines between them (so T shaped line are allowed), see section 1.3 and fig. 2.9. The coefficients are products and square roots of $1 \pm \sqrt(5)/2$.[7] This string net model

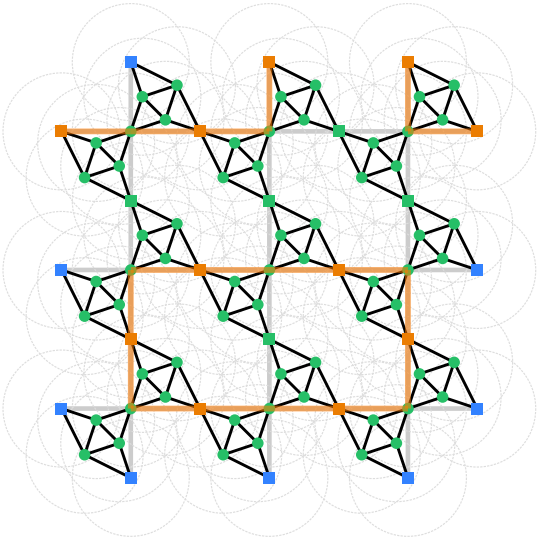

Figure 2.5: *A string net on the tessellated lattice of $\mathcal{C}_{\mathtt{SCU}}$ complexes.* Excited ports and their edges are marked orange, the other atoms have the color indicating their detuning (like in fig. 2.4). Excited ancillas are not marked. Notice, how Gauss law is satisfied at each vertex. All such string nets span $\mathcal{H}_{Loop}$. The depicted boundaries are not periodic. For a torus or PBC, the opposing blue atoms are identified, so their detuning would be 2 as well.

motivates the definition of the tessellated target Hilbert space

$$\mathbb{H}_0[\mathcal{C}_{\mathtt{FIB}}] \overset{\text{loc}}{\simeq} \mathbb{H}_T = \text{span}\,\{\,|\mathbf{S}\rangle \mid \text{String-net}\,\mathbf{S}\,\} \tag{2.15}$$

and the construction of a complex $\mathcal{C}_{\mathtt{FIB}}$ that realizes it.
The dimension of $\mathbb{H}_0[\mathcal{C}_{\mathtt{FIB}}]$ is $(1+\varphi^2)^M + (1+\varphi^{-2})^M$ where M is the number of unit cells of the honeycomb lattice and $\varphi = \frac{1+\sqrt{5}}{2}$ is the golden ratio.[9,10] Note, that this only holds for trivalent graphs, so one needs PBC in our case to satisfy this. Again, $\mathbb{H}_0[\mathcal{C}_{\mathtt{FIB}}]$ can not be decomposed into factors of Hilbert spaces. We assign one atom x^1_e to each edge. The bit projector of a trivalent honeycomb lattice vertex s now looks like

$$\mathfrak{u}_s \left(\right) = (x^1_{e_1}, x^1_{e_2}, x^1_{e_3})\,.^{2} \tag{2.16}$$

The check function, which realizes the desired string net and generates $\mathbb{H}_T$ is

$$f_{\mathtt{FIB}}(x_1, x_2, x_3) = (x_1 \oplus x_2 \equiv x_3) \vee (x_1 \wedge x_2 \wedge x_3). \tag{2.17}$$

So $f_{\mathtt{FIB}}(x_1, x_2, x_3) = 1$ for the bit configurations in $L_{\mathtt{FIB}} = \{000, 110, 101, 011, 111\}$, thus again an even number of bits of the edges can be excited, which is encoded by the first term in eq. (2.17). But in addition, two excited edges can fuse at the vertex (so all three bits are excited), which is due to the second term in eq. (2.17), so this term contributes the fusion. Without it, we would fall back to the abelian surface code from the previous section. Because $|L_{\mathtt{FIB}}| = 5$, the vertex complex can, unlike the surface code, not be realized by a single logic primitive. And because it has a odd number of ports, it is not a amalgamation of two gates. So constructing a circuit built from primitives that realize it, would require $\gtrsim 15$ atoms for a single vertex. Again a smaller complex $\mathcal{C}_{f_{\mathtt{FIB}}=1}$ can be realized, by building it from scratch. The minimal vertex complex $\mathcal{C}_{f_{\mathtt{FIB}}=1}$ has $N = 8$ atoms and is depicted in fig. 2.8 (for the proof of its minimal size see section 3.4). One can amalgamate two of these complexes at their outputs (but do not demote the resulting 'sharing' atom to a ancilla). This gives the Fibonacci model unit cell complex $C_{\mathtt{FMU}}$ for the honeycomb lattice. It contains $N = 15$ atoms and is minimal, as the vertex complexes $\mathcal{C}_{f_{\mathtt{FIB}}=1}$ building it are (and two ancillas again can not be used by both vertices together). As in the previous section,

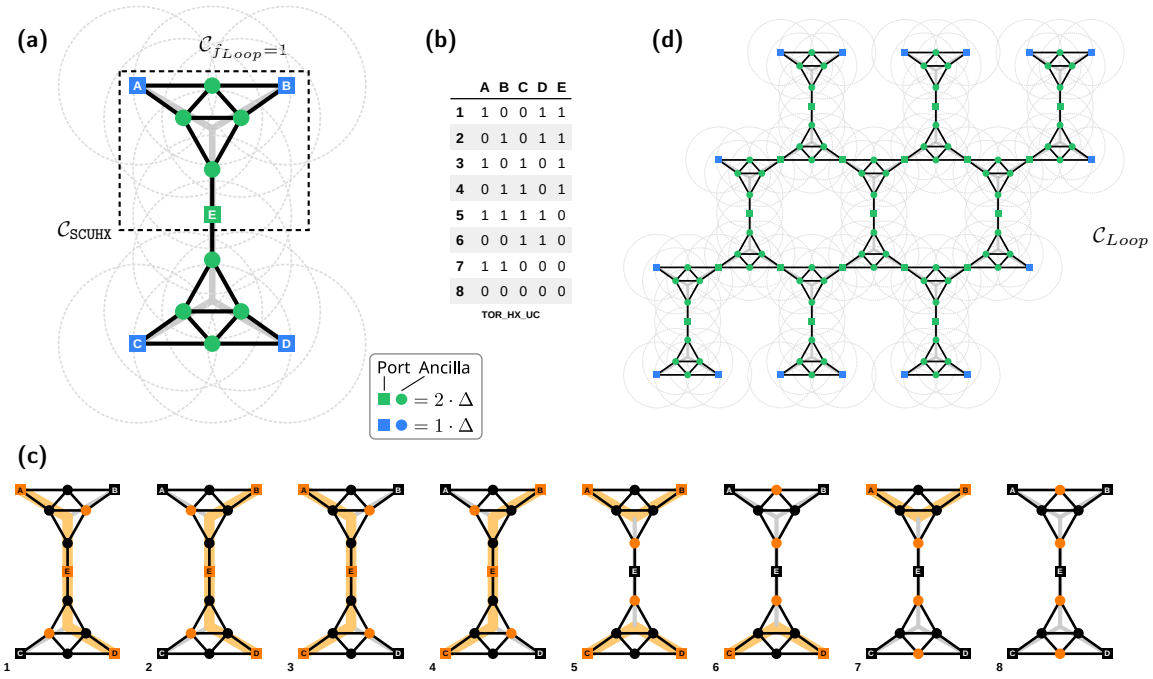

Figure 2.6: *Surface code on a honeycomb lattice.* (a) A unit cell complex $\mathcal{C}_{\texttt{SCUHX}}$ of the surface code for the honeycomb lattice, amalgamated from two $\mathcal{C}_{f_{Loop}=1}$ complexes, which are `XOR` gates (see fig. 2.1). (b,c) Truth table and ground state manifold of the complex (the data is explained in fig. 2.1). The ground state configurations realizes Gauss's law of the $\mathbb{Z}_2$-gauge theory on each vertex. This again provides a local isomorphism between $\mathbb{H}_T = \mathbb{H}_{Loop}$ and $\mathbb{H}_0[\mathcal{C}_{Loop}]$, where local unitaries are mapped onto each other. (d) Periodic tessellation $\mathcal{C}_{Loop}$ of the vertex complex $\mathcal{C}_{\texttt{SCU}}$. The copies are amalgamated at the four ports on the boundary of the complex.

tessellation of the unit cell complex leads to the Fibonacci model complex $\mathcal{C}_{\texttt{FIB}}$. A potential string net on this lattice sample is depicted in fig. 2.9.

The complex $\mathcal{C}_{f_{\texttt{FIB}}=1}$ is not unique, another realization of the check function can be achieved by modifying the `XOR` complex. The resulting complex is depicted in fig. 2.10. This alternative complex forms a alternative Fibonacci unit cell complex $\mathcal{C}_{\texttt{FMUALT}}$, also depicted in fig. 2.10. This complex again contains a `LNK` connecting both vertices, so it can be reduced to a square lattice vertex complex $\mathcal{C}_{\texttt{FMUSQ}}$ with $N = 13$ atoms (it is the amalgamation of two such modified `XNOR` gates). Note however, that $\mathcal{C}_{\texttt{FMUSQ}}$ is not minimal, there is a realization with $N = 12$ atoms, (see section 6.3). This minimal complex however is not valid (see chapter 4).

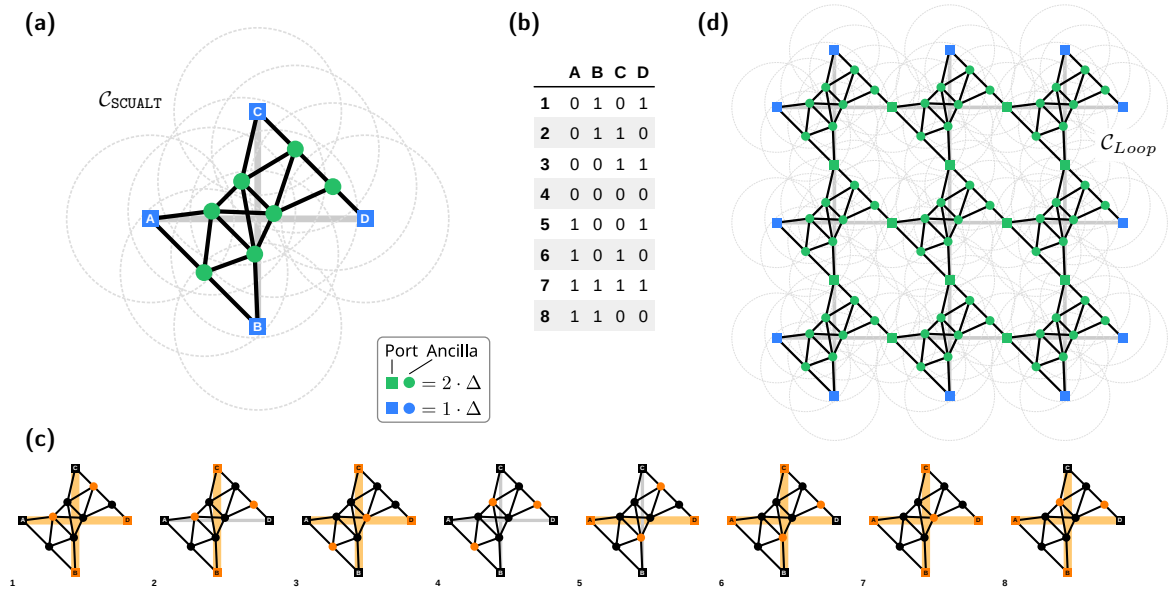

Figure 2.7: *An alternative realisation of the surface code on the square lattice.* (a) A vertex complex $\mathcal{C}_{\texttt{SCUALT}}$ of the surface code for the square lattice (in this case, the vertex complex is also identical to the unit cell). $\mathcal{C}_{\texttt{SCUALT}}$ is also minimal with $N = 11$ atoms but it is not a amalgamation of two primitive gates. But one port has degree one, so the remaining $N = 10$ atoms realize $\bar{L}_{\texttt{SCU}}$ (see section 3.3). (b,c) Truth table and ground state manifold of the complex (the data is explained in fig. 2.1). The ground state manifold realizes all configurations in which an even number of ports is excited. (d) Periodic tessellation $\mathcal{C}_{Loop}$ of the vertex complex $\mathcal{C}_{\texttt{SCUALT}}$. The copies are amalgamated at the ports (which makes the detunings uniform in the bulk).

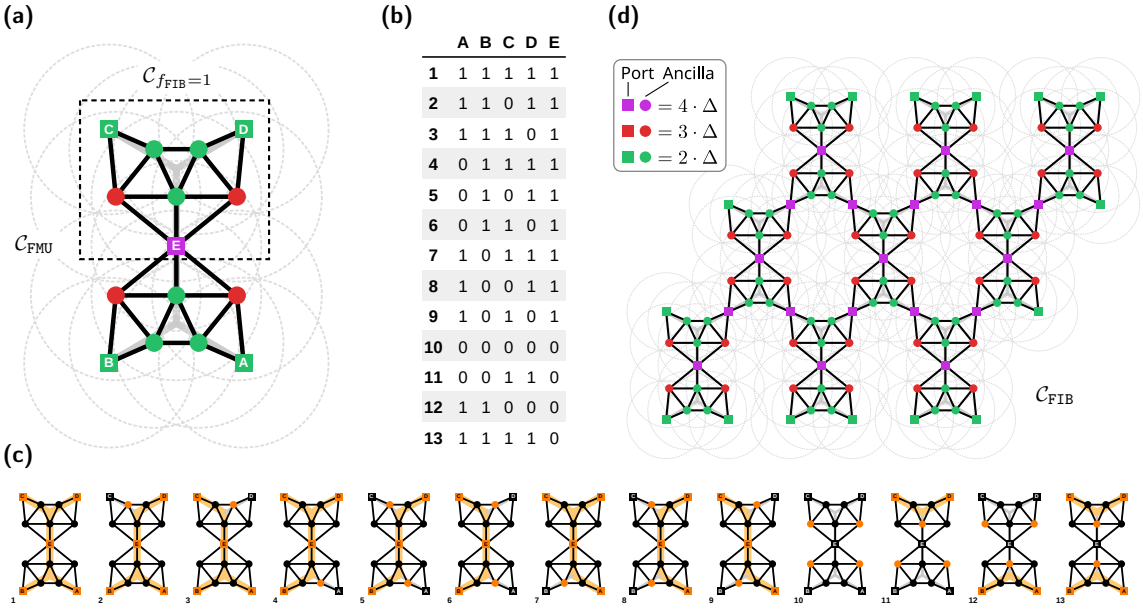

	A	B	C	D	E
1	1	1	1	1	1
2	1	1	0	1	1
3	1	1	1	0	1
4	0	1	1	1	1
5	0	1	0	1	1
6	0	1	1	0	1
7	1	0	1	1	1
8	1	0	0	1	1
9	1	0	1	0	1
10	0	0	0	0	0
11	0	0	1	1	0
12	1	1	0	0	0
13	1	1	1	1	0

Figure 2.8: *Fibonacci model.*[2] (a) The unit cell complex $\mathcal{C}_{\mathtt{FMU}}$ for the Fibonacci model. The complex is the amalgamation of two 8-atom complexes $\mathcal{C}_{f_{\mathtt{FIB}}=1}$ on the trivalent sites that form the basis of the honeycomb unit cell. The $\mathcal{C}_{f_{\mathtt{FIB}}=1}$ complex realizes the single-site check function constraint $f_{\mathtt{FIB}} = 1$ defined in eq. (2.17). Black edges denote blockades between atoms, gray edges illustrate the underlying Honeycomb lattice. (b,c) Truth table and ground state manifold of the complex (the data is explained in fig. 2.1). The ground state manifold realizes all configurations except ones where only one port is excited. This ensures, that no loop ends at the vertex. So in addition to closed loops, one can get three fusing strings at a site. This provides a local isomorphism between $\mathbb{H}_T$ and $\mathbb{H}_0[\mathcal{C}_{\mathtt{FIB}}]$. (d) Periodic tessellation $\mathcal{C}_{\mathtt{FIB}}$ of the complex $\mathcal{C}_{\mathtt{FMU}}$. The copies are amalgamated at the ports on the edges of the complex.

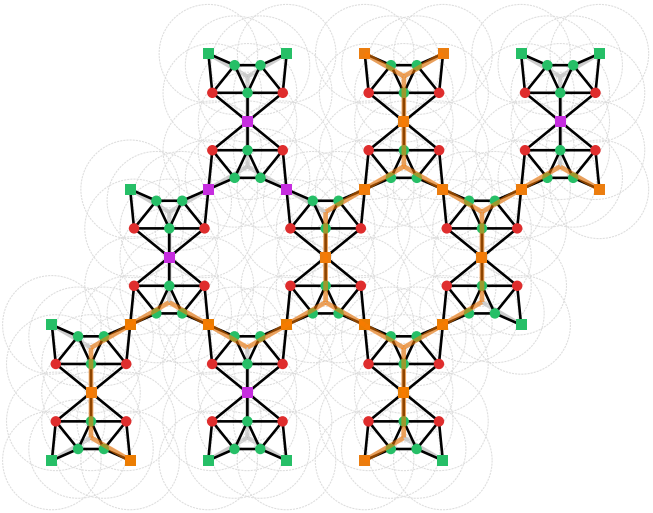

Figure 2.9: *A string net on the tessellated lattice of $\mathcal{C}_{\mathtt{FMU}}$ complexes.* Excited ports and their edges are marked orange, the other atoms have the color indicating their detuning (like in fig. 2.8). Excited ancillas are not marked. All such string nets span $\mathbb{H}_0[\mathcal{C}_{\mathtt{FIB}}]$.

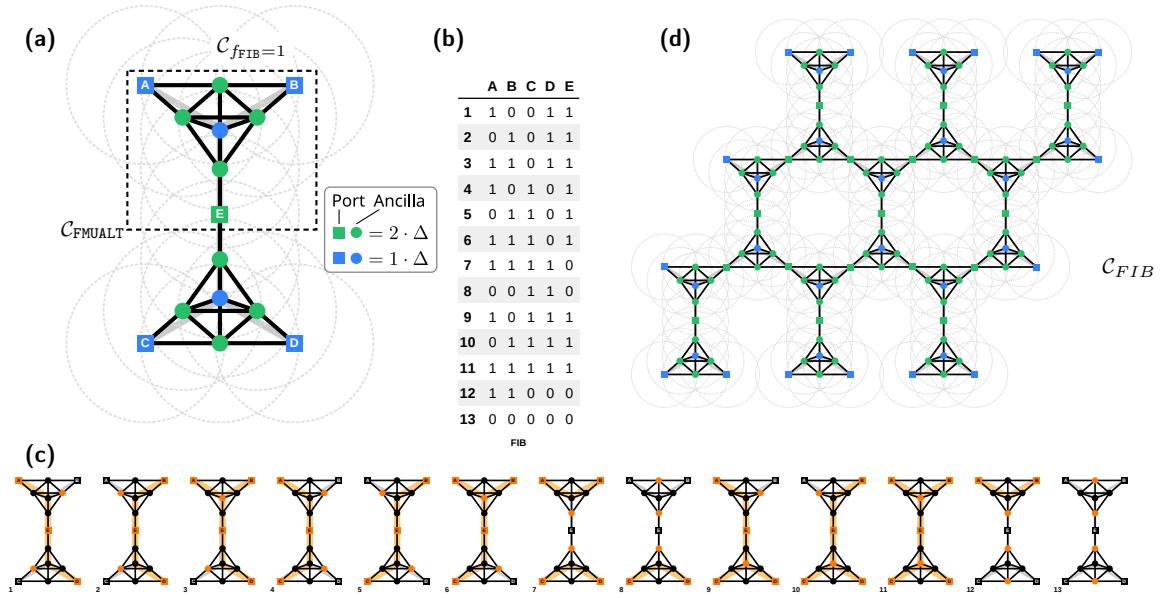

Figure 2.10: *Fibonacci model with an alternative unit cell complex.* (a) The alternative unit cell complex $\mathcal{C}_{\texttt{FMUALT}}$ for the Fibonacci model. The complex is the amalgamation of two 8-atom complexes $\mathcal{C}_{f_{\texttt{FIB}}=1}$ on the trivalent sites that form the basis of the honeycomb unit cell. They are modified `XOR` gates. (b,c) Truth table and ground state manifold of the complex (the data is explained in fig. 2.1). The ground state manifold realizes all configurations except ones where strings end at a vertex. (d) Periodic tessellation $\mathcal{C}_{\texttt{FIB}}$ of the complex $\mathcal{C}_{\texttt{FMUALT}}$. The copies are amalgamated at the ports on the edges of the complex.

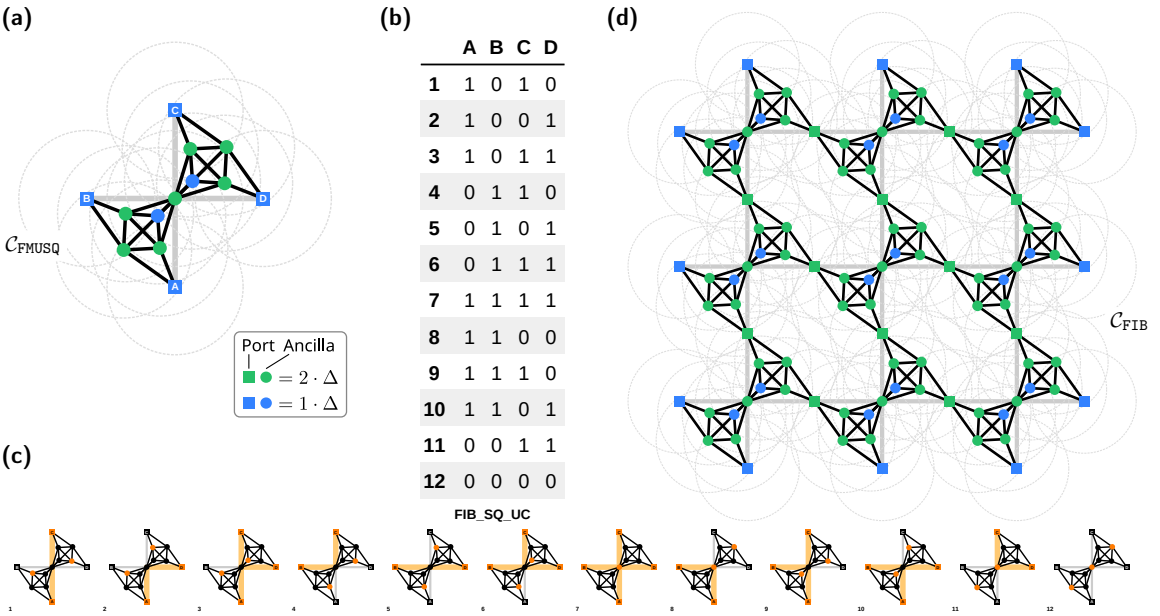

Figure 2.11: *Fibonacci model on the square lattice.* (a) The vertex complex $\mathcal{C}_{\texttt{FMUSQ}}$ for the Fibonacci model on a square lattice. The complex is obtained by contracting the `LNK` connecting the vertices in the $\mathcal{C}_{\texttt{FMUALT}}$ complex from fig. 2.10. It has $N = 13$ atoms. (b,c) Truth table and ground state manifold of the complex (the data is explained in fig. 2.1). The ground state manifold realizes all configurations except ones where only one port is excited. (d) Periodic tessellation $\mathcal{C}_{\texttt{FIB}}$ of the complex $\mathcal{C}_{\texttt{FMUSQ}}$. The copies are amalgamated at the ports on the edges of the complex.

Chapter 3

Proofs of Minimality

In this chapter we present the proof of the minimal sizes of the presented complexes.
Note 1: in this chapter we call the ground state manifold GSM.
Note 2: We say, a port has degree d, if it is connected to d other atoms, i.e. its assigned vertex in the blockade graph has degree d.

3.1 The Logic Primitives

In this section, we proof that the logic primitives can not be realized with smaller complexes that the ones given in fig. 2.1. This is trivial for the NOT, and the LNK, as they enforce the basic properties of the Rydberg blockade.

3.1.1 The CPY Complex

Lemma 1. *A CPY-complex cannot be realized with less than 4 atoms (1 ancilla).*

Proof. The copy language $L_{\texttt{CPY}} = \{000, 111\}$ is irreducible, so the realizing complex must be connected. Because $(111) \in L_{\text{GSM}}$, the ports can not be in blockade with each other. Then the only admissible blockade graph with $N = 3$ vertices is $B = (V = \{1, 2, 3\}, E = \emptyset)$, which can only realize a reducible language. □

3.1.2 The NOR Complex

Lemma 2. *A NOR-complex cannot be realized with less than 5 atoms (2 ancillas).*

Proof. There are two ways to prove this. One, that uses only maximal independent sets on graphs can be found below. This one is more basic as it uses energetic constraints for the ground states.[2]

- At first, we check if $N = 3$ atoms work for the NOR gate. The low energy Hamiltonian then is

$$H = -\Delta_1 n_1 - \Delta_2 n_2 - \Delta_3 n_3 =: E_{n_1 n_2 n_3} \,. \tag{3.1}$$

  For the GSM of the NOR complex to be degenerate, the following equations must be satisfied:

$$E_{001} = -\Delta_3 \tag{3.2a}$$
$$E_{010} = -\Delta_2 \tag{3.2b}$$
$$E_{100} = -\Delta_1 \tag{3.2c}$$
$$E_{110} = -\Delta_1 - \Delta_2 \,. \tag{3.2d}$$

  It follows immediately $\Delta_1 = \Delta_2 = \Delta_3$ and $\Delta_1 = 0$ so that all detunings must vanish. But then the ground state energy E_{GSM} vanishes as well, which implies that the state $(n_1 n_2 n_3) = (000)$ is degenerate with those four states in the GSM (which it must not be).

- we check $N = 4$ atoms. So the low energy Hamiltonian looks like this:

$$H = -\Delta_1 n_1 - \Delta_2 n_2 - \Delta_3 n_3 - \Delta_4 \tilde{n}_4 \,, \tag{3.3}$$

Let $\epsilon(n_1 n_2 n_3)$ be the energy contribution of the system coming from the ancillas alone, when the ports are in the state $(n_1 n_2 n_3)$, and under the constraint of the Rydberg blockade. We can thus define $E_{n_1 n_2 n_3} := -\Delta_1 n_1 - \Delta_2 n_2 - \Delta_3 n_3 + \epsilon(n_1 n_2 n_3)$. We have only one ancilla $\tilde{n}_4$, so either $\epsilon(n_1 n_2 n_3) = 0$ if $\tilde{n}_4 = 0$, or $\epsilon(n_1 n_2 n_3) = -\Delta_4$ if $\tilde{n}_4 = 1$. So the degeneracy of the GSM of the NOR complex demands the following four energies to be equal:

$$E_{001} = -\Delta_3 + \epsilon(001) \tag{3.4a}$$
$$E_{010} = -\Delta_2 + \epsilon(010) \tag{3.4b}$$
$$E_{100} = -\Delta_1 + \epsilon(100) \tag{3.4c}$$
$$E_{110} = -\Delta_1 - \Delta_2 + \epsilon(110) \,, \tag{3.4d}$$

which immediately implies

$$\Delta_1 = \epsilon(110) - \epsilon(010) \tag{3.5a}$$
$$\Delta_2 = \epsilon(110) - \epsilon(100) \tag{3.5b}$$
$$\Delta_3 = \epsilon(110) + \epsilon(001) - \epsilon(100) - \epsilon(010) \,. \tag{3.5c}$$

Because we require a energy gap from the ground states and the excited ones, we can derive that

$$\epsilon(000) = E_{000} \overset{!}{>} E_{100} = -\Delta_1 + \epsilon(100) = \epsilon(010) - \epsilon(110) + \epsilon(100) \tag{3.6a}$$
$$\Leftrightarrow \quad \epsilon(000) + \epsilon(110) > \epsilon(010) + \epsilon(100) \,. \tag{3.6b}$$

This is because (000) is a gapped excited state. The only kinematic constraints on the ancillas in eq. (3.6b) can come from the two inputs, since $n_3 = 0$. We show, that eq. (3.6b) can not be satisfied with just one ancilla.

The energy can be lowered when the ancilla is excited, however there may be blockades that prohibit that. Three cases can happen:

1. There are no blockades between ports and ancilla. But then the ancilla is excited in all four terms of eq. (3.6b), so that eq. (3.6b) becomes $-\Delta_4 - \Delta_4 > -\Delta_4 - \Delta_4$, which violates the gap condition.
2. The ancilla is in blockade with one input, lets say n_1. This again violates the gap condition as eq. (3.6b) becomes $-\Delta_4 + 0 > -\Delta_4 + 0$.
3. The ancilla is in blockade with both ports. Then eq. (3.6b) reads $-\Delta_4 + 0 > 0 + 0$, so $\Delta_4 < 0$, which is a contradicts the non negativity of the detunings.

So the NOR-complex requires at least 5 atoms. □

There is however a shorter proof for the minimal size of the NOR complex. The short proof uses kinematic constraints and MIS^* instead of energetic constraints. Methods from this proof are used to prove the minimal size of the remaining gates quite effectively.

Proof. It can be realized with $N = 5$ atoms. So we need to exclude $N = 3$ and $N = 4$ atoms:

1. $N = 3$: The NOR-language $L_{\texttt{NOR}} = \{001, 010, 100, 110\}$ is irreducible and forbids a blockade between the two input ports (because of (110)). The only valid blockade graph B that realizes these constraints is the line graph on three atoms. But this graph has only *two* maximal independent sets, and we need at least four to realize $L_{\texttt{NOR}}$.

2. $N = 4$: Of the six connected graphs on four vertices, only the 'tetrahedron graph', which has four vertices, and all are connected with each other, has four maximal independent sets (the other graphs have at most three). These four sets however are necessary to realize the four words in $L_{\texttt{NOR}}$. But none of these four maximal independent sets contain more than one vertex, which would be necessary to realize (110) as ground state.

□

Finally note, that by evaluating all 11 connected graphs of degree 4, that have at least four MIS^*, we find only three, that can host a NOR complex. These three are depicted in fig. 2.2.

Figure 3.1: *MIS^* of the line graph.*[2] The line graph is the only connected blockade graph on five vertices with (at least) four maximal independent sets (orange vertices), (at least) one of which has (at least) three vertices. To realize the state $|111\rangle$, the vertices 1, 3 and 5 must be chosen as ports, with 3 as output; the four maximal independent sets then realize the truth table of `AND`.

3.1.3 The AND, OR, and XNOR Complexes

Lemma 3. *`AND`-, `OR`- and `XNOR`-complexes cannot be realized with less then 6 atoms (3 ancillas).*

Proof. All these complexes must realize the state $|111\rangle$ so there are no blockades between the ports. Thus they can not be realized with complexes that contain $N < 5$ atoms as the only connected graph that satisfies this conditions is the blockade graph of the `CPY`, which can realize only two MIS^*. One can go through all 21 connected graphs with four vertices and find 11 that realize at least four MIS^*. However only the line graph can realize a MIS^* that contains three atoms. The four MIS^* of this graph are depicted in fig. 3.1. One must choose the vertices 1, 2 and 3 as ports because the languages contain $|111\rangle$. The four MIS^* then realize the language $L = \{111, 100, 010, 000\}$. This is the `AND` language. So `OR` and `XNOR` can not be realized with $N = 5$ atoms. To exclude $L_{\texttt{AND}}$ for being realized, one must use energetic constraints. The ground state degeneracy of the `AND`-GSM requires

$$E_{111} = -\Delta_1 - \Delta_3 - \Delta_5 \tag{3.7a}$$
$$E_{100} = -\Delta_1 - \Delta_4 \tag{3.7b}$$
$$E_{001} = -\Delta_2 - \Delta_5 \tag{3.7c}$$
$$E_{000} = -\Delta_2 - \Delta_4\,, \tag{3.7d}$$

which immediately implies $\Delta_4 = \Delta_5$ and therefore $\Delta_3 = 0$, which is not allowed. Thus the `AND` complex can not be realized with $N = 5$ atoms. □

3.1.4 The NAND and XOR Complexes

Lemma 4. *`NAND`- and `XOR`-complexes cannot be realized with less than 7 atoms (4 ancillas).*

Proof. The truth tables of both gates contain the states (110), (101) and (011). This implies, that no ports can be in blockade with each other. One can conclude, that these gates can not be realized with four atoms (see section 3.1.3). Lets check $N = 5$ atoms. Let one port be exited, thus one ancilla is not. The remaining ports and the remaining ancilla must realize $L = \{01, 10\}$. But because the ports can not be in blockade with each other and L is irreducible, both ports must be connected to the ancilla. This structure then can only realize a `LNK` complex with language $L_{\texttt{LNK}} = \{00, 11\}$.

So lets check $N = 6$ atoms. Three cases need to be considered:

1. One port is in blockade with all three ancillas. Let it be excited. Then the other two ports are excited as well. But then at least two of the three states $|110\rangle$, $|101\rangle$ and $|011\rangle$ cannot be realized in the GSM.

2. There is at least one port which is only connected to a single ancilla. This can be interpreted as an amalgamated `NOT`-complex. If we delete the port, subtract its detuning from the connected ancilla, and declare the latter as a new port. The new complex has five atoms and must realize the language of the original one with one letter inverted. For both gates, the GSM of this new language contains the states $|010\rangle$, $|001\rangle$ and $|111\rangle$ (plus another one that depends on the gate). The only blockade graph on five vertices with at least four MIS^*, one of which contains at least three vertices (needed for $|111\rangle$), has been identified in section 3.1.3 as the line graph. It has also been shown in section 3.1.3 that there is no assignment of detunings so that this graph can realize a fourfold degenerate GSM.

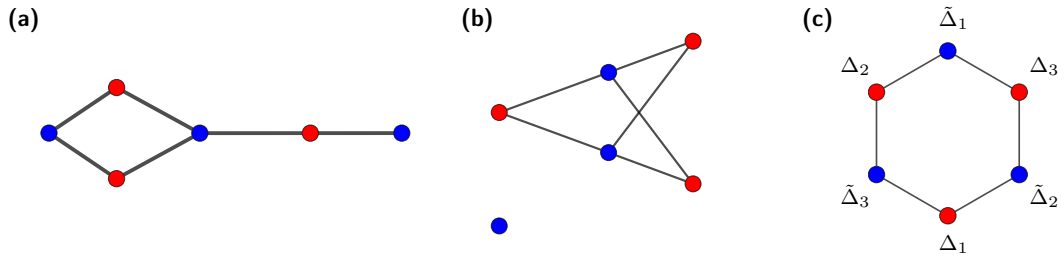

Figure 3.2: The three bipartite graphs between three ports (red) and three ancillas (blue) where all ports have degree two.[2] Note that these do not represent complete blockade graphs rather than classes of blockade graphs, as we omit blockades between ancillas. The detunings in (c) are used in section 3.1.3.

3. All ports are in blockade with exactly two ancillas. There are three possibilities to connect three ports with two ancillas each, depicted in fig. 3.2. For all of these three, one finds two ports, that when excited block all ancillas adjacent to the third port. So this third port gets excited as well. Thus at least one of the states $|110\rangle$, $|101\rangle$ or $|011\rangle$ can not be realized.

So `NAND` and `XOR` can not be realized with $N \leq 6$ atoms. *Note:* As this method used here is more effective than the energy calculations used in section 3.1.2, it gets generalized in the next section. □

3.2 A lower Bound for Complex Sizes

In this section we discuss the general analytical method to find a lower bound for the number of atoms N a complex $\mathcal{C}_L$ require to realize a irreducible language L as its GSM. The method is recursive. It relies on three mechanisms.

mechanism 1: Amputating vertices. If a port p is only connected to one ancilla a, we can delete p, and subtract its detuning from its ancilla and declare the ancilla a new port. We call this *amputation*. This is the reverse of an amalgamation. We need to make sure, that the subtraction of the detunings $\Delta_a - \Delta_p$ does not lead to a negative or zero detuning. If $\Delta_p > \Delta_a$, the port p would always be excited. This is because in states, where the ancilla would be excited, the system would reduce its energy if the port switches on instead. The port thus is superfluous and the language of the GSM is reducible. If $\Delta_p = \Delta_a$ then the for all states in the original complex where the ancilla is on, there exists a state with the same energy with the port switched on. So in the realizing language for every word x with $x_p = 0$, there exists a otherwise identical word x' only with $x'_p = 1$. This is the property 2 described in section 2.1.3. No language in this thesis has this property.

mechanism 2: Constructing subcomplexes. The following definition also justifies the final remark of section 1.5.5. Consider a complex $\mathcal{C}$ that realizes a language L and whose ports are not in blockade with each other. Select one port. We select a port p and define the sublanguage $L_P \subset L$ of words x with $x_p = 1$. let L'_p be the language which is obtained from L but the constant letter corresponding to p is deleted. We want to construct a $\mathcal{C}'_p$ complex realizing L'_p. The simplest solution is it ,to keep the geometry from $\mathcal{C}$ and increase the detuning of the port. Thereby one creates a gap between the states where p is excited and the rest of the spectrum. Because it no longer adds a degree of freedom to the GSM, p can be downgraded to an ancilla. In the GSM this new ancilla is always excited and all adjacent ancillas in blockade with it are not. This suggests, one can delete these atoms and obtain a smaller complex $\mathcal{C}'_p$ that realizes the language L'_p:

Lemma 5. *Let $\mathcal{C}$ be a finite complex, that realizes a irreducible language L, and whose ports are not in blockade with each other, $\Delta E > 0$ and $\delta E = 0$. Let p be a port with $\Delta_p > 0$ and let L_p and L'_p be defined as above. Then the structure $\mathcal{C}'_p$ one gets from $\mathcal{C}$ by deleting p and the ancilla it is in blockade with, is a L'_p complex if the ports of $\mathcal{C}'_p$ are inherited from $\mathcal{C}$.*

Proof. Because L is irreducible, $L_p \neq \emptyset$. So there are configurations, where the port p is active. Two things need to be shown: (a) The new structure $\mathcal{C}'_p$ together with its inherited ports is a complex i.e. its ground states can be labelled by configurations of those ports. (b) the language that describes the new GSM is L'_p.

Let the GSM of the new structure $\mathcal{C}'_p$ be degenerate ($\delta E = 0$) and gapped ($\Delta E > 0$). This can be achieved because we work in the PXP model and the structure is finite. Every kinematically allowed configuration in this GSM can be *extended* to a allowed configuration in the GSM of $\mathcal{C}$ because we can add the deleted atoms again and set the port to *excited* and the ancillas to *not excited*. Let $E_0(C'_p)$ denote the ground state energy of $\mathcal{C}'_p$ and $E_0(\mathcal{C})$ the one for $\mathcal{C}$. It follows that $E_0(\mathcal{C}) \leq E_0(\mathcal{C}'_p) - \Delta_p$. On the other hand, because $L_p \neq \emptyset$, there are states in the GSM of $\mathcal{C}$, where p is excited, and all its adjacent ancillas are not. *Truncating* the configuration of the port p and the ancillas, one gets an allowed configuration for $\mathcal{C}'_p$ with energy $E_0(\mathcal{C}) + \Delta_p$, implying $E_0(\mathcal{C}'_p) < E_0(\mathcal{C}) + \Delta_p$. Thus we have

$$E_0(\mathcal{C}'_p) = E_0(\mathcal{C}) + \Delta_p. \tag{3.8}$$

Using the process of extending and truncating can draw two conclusions:

1. Every configuration in the GSM of $\mathcal{C}'_p$ can be extended to a configuration in the GSM of $\mathcal{C}$ which corresponds to a word in L_p. Two things follow:
   - The configurations of L_p in the GSM of $\mathcal{C}$ can be distinguished by the ports without p. Because the structure $\mathcal{C}'_p$ inherits all other ports from $\mathcal{C}$ in the natural way, the configurations in the GSM of $\mathcal{C}'_p$ can also be distinguished by these ports. So $\mathcal{C}'_p$ is a complex realizing some language $L^?$.
   - Every word in $L^?$ can be extended to a word in L, so $\mathcal{L}^? \subseteq L'_p$.
2. Every configuration in the GSM of $\mathcal{C}$ corresponding to a word in $\mathcal{L}_p$ can be truncated to an allowed configuration of $\mathcal{C}'_p$ with energy ${}_0(\mathcal{C}'_p) = E_0(\mathcal{C}) + \Delta_p$, implying $L'_p \subseteq L^?$.

Thus $L^? = L'_p$ and therefore $\mathcal{C}'_p$ is a L'_p complex. □

This lemma thus allows us to fix a port p to be excited and ignore all ancillas in blockade with it, to examine the behaviour of the remaining atoms. They form a smaller complex (as the port and its adjacent ancillas are being ignored), which has to realize the sublanguage of words such that adding the letter x_p and set $x_p = 1$ gives the language L.

mechanism 3: Removing ancilla-ancilla blockades. lets look at a set of N Rydberg atoms, all of which have positive, nonzero detuning. We want to check, if it can be a complex $\mathcal{C}_L$ for some given language L. For them to realize a complex, one must label certain atoms as ports, realizing configurations that correspond the words in L. Let the n ports be $\{p_1, ...p_n\}$, and the $m = N - n$ ancillas $\{a_1, ...a_m\}$. We again do not allow for blockades between ports. Each port has a degree $\deg(p_i)$, which in this chapter is usually larger than one (because we can amputate ports).

We now look at a bipartite graph B. One partition are the n ports, the other are the m ancillas, and edges are between those two partitions. Also all vertices in the partition of the ports have degree $\deg(p_i)$, for $i \in \{1, ...n\}$, and the vertices of the ancilla-partition do have a degree smaller than n. We also want, that every ancilla is connected to a port so their degree is larger that one. There are, even for large complexes, rather few of such special bipartite graphs, if the number of ports is small. Examples of these graphs are depicted in figs. 3.3, 3.7 and 3.8. One can see that despite there are an enormous amount of graphs with 9 vertices, there are only 6 such graphs, when all four ports have degree two. Each such graph corresponds to an class of possible blockade graphs. The blockade graphs in this class derive from these bipartite graphs by adding some blockades between ancillas. One can now go through the MIS^* of this bipartite graph. Because all atoms have positive nonzero detuning, they are exited if they are not in blockade. The values of the detunings do not matter here. If the MIS^* does not contain all configurations of L, the class of blockade graphs can not realize a complex realizing L.

If one finds class that can realize all the configurations of L, one can investigate it further by adding ancilla-ancilla-blockades or define detunings to see if the class can indeed has a working

blockade graph to host complex $\mathcal{C}_L$. Here a numerical search, like with the program mentioned in section 2.1 can be useful. The remaining degrees of freedom are drastically reduced, compared to the ones from the general problem of finding blockade graphs.

This mechanism can also be used if there are blockades between ports, by adding the edge to the bipartite graphs.

3.2.1 The Method: Finding lower Bounds for Complexes

Here we discuss the method used in the remaining chapter and in section 6.3 to find lower bounds for the number N of atoms for a complex $\mathcal{C}$ to realize a certain language L. Note that it only works fully, if we can amputate ports (i.e. all languages in the process do not have the property 2 of section 2.1.3). The strength of it lies in the fact, that one can for the most part ignore detunings and blockades between ancillas, thus reducing the degrees of freedom for the problem. The problem of finding a lower boundary for N boils down to falsify all smaller graph classes. These are represented by graphs, where all blockades between ancillas are omitted (see above). The method is thus iterative in the number of atoms.

Step 1. At first one looks at the language L to be realized. Then one negates the first letter in the language to obtain a new language $\bar{L}$. One does this with all letters and all combinations of letters. In the worst case there are many possibilities but most useful languages (spin liquid primitives, logical gates,...) have symmetries or properties, that reduces this to only view different languages $\mathfrak{K} = \{L_1, ..L, ..\bar{L}, ...L_n\}$. If a complex realizes L and has a port p_i with degree one, one can amputate it and get a complex realizing L_i. Vice versa if a complex with $N-1$ atoms is a minimal realization of a $\mathcal{C}_{L_i}$ complex, the amalgamation of a `NOT` to the right port p_i leads to a not necessarily minimal $\mathcal{C}_L$ complex. If a $N-1$ atom complex of $\mathcal{C}_{L_i}$ however is dis-proven, we have found a minimal one. So the mentioned method must be conducted for all languages in $\mathfrak{K}$. There may be more languages than ports, but the languages are cyclic. One starts with N atoms, where we know, that there is no L complex with N atoms. A potential suitable lower bound is the number ports required minus one (we need at least all the ports). For this bound , we also know, that no other language in $\mathfrak{K}$ can be realized. Then one looks at $N+1$ atoms. We then assume one port p_i has degree one. Amputate in. We now must realize the language L_i with N atoms if this is possible with a complex C_{L_i} we amalgamate a `NOT` to its p_i port and we have found a L complex. If this is not the case, we know, there is no L complex where port p_i has degree one. One must do this for all combination of nontrivial amputations (A trivial combination of amputations would be one after which the language does not change). If we can successfully falsify a all combinations of nontrivial amputations, we can conclude that L can only be realized with a complex of $N+1$ atoms, if all ports have at least degree two.

Step 2. One then uses mechanism 2 on some port p_i to examine a upper bound z for the maximal degree of the ports. At some degree, enough ancillas are in blockade with p_i, that the subcomplex $\mathcal{C}'_p$ can not realize a necessary sublanguage L'_p. So all ports must have a degree between one and z.

Step 3. One then proceeds with mechanism three to falsify all remaining possible graph classes. This is the main step to exclude graph-classes from hosting a $\mathcal{C}_L$ complex. If all classes can be falsified, L can not be realized with $N+1$ atoms, and we set the new lower bound to $N+1$. If they can not be falsified, our lower bound remains N.

Note 1: There might be additional constraints to the complex, giving further methods to falsify classes (see section 3.5).
Note 2: One might skip step 1 if the two mechanisms used in step 2 immediately can falsify all classes with N atoms.
Note 3: As mentioned, on can improve the found lower boundary (also numerically), by extending mechanism 3. In all our examples however even if one uses only kinematic constraints to observe MIS^*, one gets a lower bound that is only one or two atoms off. Usually the method can find a working complex whose size is of order $N = 2|P|$, where $P = |\{p_1, ...p_n\}|$. This is because with this many atoms, the blockades between ancillas and ports have enough degrees of freedom, to

allow for the desired configurations of L to happen, so detunings and ancilla-ancilla blockades must be added only to energetically gap these out. In the worst case, additional ancillas must be added to do so, but in the applied cases one is sufficient.
Note 4: This method can be used to show uniqueness of complexes (up to choices in detunings) as well, as shown in sections 3.5.2 and 6.2.

3.3 The surface code $\mathcal{C}_{\texttt{SCU}}$

Lemma 6. *The vertex complex (unit cell complex) $\mathcal{C}_{\texttt{SCU}}$ of the surface code on the square lattice cannot be realized with less than 11 atoms.*

Proof. We now apply the method described in section 3.2 to show, that the surface code complex $\mathcal{C}_{\texttt{SCU}}$ requires at least $N = 11$ atoms.

At first we notice that the desired GSM of the surface code on a square lattice is symmetric under the permutation of states. It also includes $|1111\rangle$, so there can not be blockades between the ports. Further, the GSM is symmetric under the process of amputating a even number of ports, i.e. inverting a even number of letters in the words of $L_{\texttt{SCU}}$:

$$L_{\texttt{SCU}} \equiv \left\{\begin{matrix}1111\\1100\\0011\\1001\\0110\\0101\\1010\\0000\end{matrix}\right\} \xrightarrow{\text{inv. 4. letter}} \overline{L}_{\texttt{SCU}} \equiv \left\{\begin{matrix}1110\\1101\\0010\\1000\\0111\\0100\\1011\\0001\end{matrix}\right\} \tag{3.9}$$

$$\xrightarrow{\text{inv. 3. letter}} L_{\texttt{SCU}} = \left\{\begin{matrix}1100\\1111\\0000\\1010\\0101\\0110\\1001\\0011\end{matrix}\right\} \xrightarrow{\text{inv. 2. letter}} \overline{L}_{\texttt{SCU}} = \left\{\begin{matrix}1000\\1011\\0100\\1110\\0001\\0010\\1101\\0111\end{matrix}\right\} \cdots \tag{3.10}$$

The conclusion is, that the minimal toric code complex can have at most one port of degree one. Otherwise one could amputate two ports, and either end up at a smaller $\mathcal{C}_{\texttt{SCU}}$ complex, or end up with a complex realizing $\overline{L}_{\texttt{SCU}}$, which can be made to a `SCU` complex by amalgamating a `NOT` to one of its ports (thus adding one atom). Then one gets a smaller $L_{\texttt{SCU}}$ complex. So the original one was not minimal. Note, that fixing a letter x_p in $L_{\texttt{SCU}}$ ($\overline{L}_{\texttt{SCU}}$) to 1, $L_{\texttt{SCU}_p}$ ($\overline{L}_{\texttt{SCU}_p}$) is the `XNOR` (`XOR`) language. Here L_p is the language of words in L where x_p is one, but where x_p is deleted (see section 3.2). We start the iterative method with $N < 8$.

- $N < 8$: We apply method 2: If we fix a port excited it blocks at least one ancilla. The remaining $N' < 6$ atoms must realize a `XNOR` subcomplex, which requires at least $N = 6$ atoms. So the surface code can not be realized with $N < 8$ atoms.
- $N = 8$: Because only one port can have degree one, we choose a port that connects to at least two ancillas and fix it the excited state, rendering the ancilla not excited. The remaining $N = 5$ atoms again must realize a `XNOR` subcomplex which is impossible.
- $N = 9$: Three cases need to be considered:
  1. Assume one port that connects to a single ancilla. We amputate it, and the remaining $N = 8$ atoms must realize a $\overline{L}_{\texttt{SCU}}$ subcomplex, where all ports have degree ≥ 2. Fixing one of its ports p (which have degree 2) to the excited state blocking at least two

ancillas, the remaining $N \leq 6$ atoms must realize a `XOR` language (inspect $\overline{L}_{\texttt{SCU}}$ states with fixed letter $x_p = 1$ to verify this). This is impossible as a `XOR` complex requires at least $N = 7$ atoms as we've shown in section 3.1.

2. Assume a port being in blockade with three ancillas. We fix it to the excited state, blocking those three ancillas. Again the remaining $N = 5$ atoms must realize a `XNOR` logic which is impossible.
3. The case where all ports are in blockade with two ancillas remains. So we apply mechanism 3 (see section 3.2). There are six non-isomorphic bipartite graphs that connect sets of four (ports) and five vertices (ancillas), where all ports have degree 2, see fig. 3.3. We exclude graphs with disconnected ancillas because these are typically covered by the analogous step for $N = 8$. All these graphs except fig. 3.3c can be excluded from realizing a minimal `SCU` complex. This is because one can find two ports (like 1, 2 and in fig. 3.3a) which block all ancillas adjacent to a third port, so this one is excited as well (like 3 in fig. 3.3a), which must not happen in a $\mathcal{C}_{\texttt{SCU}}$ complex, as it is inconsistent with the `SCU` language. The 'cross graph' fig. 3.3c can not be excluded this way as its set of MIS^* is a superset of all MIS^* required in a $\mathcal{C}_{\texttt{SCU}}$ complex. We have to use energetic arguments instead. Because the GSM realizing L must be gapped out, we must require

$$E_{1111} = -\Delta_1 - \Delta_2 - \Delta_3 - \Delta_4 \overset{!}{<} -\Delta_1 - \Delta_2 - \Delta_3 - \Delta_8 = E_{1110} \quad \Rightarrow \quad \Delta_8 < \Delta_4\,, \tag{3.11a}$$

$$E_{1100} = -\Delta_1 - \Delta_2 - \Delta_7 - \Delta_8 \overset{!}{<} -\Delta_1 - \Delta_2 - \Delta_7 - \Delta_4 = E_{1101} \quad \Rightarrow \quad \Delta_8 > \Delta_4\,. \tag{3.11b}$$

Hence this graph cannot realize the $L_{\texttt{SCU}}$-manifold.

- $N = 10$:

1. One port is in blockade with only one ancilla. We amputate it and the remaining $N = 9$ atoms must realize a $\overline{L}_{\texttt{SCU}}$ subcomplex, where all ports have degree ≥ 2. Again we fix one of these ports in the excited state, rendering two ancillas not excited. So we can remove them and the remaining $N = 6$ atoms must realize a `XOR` language again, which however requires seven atoms.
2. Assume a port being in blockade with four ancillas. We fix it to the excited state, blocking those four ancillas. Again the remaining $N = 5$ atoms must realize a `XNOR` logic which is impossible.
3. Assume a port being in blockade with three ancillas. We fix it to the excited state, blocking those three ancillas. The remaining $N = 6$ atoms must realize a `XNOR` gate as a subcomplex. AS shown in section 6.2, there is only one blockade graph that can achieve this. So the setup for a $\mathcal{C}_{\texttt{SCU}}$ then must look like this:

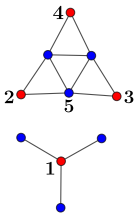

(3.12)

$L_{\texttt{SCU}}$ contains all states with a even number of ports excited. So there are two states in which ports 2 and 3 are excited (note that the ancillas adjacent to port 1 can be in blockade with ports 2 and 3, but as these ports are fixed excited, the ancillas are fixed in the not excited state and thus do not contribute anything in the following). In one of those two states, ports 1 and 4 are excited, in the other they are not. In the `XNOR` complex alone, if ports 2 and 3 are excited, port 4 is as well, because it is only in blockade with blocked out ancillas. So the second state, where port 4 is off, must be realized with the three ancillas adjacent to port 1. All ports have to be on the boundary of the complex, so the three ancillas attached to port 1 can not 'wrap' around ports 2 and 3 to reach port 4. Also port 1 can not be in blockade with ancilla

5, as it would increase its degree to four, which makes $\mathcal{C}_{\texttt{SCU}}$ impossible (see above). So the information about the state of port 1 must be passed to port 4 through the line on which ancilla 5 sits. This is a topological constraint, see section 3.5.1. It corresponds to the situation of eq. (3.19), where the two atoms marked with $\times$ are port 4 and some ancilla(s) adjacent to port 1. Note, that port 4 however is not in blockade with ancilla 5 (which is inside the green ellipse in eq. (3.19)), so one of the marked atoms in eq. (3.19) is shifted in a way that its blockade circle dos not include the entire ellipse. Then the two marked atoms (port 4 and some ancilla(s) adjacent to port 1) can not be in blockade.
These arguments imply, that port 4 can not be in blockade with any of the (non fixed) ancilla, it is thus always excited if ports 2 and 3 are, which is not consistent with $L_{\texttt{SCU}}$.

Alternatively, one could rule out all graph classes with one port of degree 3.

4. The case where all ports are in blockade with two ancillas remains. There are five non-isomorphic bipartite graphs that connect sets of four (ports) and five vertices (ancillas), where all ports have degree 2, see fig. 3.4. Again we exclude graphs with disconnected ancillas because these are covered in the case $N = 9$. One such graph however remains: fig. 3.4c, as its connected part was only excluded with energetic constraints. The classes fig. 3.4b, fig. 3.4d and fig. 3.4e can be excluded immediately because two ports can be found that block all ancillas from a third port. So if the two ports are excited, the third one is as well, which is not consistent with $L_{\texttt{SCU}}$.
The cases fig. 3.4a and fig. 3.4c remains. For the first class the following must hold:

$$E_{1111} = -\Delta_1 - \Delta_2 - \Delta_3 - \Delta_4 \overset{!}{<} -\Delta_1 - \Delta_2 - \Delta_3 - \Delta_8 = E_{1110} \quad \Rightarrow \quad \Delta_8 < \Delta_4\,, \tag{3.13a}$$

$$E_{0110} = -\Delta_2 - \Delta_3 - \Delta_5 - \Delta_8 \overset{!}{<} -\Delta_2 - \Delta_3 - \Delta_4 - \Delta_5 = E_{0111} \quad \Rightarrow \quad \Delta_8 > \Delta_4\,. \tag{3.13b}$$

So the class in fig. 3.4a is not possible for $\mathcal{C}_{\texttt{SCU}}$.
So fig. 3.4c remains. If 9 is only in blockade only with the center atom (the unlabelled one), it is excited, whenever a port is excited, this includes the states $(1111), (1110), (1100)$ and (1101). So one can repeat the argument from eq. (3.11a).
So lets assume w.o.l.g. that it is in blockade with ancilla 6 (implying it is not in blockade with 7). For port 2 to be not excited, either all ports are not excited and the center atom is, or ancilla 6 is excited, blocking ancilla 9. The second case implies:

$$E_{1001} = -\Delta_1 - \Delta_4 - \Delta_6 - \Delta_7 \overset{!}{<} -\Delta_1 - \Delta_3 - \Delta_4 - \Delta_6 = E_{1011} \quad \Rightarrow \quad \Delta_3 < \Delta_7\,, \tag{3.14a}$$

$$E_{1010} = -\Delta_1 - \Delta_3 - \Delta_6 - \Delta_8 \overset{!}{<} -\Delta_1 - \Delta_6 - \Delta_7 - \Delta_8 = E_{1000} \quad \Rightarrow \quad \Delta_3 > \Delta_7\,. \tag{3.14b}$$

which excludes this class.

□

3.4 The Vertex Complex of the Fibonacci Model $\mathcal{C}_{\texttt{FIB}}$

Lemma 7. *The vertex complex $\mathcal{C}_{f_{\texttt{FIB}}}$ of the Fibonacci model on the Honeycomb lattice cannot be realized with less than 8 atoms.*

Proof. The language to investigate is $L_{\texttt{FIB}} = \{000, 011, 110, 101, 111\}$. It contains (011), (110) and (101). We used the states of these words to show in section 3.1, that `XOR` ad `NAND` can not be realized with less than $N = 7$ atoms. Only kinematic arguments were used for this, and the argument only relied on these states (and the existence of at least another one). So it can be applied to the Fibonacci complex as well. So the Fibonacci complex can not be realized with $N = 6$ atoms or less. These three states also do not allow for any ports to be in blockade with each other. To see whether a Fibonacci complex with $N = 7$ atoms exists, we need to go through three cases.

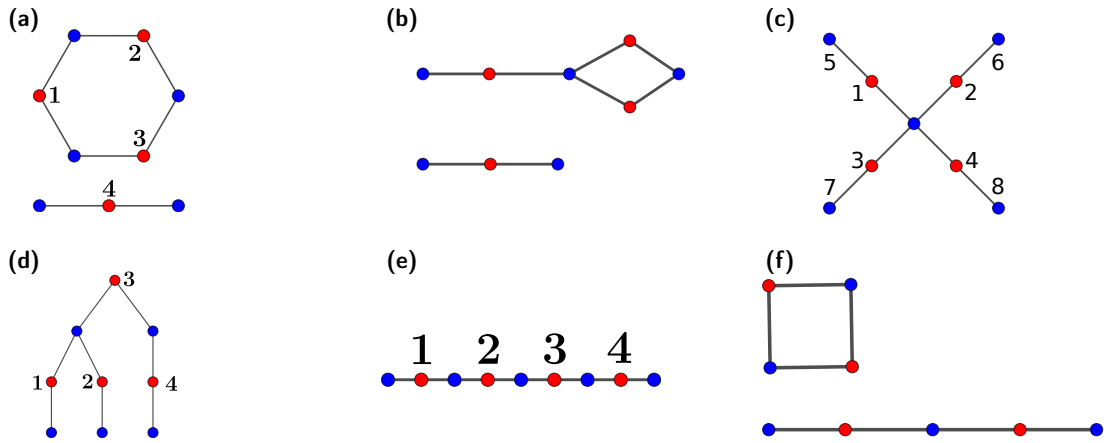

Figure 3.3: The six classes of blockade graphs for the surface code vertex complex and the crossing on nine atoms with ports of degree 2 and without disconnected ancillas.[2] Ports (ancillas) are colored red (blue) and connections between ancillas are omitted. The only class that cannot be excluded kinematically is the "cross" graph (c) with atom labels $\{1,\ldots,8\}$ and ports $\{1,2,3,4\}$, see text.

1. At least one port is in blockade with a single ancilla. We amputate it. This corresponds to inverting a letter in the symmetric $L_{\texttt{FIB}}$- language so we must realize $\overline{L}_{\texttt{FIB}} = \{100, 111, 010, 001, 011\}$ with $N = 6$ atoms. The XNOR language is a subset from this language, $L_{\odot} \subset \overline{L}_{\texttt{FIB}}$. We showed in section 6.2, that there is only one blockade graph with six atoms that realizes the XNOR language. This graph has only four MIS^*, so it can not realize the $\overline{L}_{\texttt{FIB}}$.

2. At least one port connects to three ancillas. We fix it to the excited state. It thus blocks those three ancillas. The remaining atoms (two ports, one ancilla) must realize the sublanguage $L = \{01, 10, 11\}$. As the language is irreducible, the atoms must be correlated. So the blockade graph of them is connected. But there is no graph on three vertices with (at least) three MIS^* of which (at least) one has (at least) two vertices.

3. All ports are in blockade with two ancillas. There are three graph classes to investigate. They are depicted in fig. 3.5. With a similar line of arguments as used for the surface code (the case $N = 9$ in section 3.3), one can exclude two of the three graphs (a and c). The remaining one (b), needs energetic arguments again. We have

$$E_{111} = E_{110} \quad \Rightarrow \quad -\Delta_1 - \Delta_2 - \Delta_3 = -\Delta_1 - \Delta_2 - \Delta_6. \quad \Rightarrow \quad \Delta_3 = \Delta_6. \tag{3.15}$$

The same argument with (101) (and (011)) leads to $\Delta_2 = \Delta_5$ (and $\Delta_1 = \Delta_4$). We also have to gap out unwanted states:

$$E_{111} < E_{100} \quad \Rightarrow \quad -\Delta_1 - \Delta_2 - \Delta_3 < -\Delta_1 - \Delta_5 - \Delta_6. \tag{3.16}$$

Combining both equations leads to

$$-\Delta_1 - \Delta_2 - \Delta_3 < -\Delta_1 - \Delta_5 - \Delta_3 \Rightarrow \Delta_2 > \Delta_5. \tag{3.17}$$

Hence this graph class cannot realize $L_{\texttt{FIB}}$.

□

3.5 The CRS Complex

3.5.1 Topological Constraints

For some complexes the topology of the ports play a crucial role. For example, if the CRS complex had two ports exchanged, it would become a trivial circuit of two parallel lines. So for a given

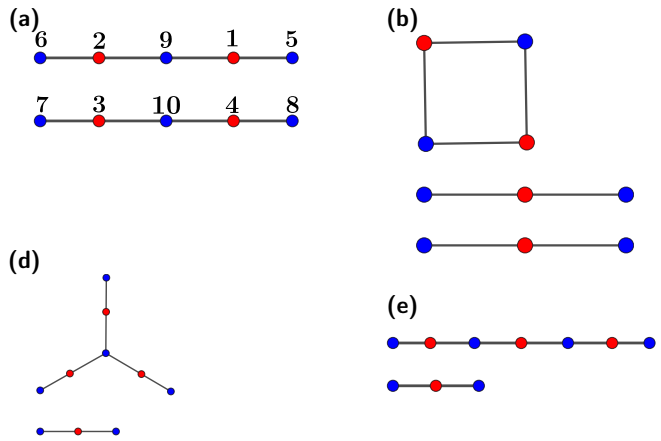

Figure 3.4: The five classes of blockade graphs for the surface code vertex complex on ten atoms with ports of degree 2 and without disconnected ancillas (except (c)). Ports (ancillas) are colored red (blue) and connections between ancillas are omitted. The only class that cannot be excluded kinematically is the "cross" graph (c) with atom labels $\{1,\ldots,9\}$ and ports $\{1,2,3,4\}$, see text.

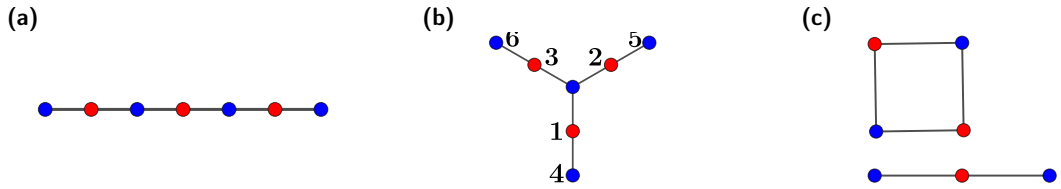

Figure 3.5: The three classes of blockade graphs for the Fibonacci vertex complex on seven atoms with ports of degree 2.[2] Ports (ancillas) are colored red (blue) and connections between ancillas are omitted. Only the graph in (b) must be energetically excluded.

counting direction (like clockwise), the ports (which lie on the boundary of the complex) thus must have a fixed pattern when counting them. For the CRS complex the pattern is $x-y-x-y$ or $y-x-y-x$, as depicted in fig. 3.6.

This property thus enforces a topological constraint to deforming a complex. So we call this property of a complex a *topological constraint*. All investigated elementary complexes in this chapter so far, except the ones in section 2.3, do not have topological constraints. The surface codes vertex primitives have completely symmetric languages, so ports can be exchanged. The primitive gates have two symmetric inputs, and one fixed output, so they have three ports, so changing their order always leaves the inputs adjacent to each other as seen in (ii):

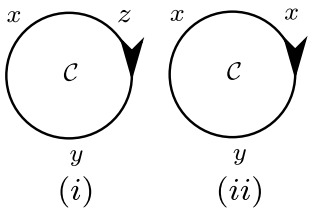

(3.18)

In general also three ports can have topological constraints, as seen in (i). In the picture y follows z, but after exchanging x and y, x follows z.

However these constraints become nontrivial, when one has four or more ports and information must 'flow' through the complex along a certain axis i.e. the logic of two logical ports is independent of the other, and not a reducible language. The crossing has the property, that information must flow through the two axis independently. The counting order of the ports lets the complex assign directions 'up', 'down', 'left' and 'right', as depicted in fig. 3.6. Ports at the

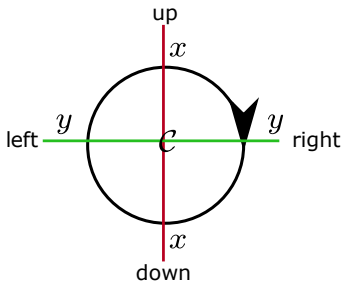

Figure 3.6: A CRS complex $\mathcal{C}$. We have two x-ports and two y-ports. Each port gets a direction assigned, and these define two axis, through which information must pass. Because the ports lie on the boundary, information must pass through the red line without circumventing the 'up' and 'down' ports, and through the green line without circumventing the 'left' and 'right' ports.

positions labelled x (y) are called x- (y-)ports. For the CRS complex, both x- (y-) ports have to be in the same state. For a $\overline{L}_{\text{CRS}}$ complex (see section 3.5) one x-type is the inverse of the other ($x_2 = \bar{x_1}$), while the y-ports still share the same state (or vice versa).

The following applies to complexes that have the structure of fig. 3.6 (They do not have to be crossings as they may have other ports).

Lemma 8. *Lets look at two ports with same fixed vertex degree, and both connect to the same ancilla. Then*

1. *both ports are either x-ports or y-ports (w.o.l.g. one can choose).*
2. *either the x-ports are rendered uncorrelated by the y-ports or there are states where the x-ports are not excited and the x-ports are rendered uncorrelated i.e. the complex can not support a topological constraint where the x-ports are independent of the y-ports.*

Proof. As both ports are connected to the same ancilla, if one is excited the other one is as well so the have to be the same type, lets say both are x-ports. Two cases can happen:

- The two ports are not connected.

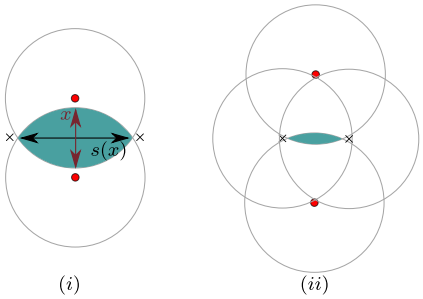

(3.19)

All the mentioned ancillas lie within the green ellipse.

case 1: It holds $r < (2-\sqrt{3})r_B \Rightarrow s(r) < r_B$, see (ii). In that case two atoms can pass information from left to right by placing them at the positions market with $\times$. They are thus in blockade with each other. So information can be passed through them. If one of them is excited every atom in the ellipse is blocked (see (ii)). Note, that one of them must be excited at some point, otherwise there would be no connection between the left and the right side. Thus the two ports are completely independent of each other and the sub language created by those ports is reducible i.e. the two x-ports are uncorrelated. This is exactly **not** the property of the crossing. However the two placed atoms can also not be in blockade with each other. Then they either must circumvent the ports to pass information from left to right (remember conditions for blockades with the ports). This can not happen as the ports lie on the boundary of the complex. Or they are in blockade with atoms in the ellipse. But if one of the two x-ports is excited, all atoms in the ellipse are blocked out. This again renders the left side independent from the right side thus the x-ports are uncorrelated.

case 2: If $r < (2-\sqrt{3})r_B$ thus $s(r) > r_B$, (see (i)), no information can be passed directly 'through' the ellipse like in the last case (again note the condition for the ports). So the remaining atoms must be in blockade with atoms in the ellipse again, and the same argument as above holds.

- the ports are connected.

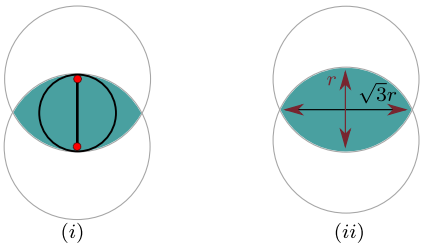

(3.20)

Then the minor axis $r \geq r_B$ (black circle) of the ellipse is $r > r_B$ and The major axis is $s(r) > r$. So again, no blockade can be established through the ellipse. This is again the same as in *case 2* above. Finally note, that for four atoms (which can be ports) the following situation can trivially not happen if the black marked blockades should be the only ones:

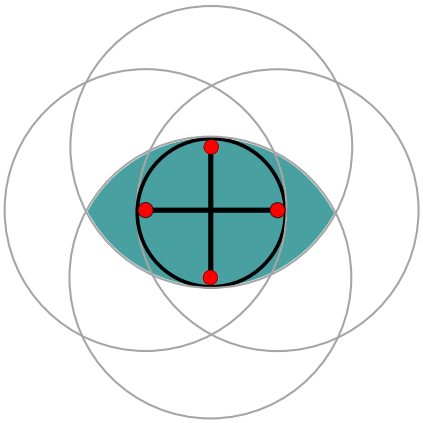

(3.21)

This also would violate the assumption, that the graphs are connected. But there have to be additional bonds in this scenario which make this configuration connected (In fact, the given minimal CRS complex revolves around a similar structure).

□

We say, a complex violates the topological constraint, if the complex satisfies the conditions for the lemma. Note that when there is no sub complex on one side of the ellipse, the topological constraint is trivially violated. A conclusion is, that complex that satisfies the conditions of the lemma, cannot realize a CRS or $\overline{L}_{\texttt{CRS}}$ (see below).

3.5.2 Minimality of the CRS Complex.

With the setup of topological constraints section 3.5.1 at hand, we can now proof the following lemma:

Lemma 9. *The complex $\mathcal{C}_{\texttt{CRS}}$ of the surface code on the square lattice cannot be realized with less than 10 atoms.*

Proof. We again use the method introduced in section 3.2, and the (topological) labelling scheme from fig. 3.6.

$$L_{\texttt{CRS}} \equiv \begin{Bmatrix} 1111 \\ 1010 \\ 0101 \\ 0000 \end{Bmatrix} \xrightarrow{\text{inv. 1. letter}} \overline{L}_{\texttt{CRS}} \equiv \begin{Bmatrix} 0111 \\ 0010 \\ 1101 \\ 1000 \end{Bmatrix} \xrightarrow{\text{inv. 2. letter}} \overline{\overline{L}}_{\texttt{CRS}} \equiv \begin{Bmatrix} 0011 \\ 0110 \\ 1001 \\ 1100 \end{Bmatrix}. \tag{3.22}$$

Note that the language is symmetric, and inverting the first and third letter does not change the CRS language as it corresponds to inverting both x-ports (or both x-ports). If a CRS complex would have two x-ports (or x-ports) with degree one, one can just invert both (by amputation) and the result is a smaller CRS complex. Inverting the first and second letter corresponds to amputating a x- and a x-port. This results in the ICRS manifold. Inverting more than two letters would mean, one could amputate three or more ports. Then again both x-ports (or both x-ports) are being amputated, and the resulting complex would again realise one of the three languages $L_{\texttt{CRS}}$, $\overline{L}_{\texttt{CRS}}$ or $L_{\texttt{ICRS}}$ (up to permutation of the ports), but with a 2 atom smaller complex. Inverting three or more letters always implies inverting two x- or two x-ports. So if ports are in blockade with only one atom, it can only be one x-port and/or one x-port. Because $|1111\rangle$ is in the GSM, there can be no blockades between the ports. *For the two inverted manifolds, this is not true.* We however assume, there is no such connection in the following cases and deal with it afterwards.

Let us now systematically exclude the existence of a CRS complex with $N \leq 9$ atoms.

- $N \leq 5$: The ports must be connected to a ancilla for the complex to be connected. With $N = 5$ atoms the complex has the CPY GSM (with three copies) as MIS^* which is not the desired one.

- $N = 6$: If at least one port has degree two, it is connected to both ancillas. We can fix it to be excited, rendering both ancillas not excited. Thus the other ports, which are connected only to the as well are excited to minimize the energy (remember, we only look at irreducible languages so ports do not have zero detuning). So one of the states $|1010\rangle$ or $|0101\rangle$ can not be realized. ICRS is not possible with four atoms, as four unconnected ports are just uncorrelated. So the CRS with 6 atoms where one x and one x-port have degree one is not possible, So a $N = 6$ atom sized CRS complex where two ports are in blockade with only one ancilla can not be realized. If only one port is connected to only one ancilla, we can amputate it. The resulting $\mathcal{C}_{\overline{L}_{\texttt{CRS}}}$ can not be realized with 5 atoms as they again form a four legged CPY complex and realize some MIS^* of it as GSM.

- $N = 7$:

  1. If two ports are in blockade with only to one ancilla, we amputate both. But ICRS can not be realized with the remaining five atoms. Here one uses the same argument used to show that CRS is not possible with five atoms.
  2. If one port is in blockade with only one ancilla, we amputate it. Then $\mathcal{C}_{\overline{L}_{\texttt{CRS}}}$ with $N = 6$ atoms, where no port has degree one, must be realized:
     This is impossible. Again, all ports must be connected to both ancillas so if one port is excited the other are as well. Then $|1101\rangle$ and $|1000\rangle$, both of witch must be in GSM $\overline{L}$ can not be realized.
  3. If at least one port has degree three, it again blocks all ancillas, rendering the three other ports uncorrelated.
  4. The case where all ports have degree two remain. There are three non-isomorphic bipartite graphs that connect sets of four (ports) and five vertices (ancillas), where all ports have degree 2, and no double edges occur, fig. 3.7. There are no graphs with free ancilla, as $N = 6$ crossings where all ports have degree 2 are not possible due to the blockade rendering ports uncorrelated. An additional ancilla adds only energetic constraints, none to the degrees of freedom coming from port-ancilla-blockades. The graph in fig. 3.7c violates the Rydberg blockade. Port 1 has to be connected with either port 2 or port 3 which would result in port-port blockades
     (and one port having degree 3). In the graph in fig. 3.7b if port 1 is excited, port 2 is excited as well. So they have to be both either x-ports or y-ports. Then however the topological constraint is violated. The same is true for graph in fig. 3.7c. Here however we can also choose ports 1 and 4 as x-ports, which would satisfy the topological constraint. But if they are excited, ports 2 and 3 are as well, a CRS complex can not be realized.

- $N = 8$:

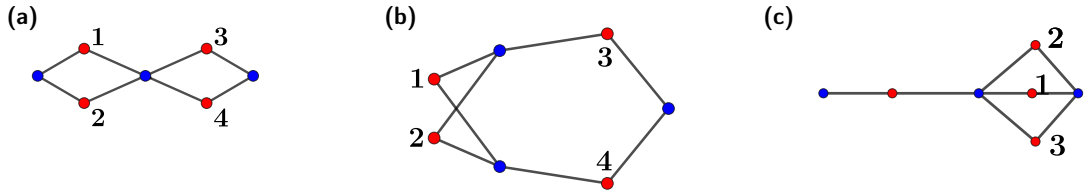

Figure 3.7: The remaining three classes of blockade graphs for the CRS complex on seven atoms with ports of degree 2 and without disconnected ancillas. Ports (ancillas) are colored red (blue) and connections between ancillas are omitted.

1. If two ports are in blockade with only one ancilla, we amputate them. So one has to realise ICRS with $N = 6$ atoms where all ports have degree 2:
   This is impossible because all four ports are connected to the same two ancillas, so if one port is excited, the others are as well so states like $|1100\rangle$, which are in $\mathrm{GSM}_{\mathtt{ICRS}}$ can not be realized.
2. If one port is blockade with only one ancilla, we amputate it and must realize $\overline{L}_{\mathtt{CRS}}$ with $N = 7$ atoms where all ports have a degree larger than one:
   This is not possible. If one port has degree three, it connects to all ancillas, rendering the other ports excited again. If all ports are in blockade with two ancillas, the graphs of fig. 3.7a and fig. 3.7a are the ones we need to check. (we already showed, that fig. 3.7a violates the Rydberg blockade). But both have the property, that if three ports are excited, all four are, thus they can not realize $\overline{L}_{\mathtt{CRS}}$, as it contains states like $|1110\rangle$.
3. At least one port is in blockade with three ancillas. W.l.o.g let it be a x-port. We can fix it to be excited. Therefore those three ancillas must be off. To realize a CRS complex, one of the remaining ports has to be the second x-port and must be excited as well, and the ports must be arranged to satisfy the topological constraint. This second x-port is in blockade with at least two ancillas (otherwise it could be amputated). There is only one ancilla not in blockade with the fixed port. So the second x-port has to be in blockade with one (or more) of the three blocked ones. Then the topological constraint is violated. Note that the fixed port is in blockade with additional ancillas, but they are fixed to be not excited so these dummy ancillas don't play a role in the information flow.
4. All ports are in blockade with two ancillas. There are seven non-isomorphic bipartite graphs that connect sets of four (ports) and five vertices (ancillas), where all ports have degree 2, and no double edges occur, fig. 3.8. Again graphs with free ancilla do not need to be considered. None of those can realize CRS, because the graphs in fig. 3.8b, fig. 3.8c, fig. 3.8d, fig. 3.8f violate the topological constraint. The graphs fig. 3.8a, fig. 3.8e, have the ports 1, 2, 3, where if two are excited, the third one is as well, in a CRS complex only pairs of two can display this behavior (they are the (x-port,y-port) pairs). The graph in fig. 3.8g has only one way to satisfy the topological constraint: 1 and 3 are the x-ports, 2 and 4 are the y-ports. But if the x-ports are excited, all ancillas are blocked and the y-ports are excited as well and vice versa. So this graph can not realize a CRS complex.

- $N = 9$:

1. If two ports are in blockade with only one ancilla, we amputate them. So one has to realise a ICRS complex with $N = 7$ atoms where all ports have degree larger than 1:
   If one port is in blockade with three ancillas, we fix it in the excited state. Then all ancillas are off rendering the other ports excited as well. So in a complex with $N = 7$ atoms all ports have degree two. One can again check the graphs in fig. 3.7a and fig. 3.7b. Both must realize the state where port 1 and port 4 are excited, the others not. But if those two are excited, port 3 and 4 are excited in those graphs.

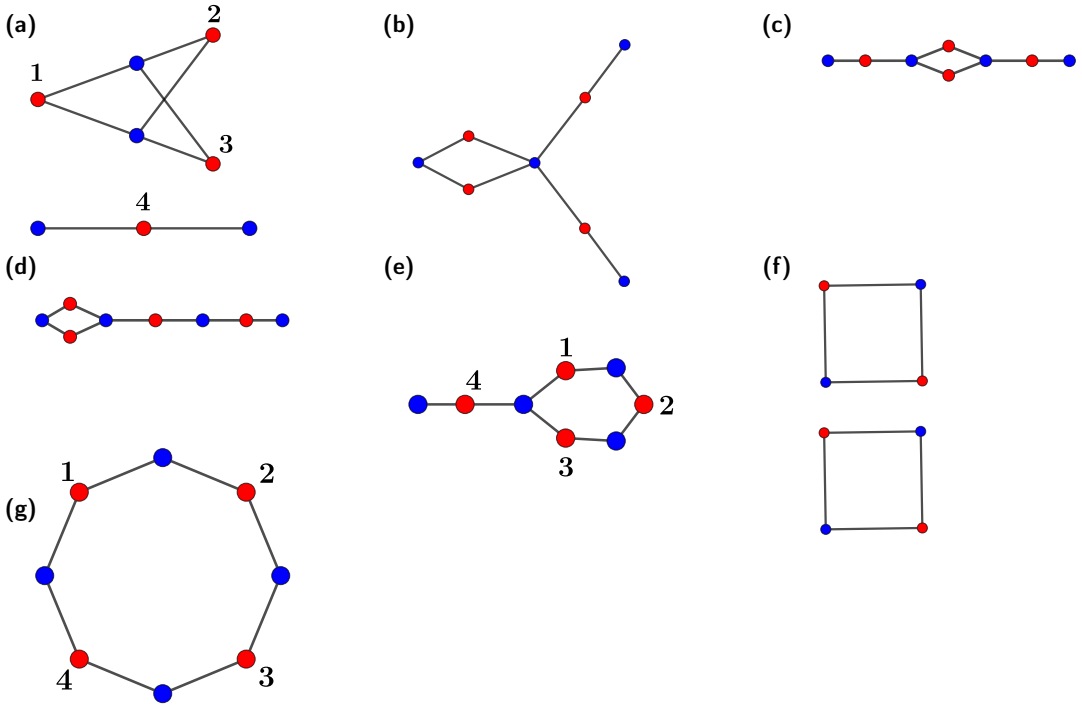

Figure 3.8: The remaining seven classes of blockade graphs for the CRS complex on eight atoms with ports of degree 2 and without disconnected ancillas. Ports (ancillas) are colored red (blue) and connections between ancillas are omitted.

2. If there is one port with only one ancilla, we amputate it and must realize $\overline{L}_{\texttt{CRS}}$ with $N = 8$ atoms where all ports have a degree larger than one:
If one has degree three, we can fix it in the excited state. All other ports must be connected to the remaining ancilla. So these remaining four atoms realize a CPY complex a subset of the states $\{|000\rangle, |111\rangle\}$. They should however realize $|011\rangle$ or $|101\rangle$ (depending on which port was the amputated one). If all ports have degree two one looks at fig. 3.8. The argument is the same as for why a CRS complex can not be realized with them.

3. At least one port is in blockade with three ancillas. W.l.o.g let it be a x-port. We can fix it to be excited. It blocks three ancillas, so two others remain. Because very port has at least degree two, the other x-port can be in blockade with none or one of the blocked ancillas, or it can be in blockade with both remaining ancillas. The first two cases are the same as for a CRS-complex with $N = 8$ atoms. In the second case both x-ports, (which are both excited due to the first one fixed and the second one copying this state) block all five ancillas. So the remaining ports can both only be excited as well, which is not the case for a CRS - complex.

4. All ports have degree two. Again we look at the graphs in fig. 3.3, where again graphs with free ancilla do not need to be considered. The graphs in fig. 3.3b and fig. 3.3f violate the topological constraint. The graph in fig. 3.3a can not realize a CRS- complex as one can choose the three ports 1, 2 and 3, and if two are excited the third one is as well. The graph in fig. 3.3c can not realize a CRS- complex, as it has to violate the topological constraints. This is because fixing ports 1 and 4 excited makes ancillas 5 and 8 dummy ancillas, and no information can pass from 1 to 4. The graph in fig. 3.3d can not realize a CRS- complex, because port 3 gets excited whenever either ports 1and 4 or ports 2 and 4 are excited. Such behavior can not occur for the ports of a crossing. The graph in fig. 3.3e can not realize a CRS- complex. If ports 1 and 3 are, lets say, x-ports, the must be excited the same time. Then however the y-port 2 is excited as well. If ports 2 and 3 are the x-ports now, 1 and 4 are the x-ports. This labelling does

not allow for the outer most ancilla to be in blockade and bring the complex to a circle shape, because the labelling would violate the topological constraint. If they are open however, one can reshape the line to a S-shape, which would allow for the topological constraint to be satisfied. However fixing ports 2 and 3 excited, the complex has to violate this constraint again as no information can pass from port 1 to port 4.

So we showed, that the CRS can not be realized with $N = 9$ atoms. Repeating this for $N = 10$ atoms requires for a ICRS complex to happen with $N = 8$ atoms where all ports have degree 2. This however can not be excluded because the graph in fig. 3.8g can have the states of ICRS as GSM. If two adjacent ports are excited (like 1 and 4 or 4 and 3) the remaining unblocked ancilla can be excited, blocking the remaining two ports. Using the rotation symmetry of this graph, this realizes all the states of $L_{\texttt{ICRS}}$. (see. fig. 2.3)c. To gap out the state $|1111\rangle$, energetic constraints must apply. The ancillas must have larger detunings than the ports. If the ports have detuning 1 this implies that the ancillas have detuning 3, so $E_{\text{GSM}} = -5$. To gap out all states where at least two ancillas are excited (which have $E \leq -6$) we finally add the ancilla-ancilla- blockades: all ancillas must be in blockade with each other. The realizing complex is shown in fig. 2.3c. In fact it is the only one (up to the choice of port detunings) that can realize a ICRS with $N = 8$ atoms. Adding two NOT ports to two adjacent ports gives the depicted (not necessarily unique) smallest CRS complex with $N = 10$ atoms.

The only thing left to discuss is, that $\overline{L}_{\texttt{CRS}}$ and $L_{\texttt{ICRS}}$ allow for blockades between ports. But both languages require their complexes, to transfer information from the left side to the right side,i.e. satisfy topological constraints. As shown in section 3.5.1, this can not happen when two ports are in blockade. □

Chapter 4

Considering Van der Waals

In this thesis, complexes were constructed in the PXP model. In the following chapter we look at the complexes with the Van der Waals interaction in mind. We check if, and how valid the PXP approximation is for the found complexes. Lastly we take a look at potential string net vertex complexes in a pure Van der Waals model.

4.1 Geometries of Complexes

So far we have optimized complexes by their size, that is the minimal number of atoms, they require to realize a given language. We ended up with a blockade graph B, local detunings Δ and assigned ports l, that realize a desired language as ground state manifold (see section 1.5). In our approach, these blockade graphs are unit disk graphs, where the 'unit' is the blockade radius r_B. A geometry $G_\mathcal{C}$ that realizes such a graph is called unit disk embedding of B. Whether such a embedding exists or not is in general not clear, answering that question usually is NP-hard. So far, it was only relevant, that a geometry and thus a unit disk embedding exists. When there exists such a planar geometry $G_\mathcal{C} = (\mathbf{r}_i)_{i\in V} \in \mathbb{R}^{2N} \equiv \mathfrak{C}_N$ that realizes a given blockade graph B, there exist many of such geometries. In most cases, there is just some 'wiggle' room for the atoms. However there can be cases, in which there exist several valid geometries, that can not continuously be transformed into each other without violating the blockade constraints, for example:

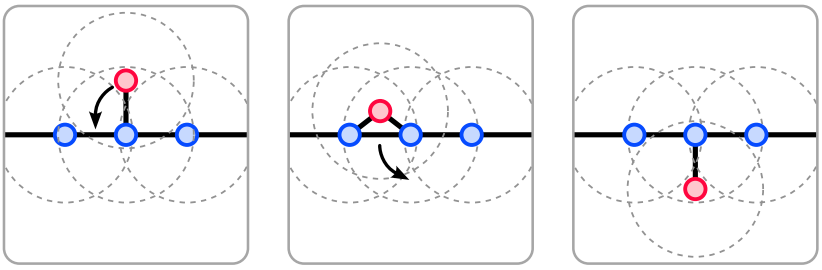

[2]

This can lead to disconnected regions in the configuration space $\mathfrak{C}_N$, that realize a given blockade graph. In fig. 4.3b another similar thing happens: the atoms can break the symmetry and go to different sides. So for a fixed geometry of each unit cell complex of a lattice, this can lead to these complexes having different chirality.

To geometrically optimize a complex, we need to quantify what we mean by a 'good' complex. To this end we define a $\Gamma : \mathfrak{C}_N \to \mathbb{R}$ that quantifies the desired quality we seek to optimize. One possible candidate would be

$$\tilde{\Gamma}(G_\mathcal{C}) = \frac{\delta E}{\Delta E} \tag{4.1}$$

where δE and ΔE are the width and the gap of the ground state manifold (see fig. 1.6). However this function (its configuration space) scales exponentially with the size of the complex N, because we need to compute the low energy spectrum of the complex to evaluate it. Even with $\Omega_i = 0$ this the NP-hard QUBO problem (recall section 2.1). Furthermore, $\tilde{\Gamma}$ simply vanishes in the

PXP-model when the blockade constraints are satisfied, because then $= 0$. So a finer optimization function is needed, that can be directly computed from the complex itself: The *Robustness*.

4.2 Robustness as Optimization Parameter

To motivate the definition of the Robustness, we review the blockade radius in the PXP model: In the limit of $\Omega_i = 0$, the blockade radius r_B is the distance at which the Van der Waals interaction matches its detuning, so $C_6 \, {r_B}_i^{-6} = \Delta_i$. The detunings vary from atom to atom in the complexes, so their blockade radius changes. However, we like to work with a unique blockade radius r_B, as we have in all previous chapters of this thesis. In the following, we interpret a given blockade graph B as the encoding of the constraints we would like to realize with a structure $\mathcal{C}$ of yet unknown geometry $G_\mathcal{C}$.

We now introduce two dimensionless quantities. First, the *robustness* of a structure w.r.t. a given blockade graph $B = (V, E)$ is defined as

$$\xi_B(\mathcal{C}) := \frac{\min\limits_{(i,j)\notin E} d(\mathbf{r}_i, \mathbf{r}_j) - \max\limits_{(i,j)\in E} d(\mathbf{r}_i, \mathbf{r}_j)}{\min\limits_{(i,j)\notin E} d(\mathbf{r}_i, \mathbf{r}_j) + \max\limits_{(i,j)\in E} d(\mathbf{r}_i, \mathbf{r}_j)} \,, \tag{4.2}$$

where $d(\mathbf{r}_i, \mathbf{r}_j)$ denotes the Euclidean distance. The robustness is a scale-invariant, finite number $\xi_B(\mathcal{C}) \in [-1, 1]$. If $\xi_B(\mathcal{C}) > 0$ the unit disc embedding $G_\mathcal{C}$ realizes the blockade graph B for blockade radii in some interval. The larger $\xi_B(\mathcal{C})$, the more positional freedom the atoms have, thus the embedding is more robust against atoms 'wiggling around'. Equivalently, more robust embeddings realize the blockade graph for a wider range of blockade radii. Thus a robust embedding is more valid in the Van der Waals model, as this allowed wider range separates blocked atoms further from unblocked ones, leaving blocked atoms in the strong interacting regime, and ones that are not in the low interacting regime. If $\xi_B(\mathcal{C}) < 0$, the unit disk graph induced by $G_\mathcal{C}$ does not match the prescribed blockade graph B. Similarly, we define the *spread* of a structure $\mathcal{C}$ as

$$\begin{aligned} s(\mathcal{C}) &:= \frac{\max_i r_{Bi} - \min_i r_{Bi}}{\max_i r_{Bi} + \min_i r_{Bi}} \\ &= \frac{(\max_i \Delta_i)^{1/6} - (\min_i \Delta_i)^{1/6}}{(\max_i \Delta_i)^{1/6} + (\min_i \Delta_i)^{1/6}} \,. \end{aligned} \tag{4.3}$$

The spread $s \in [0, 1]$ quantifies the variations of the blockade radii due to the changing detunings of the atoms. Just as eq. (4.2), the spread does not depend on the total length scale, neither does it depend on the C_6 coefficient of the Van der Waals interaction. We can now take into account the variability of the blockade radius, and partly the Van der Waals model without abandoning the PXP model: We call a structure $\mathcal{C}$ a *valid implementation*, if

$$s(\mathcal{C}) < \xi_B(\mathcal{C}) \,. \tag{4.4}$$

This condition ensures, that the geometry $G_\mathcal{C}$ can be scaled in a way, that all distances of atoms that should (not) be in blockade according to B, are smaller (larger) than the smallest (largest) blockade radius of the structure $\mathcal{C}$. This condition is scale invariant, so we do not need to specify r_B and thus a length scale in the following. Not all complexes are valid. The one depicted in fig. 6.2a has no valid geometry (note, that it is already optimal in the sense defined in section 4.3). All other complexes in this thesis are valid, i.e. they have a valid geometry.

4.3 Numerical Optimization

These considerations suggest that the robustness ξ_B is a reasonable measure for the quality of geometries. We set $\Gamma = -\xi_B$ to maximize the robustness by minimizing Γ. As input we give a blockade graph B, together with detunings Δ and labels l. These are fixed and define the functional properties of the complex. In particular, the spread $s(\mathcal{C})$ is constant. We now optimize for geometries that satisfy the validity constraint eq. (4.4), and that maximize the the margin between spread and robustness. We call a complex $\mathcal{C}$ *globally (locally) optimal* if $\xi_B(\mathcal{C}) > 0$ and its geometry is a global (local) minimum of Γ in $\mathfrak{C}_N$. For the minimization we use the `SciPy`

implementation[24] of simulated annealing, in combination with a local optimization that uses the Nelder-Mead algorithm.[25,26] The `SciPy` method is `scipy.optimize.dual_annealing`[24,27,28] Our stochastic algorithm starts with a random initial geometry (that may, or may not realize the blockade graph). However one can start from the ones given throughout this thesis, as they are often close to the found optimum. The algorithm then completes iterations of jumps. Each jump in $\mathfrak{C}_N$ is completed with a probability depending on the distance of the jump and the variation of the objective function. The annealing is thus able to basin hop. The probability to do so is high, as the search space is large ($\mathbb{R}^{2N}$ for N atoms). After each jump, a local search is conducted by the Nelder Mead algorithm. Note, that this algorithm does not use derivatives, and it is non probabilistic. After $\lesssim 2000$ iterations, the algorithm stops and returns the (potentially global) minimum of the robustness, and the final geometry. Remember that the robustness is a scale-invariant quantity, so that the scale of the optimized geometry is arbitrary. We thus can renormalize the length scale by setting the blockade radius

$$r_B := \frac{1}{2}\left[\max_{(i,j)\in E} d(\mathbf{r}_i,\mathbf{r}_j) + \min_{(i,j)\notin E} d(\mathbf{r}_i,\mathbf{r}_j)\right] \stackrel{!}{=} 1\,. \tag{4.5}$$

As we see in fig. 4.1c, there are atoms, that still have 'wiggle' room in the optimized complex without changing the robustness. This is because the robustness only looks for maximal blockades and minimal 'un blocked' distances. So the function has usually continuous valleys of minima,whose complexes change by 'wiggling' these atoms around. The source code is available at DaRUS.[23]

At first, we apply the algorithm to the logic primitives. All the logic primitives depicted in section 2.2 and the crossing fig. 2.3 are optimal in the defined way, although we did not construct them with that in mind. We also believe, that they are globally optimal, although we did not prove this (the optimization can not provably return a global optimum). As depicted in fig. 2.2, all logical gates are constructed from the three variations of the `NOR` gate (except `XNOR` and `XOR`). All logical gates have thus the same robustness as the `NOR`-gate they are based upon. In fig. 4.1, a random starting point is depicted (and in (c) the constructed gate) together with the three optimal `NOR` gates. Their Robustness and their spread is shown. We find for these (and thus all logical gates, including `XNOR` and `XOR`, which have the same triangle structure as one of the `NOR` gates):

$$s(\mathcal{C}^{(\mathrm{opt})}_{\texttt{NOR}\triangle}) = 0.058 < 0.268 = \xi(\mathcal{C}^{\mathrm{opt}}_{\texttt{NOR}\triangle}), \tag{4.6}$$

$$s(\mathcal{C}^{(\mathrm{opt})}_{\texttt{NOR}\circ}) = 0.058 < 0.236 = \xi(\mathcal{C}^{\mathrm{opt}}_{\texttt{NOR}\circ}), \tag{4.7}$$

$$s(\mathcal{C}^{(\mathrm{opt})}_{\texttt{NOR}}) = 0.0 < 0.0924 = \xi(\mathcal{C}^{\mathrm{opt}}_{\texttt{NOR}}). \tag{4.8}$$

Note, that $\xi(\mathcal{C}_{\texttt{NOR}\triangle}) > \xi(\mathcal{C}_{\texttt{NOR}})$. So the `NOR` complex based on triangles may be more robust in some settings, than the ring shaped one. The optimized `ICRS` complex is depicted in fig. 4.4. The optimized `CRS` complex is again the same as the optimized `ICRS` complex, with two amalgamated `NOT`'s, which have some 'wiggle' room. Lastly, we optimized string net unit cell complexes. The found complexes are depicted in fig. 4.2 (surface codes) and fig. 4.3 (Fibonacci models). The Fibonacci model unit cell depicted in fig. 2.8 is not valid as constructed. However the blockade graph has a valid geometry. At this point note, that the described optimization is not reducible to subcomplexes. However the shortest blockades occur within the unit cell complex, when observing the presented tessellated lattices form fig. 2.4-fig. 2.11. So the interesting part are free edges. However in the depicted unit cell complexes, each one has a free edge, that is just barely outside the blockade radius, so only minor changes are to be expected when optimizing tessellated languages.

4.4 Complexes in the Van der Waals Model

Lastly we notice, that complexes can be realized a lot smaller when using the additional degrees of freedom from the real Van der Waals interaction. In fig. 4.5 the two vertex complexes for the surface code and the Fibonacci model are depicted, where now the interaction between the Atoms are given by the Van der Waals potential with $C_6 = 1$. Note, that the complex in fig. 4.5a also realizes the `XOR` gate. The atoms require only $N = 4$ atoms, in contrast to the seven (surface code) and eight (Fibonacci model) atoms they need in the PXP model, and

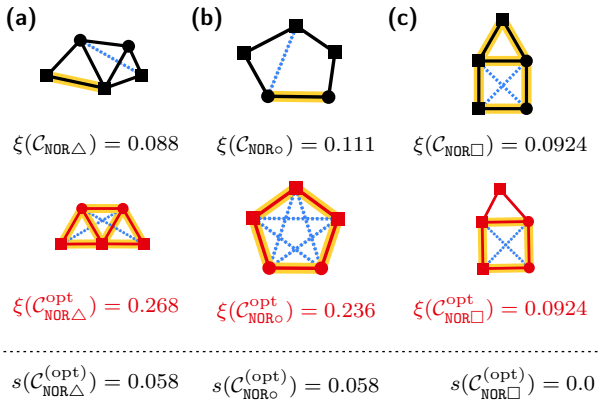

Figure 4.1: *Optimization (NOR gate).* (a)[2] and (b)[2] Comparison of perturbed (black) and optimized (red) geometries for the three minimal NOR-complexes. Maximum distance blockades are highlighted yellow, minimum distances of unblocked atoms are indicated by dashed blue edges. The optimal geometries are highly symmetric and match the manually constructed ones in fig. 2.1 and fig. 1.10c. Robustness for each complex is printed below the geometries and the spread on the bottom of each column (we omit blockade graph indices). Note that $\xi(\mathcal{C}^{\text{opt}}_{\texttt{NOR}\triangle}) > \xi(\mathcal{C}^{\text{opt}}_{\texttt{NOR}\circ})$. This makes the 'triangle version' NOR$\triangle$ potentially more robust than the ring-shaped NOR$\circ$. For all geometries the validity constraint $s(\mathcal{C}) < \xi(\mathcal{C})$ is satisfied. Note, that NOR has no spread, as all detunings are the same. (c) The constructed third NOR gate from fig. 2.2 contains only blocked edges of the same length. Thus we expect and find, that the optimization does not change the robustness. However there are degrees of freedom. The 'top' atom can thus 'wiggle' a certain amount, without changing the robustness, (in the constructed symmetric case depicted it is placed, so that all blockade edges in the complex have the same length).

they share, up to scaling, the same geometry. The complexes still have degenerate ground state manifolds. This suggests unit cell complexes, that are amalgamations of two copies of these vertex complexes. This is the same procedure as for the PXP model. The resulting complexes are depicted in fig. 4.6. Tessellating them would result in a honeycomb lattice where one atoms sits on each vertex and edge - so quite simple. However a big point must be made: The amalgamation does not work any more in the Van der Waals model, as there are residual interactions between atoms from the amalgamated complexes. However, additional links can be added with may reduce these interactions. Indeed, the unit cell complexes complexes in fig. 4.6 are not degenerate. For them we numerically[23] find at best $\frac{\delta E}{\Delta E} \approx 0.2$ by optimizing the detunings.

We close with a remark on a experimental note: Although the Van der Waals interaction depicts the real physical setting instead of an approximation, these complexes may be harder to realize, as they require an exact positioning and fixation of the atoms, which must be very fine tuned (compared to the PXP model, where atoms can move around as long as they do not violate the blockade graph). However an interesting advantage of the Van der Waals model is a potential uniformity of detunings. The complex depicted in fig. 4.7 is a LNK complex, that can rise detunings. So if a atom has detuning $\Delta = 1$, we can amalgamate this complex with it using port A, and it gets a new detuning $\Delta = 2$ (the sum of the two amalgamated atoms). This is the same detuning like the ancilla and the linked port B have. Such a LNK can not exist for the PXP model because one of the two ground sates has odd, the other even ground state energy (as all atoms have detuning two, except for one, which has detuning one). So by using this complex, circuits can be realized with only one uniform detuning, which is useful for experimental applications, as different detunings are hard to realize.

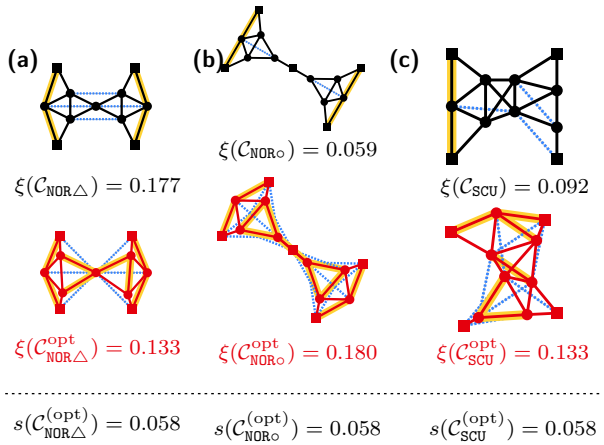

Figure 4.2: *Optimization of the surface code unit cell complexes.* Comparison of perturbed (black) and optimized (red) geometries for the three surface code unit cell complexes. The depicted data is explained in fig. 4.1. For all geometries the validity constraint $s(\mathcal{C}) < \xi(\mathcal{C})$ is satisfied. Note, that the complex in (c) has the same robustness as the one in (a).[2] They share the same maximum blocked edge, and the minimal free edge is barely larger than the blockade radius.

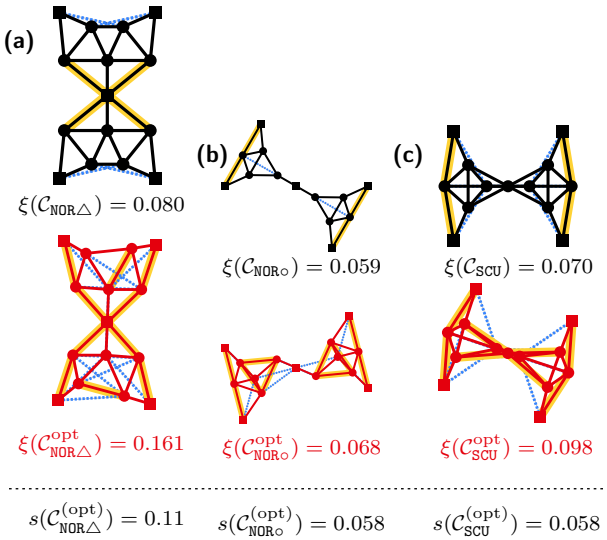

Figure 4.3: *Optimization of the Fibonacci model unit cell complexes.* Comparison of perturbed (black) and optimized (red) geometries for the three Fibonacci model unit cell complexes. The depicted data is explained in fig. 4.1. Note, that the unoptimized complex in (a)[2] is not valid. The blockade graph however has a valid geometry (the optimized one). For all other geometries the validity constraint $s(\mathcal{C}) < \xi(\mathcal{C})$ is satisfied.

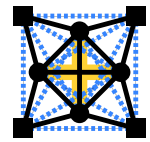

$\xi(\mathcal{C}_{\texttt{ICRS}}) = 0.155$

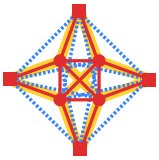

$\xi(\mathcal{C}^{\text{opt}}_{\texttt{ICRS}}) = 0.254$

$s(\mathcal{C}^{(\text{opt})}_{\texttt{ICRS}}) = 0.091$

Figure 4.4: *Optimization of the* `ICRS` *complex.* The optimized geometry for the `ICRS` complex. Note, that it is almost the same as the unoptimized one, except the edges to the ports are rescaled, so they match the longer 'diagonal' edges. This reduces $\min_{(i,j)\notin E} d(\mathbf{r}_i, \mathbf{r}_j)$. The depicted data is explained in fig. 4.1. For all minimal and `ICRS` complexes in this thesis $s(\mathcal{C}) < \xi(\mathcal{C})$ is satisfied.

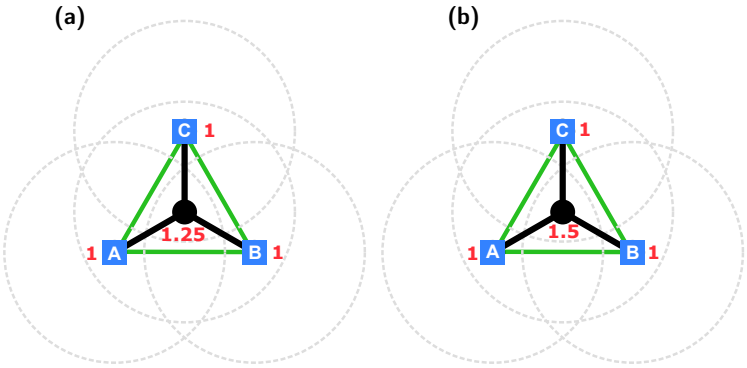

$V_{\text{green}} = 0.75$ $V_{\text{black}} = 36$

$V_{\text{green}} = 0.5$ $V_{\text{black}} = 14$

Figure 4.5: *Surface code and Fibonacci vertex complexes.* The detunings of complexes are red numbers next to their atoms, the two possible distances between atoms are marked as black and green edges. (a) The surface code vertex complex in the Van der Waals model. The complex also realizes a `XOR` gate. Its ground state manifold is exact when enforcing the geometry as depicted. All lengths are given in terms of the strength of the Van der Waals interaction with the coefficient $C_6 = 1$. Note, that $V_{\text{black}} \gg 1$, so it acts as effective Rydberg blockade. (b) The Fibonacci model vertex primitive in the Van der Waals model. Note, that the complex has, up to scaling, the same geometry as the surface code vertex primitive complex. Its ground state manifold is exact when enforcing the geometry as depicted. All lengths are given in terms of the strength of the Van der Waals interaction with the coefficient $C_6 = 1$. Note, that $V_{\text{black}} \gg 1$, so it acts as effective Rydberg blockade.

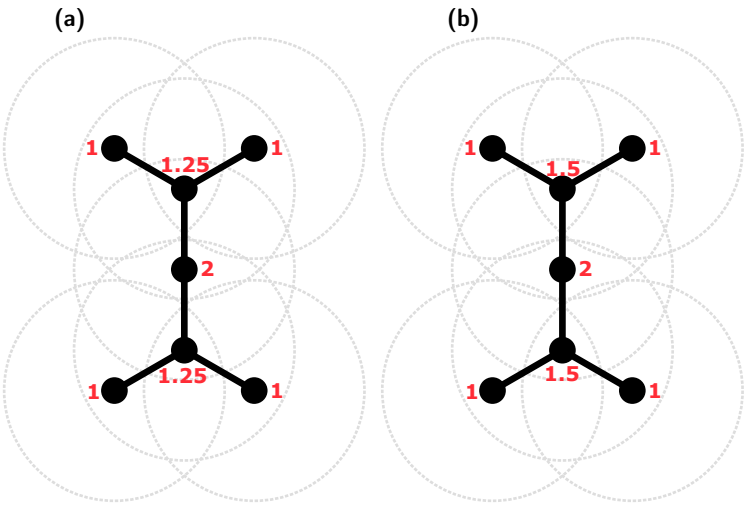

Figure 4.6: *surface code and Fibonacci model unit cell).* The detunings of complexes are red numbers next to their atoms. (a) The unit cell complex for the surface code in the Van der Waals model, created by amalgamating two `XOR` gates from fig. 4.5. The complex is six atoms smaller than its corresponding complex in the PXP model, making it almost half size. However its ground state manifold is not degenerate. Optimizing it analytically and numerically[23] lead to $\frac{\delta E}{\Delta E} \approx 0.2$. (b) The unit cell complex for the Fibonacci model in the Van der Waals model, created by amalgamating two `XOR` gates from fig. 4.5. The complex is eight atoms smaller than its corresponding complex in the PXP model, making it more than half size. However its ground state manifold is not degenerate. Optimizing it analytically and numerically[23] lead to $\frac{\delta E}{\Delta E} \approx 0.2$.

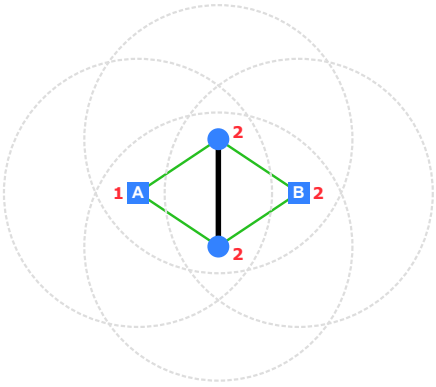

$V_{\text{green}} = 2.3,\ V_{\text{black}} = 1.1,\ V_{AB} = 0.1$

Figure 4.7: *The* `LNK` *complex in the Van der Waals model.* The data is explained in fig. 4.5. With the given distances of the atoms (lengths are again measured in interaction strength, see fig. 4.5), the depicted complex realizes a `LNK` complex, that, when amalgamated, raises a detuning. That means that if a atom has detuning Δ_1, and it is amalgamated with port A of this complex, its new detuning is $\Delta = 2$, which is the same as the one from port B (that has the same state as the amalgamated atom), and from all ancillas. So all detunings is the system are now 2. The degenerate ground state energy of this `LNK` is $E_{\text{GSM}} = -2.9$, the gap is $\Delta E = 0.9$.

Chapter 5

Conclusion and Outlook

In this thesis we use arrangements of Rydberg atoms, called complexes, to realize logical languages by exploiting the Rydberg blockade in the PXP model. The intrinsic logic of the Rydberg blockade is the `NOT` logic. In this thesis we aimed to find all minimal complexes for all Boolean primitives including a 'link' `LNK` and a 'copy' `CPY`. All these complexes can be realized with $N \leq 7$ atoms. We found, that complexes that realize inverted gates (like `OR`, which is an inverted `NOR`) differ by size of one atom. This exploits the intrinsic negating nature of the blockade. In the second step we developed vertex and unit cell complexes for string nets on a square or honeycomb lattice. The investigated models are the surface code, which imposes Gauss's law for a $\mathbb{Z}_2$ gauge theory with a charge free background on each vertex, and a Fibonacci model, where, in addition, strings can fuse at vertices. The non unique string net complexes contain $N = 13$ atoms (surface code) and $N = 15$ atoms (Fibonacci model) on the honeycomb lattice. Some of complexes can be reduced by removing a `LNK` in the center, which corresponds to contracting a edge in the honeycomb lattice. The resulting complexes realize these models on the square lattice.

To find these complexes and to prove their minimal size, we developed an analytical method, that exploits properties of the realizing language. This was complemented by a numerical search for small complexes. The method reduces the problem of going trough all graphs by ignoring blockades between ancilla and by reducing large graphs to smaller ones by performing amalgamations or by evaluating subgraphs.

Finally we optimize complexes in hindsight of the Van der Waals interaction. The robustness must be larger than the spread, which introduces the changing blockade radii due to the Van der Waals model. We found, that all complexes except the one in fig. 6.2a have a valid geometry. The logic primitives even are optimal by construction. Lastly we we depict the gates completely in the Van der Waals model.

With that now have the tools at hand to realize Rydberg complexes for geometric programming or to built string nets, that potentially can host topological phases, which can perform fault tolerant (universal) quantum computing. In fact, such Rydberg arrays, emerge from geometric programming, so we connected these two fields. This forms a good basis to continue the research on the Rydberg complexes, as many interesting questions were raised during writing this thesis. We thus conclude this thesis with some remarks on directions for future research:

Beyond the PXP model We briefly look at the Van der Waals model in the last chapter. However the most important concept of our research, the amalgamation of complexes, fails, when Van der Waals interactions are turned on, so the depicted complexes themself are not very useful. Key here is the observation of the width δE when amalgamating complexes. In our model $\delta E = 0$. This must no longer be the case in the Van der Waals model (look at the complexes depicted in fig. 4.6). The most important amalgamation then is the amalgamation of `LNK` complexes, which can be used to separate operational complexes from each other and reduce the width δE. How the best complexes in the Van der Waals model look like is an open question.

Quantum phase diagrams In this thesis, we only studied the ground states of Hamiltonians like eq. (1.36) without quantum fluctuations ($\Omega_i = 0$). As demonstrated in Refs,[1] these fluctuations in combination with the strong interaction of the blockade gives rise to interesting many-body quantum phases at zero temperature. Thus, the natural next step could be to investigate the quantum phase diagram of the spin liquid primitives and their tessellated lattices, for example

numerically, using DMRG. The unit cell consists of $N \approx 15$ atoms for the Fibonacci model, which makes the analysis of two or three unit cells with it a feasible approach. Note, that, even with additional `LNK` complexes in between, the unit cell primitives in the Van der Waals interaction are ≈ 5 atoms smaller, so an entire plaquette could be observed, if a small δE is taken into account. Analytically, one could derive the effective Hamiltonians on the constructed low-energy manifolds for finite but small Rabi frequencies $\Omega_i \ll \Delta E$ in perturbation theory using a Schrieffer Wolff transformation and examine the interactions in low energy subspace. Note, that the relative strength of these interactions can depend on the specific complex used to implement the local constraints. This raises the subsequent question whether these interactions can be *tuned* by modifications of the used complexes.

Dynamical preparation In recent experiments,[29] dynamical preparation schemes have been used to drive long-range entangled many-body systems out-of-equilibrium. This can be done with adiabatic protocols $\Omega_i(t)$ and $\Delta_i(t)$, where the Rabi frequency ensures the coupling of different excitation pattern, the detuning increase continuously to its set target value. This allows the preparation of the system given by our classical Hamiltonian eq. (1.38) in non trivial superpositions of the low energy states. It would be interesting to study these effects on the tessellated lattices presented in this thesis.

Chapter 6

Appendix

6.1 Appendix A: Brief Overview of Phases in the Landau Paradigm

6.1.1 Classical Phases

To describe classical phases one uses Landau theory, so one defines an local order parameter which locally describes the system. If this parameter is the same everywhere, the system is in a certain phase. One can now change global system parameters like pressure or temperature. As long as the system stays in a phase the order parameter changes smoothly. At certain critical parameters (ex. critical temperature T_C) the system can changes into a different phase. Formally this is derived from the free enthalpy G. If $S = \frac{\partial G(T,p)}{\partial T}$ is not continuous, one has a phase transition of the first order. If they are but $C_p = \frac{\partial S}{\partial T}\Big|_p = \frac{\partial^2 G(T,p)}{\partial T^2}$ are not, it is a second order transition. In general, if $G \in C^n$ in a neighbourhood of the t transition, the phase transition is of order $n+1$. The symmetry of the system defines, how it 'looks like' macro and microscopically (compare ice and water). So the change of symmetry is key to classify phase transitions as we briefly discuss in sec 6.1.2.

An example is the melting of ice. In ice and water the heat capacities are (almost constant) over temperature. However at a critical temperature ($273.5K = 0°C$ as we know under normal atmospheric pressure) the heat capacity is not continuous. But in addition, if we add heat at that point, temperature stays (these are the famous 333kJ/kg). So $\Delta Q = T\Delta S$ implies a non continuous change of Entropy at that point. That is clear as well because the symmetric ice crystals break up. So melting is a phase transition of the first order. The above construction is not limited to temperature as the example for a second order phase transition shows: The transition from ferro- to paramagnetism at the Curie temperature. The free enthalpy at constant pressure here is (see[30] as source, and for more details)

$$G(T, M) = -SdT - MdH\,. \tag{6.1}$$

Here the magnetisation M is the order parameter. expanding G in M one gets

$$G(T, M) = a(T - T_C)M^2 + bM^4\,. \tag{6.2}$$

The free enthalpy has to be at a maximum for the phase to be stable, so one gets

$$\frac{\partial G}{\partial M}\Big|_T = 2a(T - T_C)M + 4bM^3 \stackrel{!}{=} 0\,, \tag{6.3}$$

which leads to $M = 0$ for $T > T_C$ or $M^2 = -\frac{a(T-T_C)}{2b}$ for $T < T_C$. Notice that at these points $G = 0$ for $T > T_C$ and $G \propto (T - T_C)^2$ for $T < T_C$.so $\frac{\partial G}{\partial T}\Big|_M$ is continuous a t $T = T_C$ but $\frac{\partial^2 G}{\partial T^2}\Big|_M$ is not continuous at $T = T_C$ thus the phase transition is of second order.
Notice, that again a symmetry breaks at the transition, so the paramagnetic state, which is highly isotropic (without, or weak external fields) breaks and the ferromagnetic state has a much lower symmetry due to the ordered magnetic moments. Here however, the state has two ground states,

in which it can decay (without external fields) depending on the orientation of the magnetic moments. This is called spontaneous symmetry breaking.

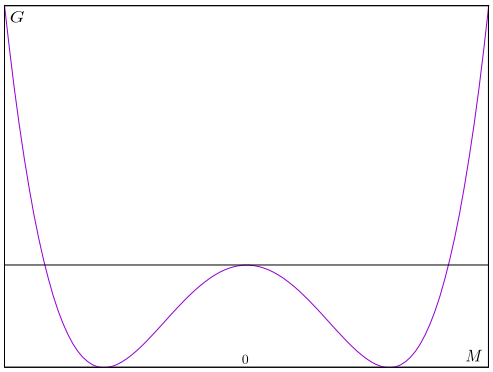

Figure 6.1: G over M for $T < T_C$. The symmetric state of $M = 0$ becomes unstable and there are two stable ground states for the system with lower symmetry, in one of which the system can spontaneously decay.

6.1.2 Quantum Phases and Spontaneous Symmetry Breaking

This section follow the lecture notes of N. Lang.[31] All these observations can be transferred to quantum phases as well. In this thesis it is always $T \Rightarrow 0$. The phase transition occurs due to non commuting terms in the Hamiltonian, and the parameters of the Hamiltonian are the system variables (and not T). An example is the traverse Ising model in 1D given by

$$H = -J \sum_{i=1}^{L} \sigma_i^z \sigma_{i+1}^z - h \sum_{i=1}^{L} \sigma_i^x \,, \tag{6.4}$$

with the coupling strength $J > 0$ and the traverse field $h > 0$. Note that this is a (entangled product of eigenstates of $\sigma_i^z \sigma_{i+1}$:.) $[\sigma_i^z \sigma_{i+1}^z, \sigma_i^x] \neq 0$ so there are quantum fluctuations. The local There are two regimes of the system.

$J \ll h$ and $J \gg h$. In the first case the system is in the paramagnetic phase, all states are oriented in x direction by h, leaving the z direction unaffected. The ground state thus is $G_+ = |+ + +...+\rangle$, where $|+\rangle$ is the eigenstate with eigenvalue $+1$ of σ^x in h-direction. Here the correlation function $\lim_{|i-j|\to\infty} \langle G_+| \sigma_i^z \sigma_j^z |G_+\rangle = 0$ because the spins do not (very weakly) interact in z direction so the system in this direction is non trivially unordered.

The case $J \gg h$ is the ferromagnetic phase. due to the strong spin interactions and the lack of the external field the spins align, however the direction is arbitrary and dependent on the orientation of the majority of spins, which is subject to fluctuations so it behaves chaotic. Either way the general ground state is the superposition of the two degenerate gapped ground states $|G_\uparrow\rangle = |\uparrow, \uparrow, .. \uparrow\rangle$ and $|G_\downarrow\rangle = |\downarrow, \downarrow, ... \downarrow\rangle$. So the ground state is $|G\rangle = \alpha |G_\uparrow\rangle + \beta |G_\downarrow\rangle$ and the correlation function now becomes $\lim_{|i-j\to\infty} \langle G| \sigma_i^z \sigma_j^z |G\rangle = 1$, which is clear because all states are aligned in the eigenbasis of σ^z, so it acts either as $+1$ or as -1 on both spin sites. Thus the signs cancel and $\langle\uparrow|\uparrow\rangle = \langle\downarrow|\downarrow\rangle = 1$. So the system is ordered. However, σ_i^z is a site dependent local order parameter so the system is not topologically ordered.

In the two cases above, the system is gapped, and the order parameter distinguishes them. At the phase transition, the gap closes, because the higher non oriented states close it. In this area, the correlation function based on the σ_i^z, the local order parameter, is continuous but not differentiable. The system thus has a phase transition of second order. This implies that with increasing field, the order by the interaction is destroyed, and a unordered system in z is established. Thus the correlations go from 1 (perfect correlation) to 0 no correlation (continuous).

But as discussed in the previous section, when the system enters the ferromagnetic the spins align thus the entire system becomes less symmetric. The spin alignment can be seen as more

symmetric with a philosophical point of view, however the symmetry group of the Hamiltonian is

$$G_S = \{\mathbb{1}, X\}, \text{ with } X = \prod_i \sigma_i^x \,. \tag{6.5}$$

This is because $[\sigma_i^z \sigma_{i+1}^z, \sigma_i^x] \neq 0$ due to the anti-commutation of the Pauli-matrices, products of all $[\sigma_i^z \sigma_{i+1}^z, X] = 0$ because there are always two σ_x to anti commute with the two $\sigma_i^z \sigma_{i+1}^z$ so the signs cancel. However there are no more operators to commute with H since all can be created from Pauli matrices and this is the only operator that commutes with all products of two σ^z and single σ^x. And since $X\,|G_+\rangle = |G_+\rangle$ (because it is a product of $+1$-eigenstates of the σ_i^x), this is the symmetry ground of the paramagnetic phase. In the ferromagnetic phase however, it is $X\,|G_\uparrow = |G_\downarrow\rangle\rangle$ and $X\,|G_\downarrow = |G_\uparrow\rangle\rangle$ (because σ^x flips the σ^z eigenstates.) So the symmetry group G_F of the ferromagnetic phase only is $G_F = \{\mathbb{1}\} \subsetneq G_S$. This is called *spontaneous symmetry breaking (SSB)* because the states $G_\downarrow$ and $G_\uparrow$ break the symmetry and (also as described above) the system is in a superposition and upon measurement collapses spontaneously into one of the two orientations.

Famous examples of SSB are the breaking of the $U(1)$ particle number symmetry in superconductors, or breaking of the same $U(1)$ symmetry of complex rotations in the (abelian) Higgs-mechanism.

6.2 Appendix B: Uniqueness of the Blockade Graph of $L_{\texttt{XNOR}}$ and $L_{\texttt{XOR}}$

The minimal complexes do not have to be unique (see section 2.2). However the blockade graph of the minimal $L_{\texttt{XNOR}}$ complex is.

Proof. The minimal blockade graph consists of $N = 6$ atoms, so lets assume, we have six atoms at our disposal. We now try to construct a complex that realizes $L_\odot = \{001, 010, 100, 111\}$ systematically. Lets assume, there exists such a complex. Three cases can occur:

1. At least one port is only in blockade with one ancilla. We amputate it. The remaining 5 atoms must realize $\overline{L}_\odot = \{101, 110, 000, 011\}$, which is impossible as proven in section 3.1.4.

2. A port is in blockade with all three ancillas. If it is excited, all ancillas are not, thus all other ports are excited as well. But the states $|100\rangle$, $|010\rangle$ and $|001\rangle$ must be realized, which then can not work.

3. So all ports are in blockade with two ancillas. The three graph classes for this are depicted in fig. 3.2. The first two graphs can be excluded from realizing the desired GSM, as they are inconsistent with the states $|100\rangle$, $|010\rangle$ and $|001\rangle$. So the graph fig. 3.2c remains. Without additional blockades between ancillas, this graph can realize $\{000, 001, 010, 100, 111\} \supset L_\odot$, with its MIS^*.

   Let $\Delta_{1,2,3}$ denote the detunings of the three ports and $\tilde{\Delta}_{1,2,3}$ the detunings of the three ancillas (where $\tilde{\Delta}_i$ describes the ancilla opposite of port i, fig. 3.2). In the state $|100\rangle$ only the first port is excited. Its opposite ancilla must be excited as well to block the two other ports. To balance this state energetically with the state $|111\rangle$, the detuning of the ancilla must equal the sum of the detunings of its two adjacent ports. Due to the permutation symmetry of $L_\odot$ and the rotation symmetry of the "hexagon graph", this argument is valid for all three ancillas:

   $$\tilde{\Delta}_1 = \Delta_2 + \Delta_3 \,, \quad \tilde{\Delta}_2 = \Delta_1 + \Delta_3 \,, \quad \text{and} \quad \tilde{\Delta}_3 = \Delta_1 + \Delta_2 \,. \tag{6.6}$$

   Remember that all detunings are positive, which implies for any pair of ancillas

   $$-\tilde{\Delta}_i - \tilde{\Delta}_j < -\Delta_1 - \Delta_2 - \Delta_3 = E_{111} \,. \tag{6.7}$$

   The state $|111\rangle$ must be in the in the GSM so E_{111} is the lowest possible. To achieve this, there have to be blockades between all pairs of ancillas to prevent two of them being excited at the same time, lowering the energy of the GSM below E_{111}. This yields the blockade graph of the XNOR-complex depicted in fig. 2.1. The choices of the port detunings $\Delta_i > 0$ are arbitrary. The detunings of the ancillas are then fixed by eq. (6.6).

We conclude that the blockade graph of the minimal realization of a XNOR-complex with six atoms is unique up to the choice of the port-detunings. In addition, we proved that no *strict superset* of $L_{\odot}$ can be realized by a complex with six atoms or less (this is used in section 3.4). With the same method, one can conclude, that the XOR complex has a unique realization with $N = 7$ atoms.

If one port has degree one, we amputate it. The resulting complex thus must realize a XNOR logic (the result is the same, whether the amputated port is an in- or output). So in this case, we get a unique XOR complex.

If a port has degree three, we fix it to the exited state. The remaining two ports and singe ancilla must realize a LNK complex, because ports can not be in blockade with each other and the language is irreducible. But the two ports must realize (10) and (01), so a NOT logic instead of a LNK logic. So this case can not happen.

If all ports have degree two, we must look at the three graph classes depicted in fig. 3.5. These can not realize the XOR logic for the same reasons they can not realize the vertex complex of $\mathcal{C}_{\texttt{FIB}}$. So the presented seven atom XOR complex is unique (up to the aforementioned choice of detunings). □

6.3 Appendix C: Minimal Complex for Fibonacci Anyons on a Square Lattice

In fig. 6.2 a minimal vertex complex for the Fibonacci model $\mathcal{C}_{\texttt{MFMUSQ}}$ on a square lattice is depicted. It consists of $N = 12$ atoms. Note that it is not valid in the sense of chapter 4.

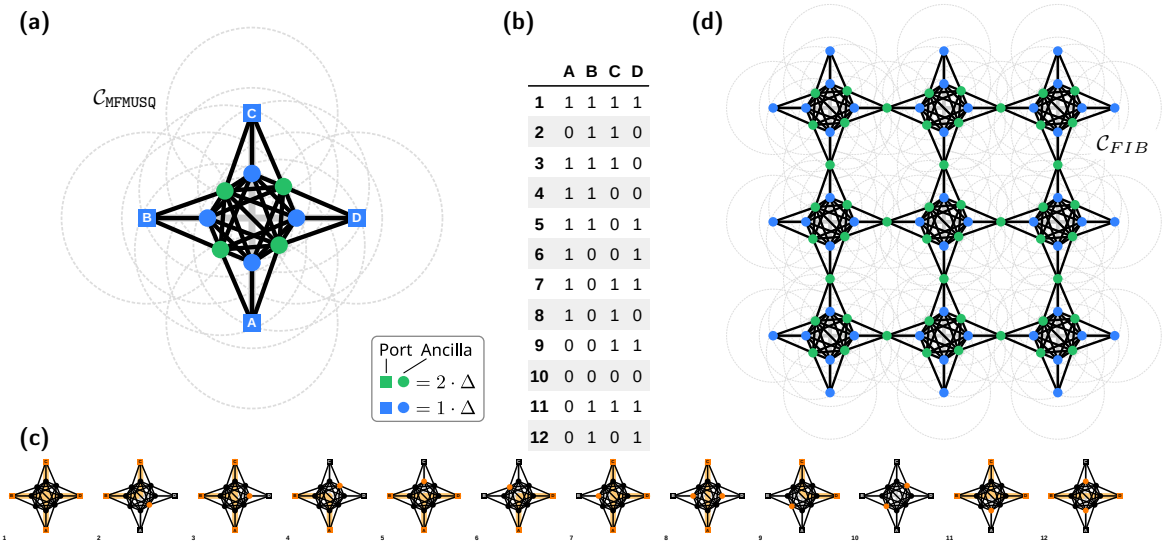

Figure 6.2: *A minimal vertex complex for the Fibonacci model on a square lattice.* (a) The minimal vertex complex $\mathcal{C}_{\texttt{MFMUSQ}}$ for the Fibonacci model on a square lattice. It has $N = 12$ atoms. (b,c) Truth table and ground state manifold of the complex (the data is explained in fig. 2.1). The ground state manifold realizes all configurations except ones where only one port is excited. (d) Periodic tessellation $\mathcal{C}_{\texttt{FIB}}$ of the complex $\mathcal{C}_{\texttt{MFMUSQ}}$. The copies are amalgamated at the ports of the complex.

Lemma 10. *The vertex complex (unit cell complex)* $\mathcal{C}_{\texttt{MFMUSQ}}$ *of the surface code on the square lattice cannot be realized with less than 12 atoms.*

Proof. At first we look at the language, and how it behaves under inversion of ports. We find in

the case of a square lattice

$$L_{\texttt{FMU}} \equiv \left\{\begin{matrix}1111\\1100\\0011\\1001\\0110\\0101\\1010\\0000\\1110\\1101\\1011\\0111\end{matrix}\right\} \xrightarrow{\text{inv. 4. letter}} \overline{L}_{\texttt{FMU}} \equiv \left\{\begin{matrix}1110\\1101\\0010\\1000\\0111\\0100\\1011\\0001\\1111\\1100\\1010\\0110\end{matrix}\right\} \tag{6.8}$$

$$\xrightarrow{\text{inv. 3. letter}} \overline{\overline{L_{\texttt{FMU}}}} = \left\{\begin{matrix}1100\\1111\\0000\\1010\\0101\\0110\\1001\\0011\\1101\\1110\\1000\\0100\end{matrix}\right\} \xrightarrow{\text{inv. 2. letter}} \overline{\overline{\overline{L_{\texttt{FMU}}}}} = \left\{\begin{matrix}1000\\1011\\0100\\1110\\0001\\0010\\1101\\0111\\1001\\1010\\1100\\0000\end{matrix}\right\} \cdots \tag{6.9}$$

Note, that inverting the first letter as well does not lead to the original language. Because these languages are obtained by inverting ports, they can be realized by amputating or amalgamating ports to the $\mathcal{C}_{\texttt{MFMUSQ}}$ complex, and we only look at the amputation, as amalgamating would make the complex larger. All of these languages contain either $L_{\texttt{SCU}}$ or $\overline{L}_{\texttt{SCU}}$ as subset, so they require at least $N = 10$ (or $N = 9$ atoms for $\overline{L}_{\texttt{SCU}}$.). All other cases were excluded kinematically, except the cross class in fig. 3.3c, with which we deal separately. So if we amputate two ports, we have $N = 9$ atoms left to realize a complex that has to realize $L_{\texttt{SCU}}$ as sublanguage, which is not possible as this has been ruled out kinematically (again, we deal with fig. 3.3c separately). So only the first two languages are to be looked at. Because $L_{\texttt{FMU}}$ contains $L_{\texttt{SCU}}$ as subset, which requires at least $N = 11$ atoms we only need to exclude all graph classes with $N = 11$ for $L_{\texttt{FMU}}$ and with $N = 10$ for $\overline{L}_{\texttt{FMU}}$.

- $N = 11$:
  1. We start by proving, that $\overline{\overline{L_{\texttt{FMU}}}}$ can not be realized with $N = 9$ atoms. The only case we need to look at is fig. 3.3c, as this class was only kinetically excluded from realizing a $\mathcal{C}_{\texttt{SCU}}$. However we find:

$$E_{1111} = -\Delta_1 - \Delta_2 - \Delta_3 - \Delta_4 \overset{!}{<} -\Delta_2 - \Delta_3 - \Delta_4 - \Delta_5 = E_{0111} \quad \Rightarrow \quad \Delta_5 < \Delta_1\,, \tag{6.10a}$$

$$E_{0011} = -\Delta_3 - \Delta_4 - \Delta_5 - \Delta_8 \overset{!}{<} -\Delta_1 - \Delta_3 - \Delta_4 - \Delta_6 = E_{1011} \quad \Rightarrow \quad \Delta_5 > \Delta_1\,. \tag{6.10b}$$

     So this case is not possible.
  2. We now show, that $\overline{L}_{\texttt{FMU}}$ is not possible with $N = 10$ atoms. The classes are depicted in fig. 3.4. Only the classes in fig. 3.4a and fig. 3.4c are to be checked. The other three can be excluded immediately as one can find one (in fig. 3.4b) or two (in fig. 3.4d and

fig. 3.4e) ports that, when excited, block all ancillas from a third port. So this third port is excited as well. This is inconsistent with $\overline{L}_{\texttt{FMU}}$.
We exclude fig. 3.4a. Because $\{1111, 1110, 1101, 1011, 0111\} \in \overline{L}_{\texttt{FMU}}$, We have

$$\Delta_5 = \Delta_1 \,, \tag{6.11}$$
$$\Delta_6 = \Delta_2 \,, \tag{6.12}$$
$$\Delta_7 = \Delta_3 \,, \tag{6.13}$$
$$\Delta_8 = \Delta_4 \,. \tag{6.14}$$

Because $(1100) \in \overline{L}_{\texttt{FMU}}$, but $(0011) \notin \overline{L}_{\texttt{FMU}}$, we can conclude, that ports 5 and 6 are in blockade and $\Delta_9 < \Delta_1 + \Delta_2$. This ensures that $E_{1100} < E_{0011}$. But then

$$E_{0001} = -\Delta_4 - \Delta_7 + \epsilon(0001) > -\Delta_1 - \Delta_2 - \Delta_4 - \Delta_7 = E_{1101}. \tag{6.15}$$

This is because $\epsilon(0001)$ equals either$-\Delta_5$ or $-\Delta_6$ or $-\Delta_7$, all of which are smaller than $-(\Delta_1 + \Delta_2)$. So this graph class can not realize $\overline{L}_{\texttt{FMU}}$.
We now exclude fig. 3.4b. If ancilla 9 is only in blockade with the center atom, it is always excited if a port is. So we use the identical argument we used for fig. 3.4a above. Lets thus assume w.o.l.g., that 9 is in blockade with 6. We then find

$$E_{1011} = -\Delta_1 - \Delta_3 - \Delta_4 - \Delta_6 \overset{!}{<} -\Delta_3 - \Delta_4 - \Delta_5 - \Delta_6 = E_{0011} \quad \Rightarrow \quad \Delta_5 < \Delta_1 \,, \tag{6.16a}$$

$$E_{0001} = -\Delta_4 - \Delta_5 - \Delta_6 - \Delta_7 \overset{!}{<} -\Delta_1 - \Delta_4 - \Delta_6 - \Delta_7 = E_{1011} \quad \Rightarrow \quad \Delta_5 > \Delta_1 \,. \tag{6.16b}$$

So again this class can not realize $\overline{L}_{\texttt{FMU}}$.
Lastly we must exclude a $N = 10$ atom class, where ports have degree three, from realizing $\overline{L}_{\texttt{FMU}}$. Let us assume we have such a port. We fix it to the excited state thus blocking all three ancillas. The remaining subcomplex containing $N = 6$ atoms must realize the states $(110), (101)$ and (011). These however require at least seven atoms, so this setting is not possible.

3. Now we only need to exclude all classes with $N = 11$ atoms, where all ports have degree ≥ 2, from realizing $\mathcal{C}_{\texttt{MFMUSQ}}$. At first we look at classes that have ports with degree four. The argument to exclude these is exactly the same as used three lines above.

4. The case of classes where all ports have degree two or three remains. We only look at classes where only one port has degree three, as excluding them excludes all with more such ports as well.

   There are nine relevant classes to discuss. Two are fig. 3.4a and c, the other seven are depicted in fig. 6.3. All other classes with free ancilla have connected parts of in sum ten atoms, that have been excluded from realizing the surface code only with kinematic constraints.

   We can immediately exclude the classes in fig. 6.3c and fig. 6.3d, as we find port(s) in them, that block all ancillas to another port. So if these port(s) are excited, the other port is as well and this is inconsistent with $L_{\texttt{FMU}}$.

   – We deal with fig. 6.3a, which immediately excludes fig. 3.4a, as it is just obtained from fig. 6.3a by removing a free ancilla and its degrees of freedom. w.o.l.g. let 11 be connected with 8 at first. Because (1111) and (1110) are ground states, $\Delta_8 = \Delta_4 + \Delta_{11}$. Note, that ancilla 11 then can not be in blockade with ancilla 7, because otherwise $E_{1100} < E_{\text{GSM}}$ (because that ancilla has detuning $\Delta_8 = \Delta_4 + \Delta_{11}$, as $E_{1110} = E_{1111}$, similarly $\Delta_7 = \Delta_3 + \Delta_{11}$). The same argument implies, that ancilla 11 can not be in blockade with ancilla 6 and with ancilla 5. We must realize $(1001), (1011)$ and (1101) as ground state. All this together implies :

$$E_{1001} = -\Delta_1 - \Delta_4 - \Delta_6 - \Delta_7 - \Delta_{11} = -\Delta_1 - \Delta_2 - \Delta_4 - \Delta_7 - \Delta_{11} = E_{1101} \,, \tag{6.17}$$

from which we can conclude $\Delta_2 = \Delta_6$ (and similarly $\Delta_3 = \Delta_7$), and that ancilla 6 can not be in blockade with ancilla 7. Then however $E_{1000} = E_{1100}$, which is again inconsistent with $L_{\texttt{FMU}}$.
If 7 is in blockade with 8, then $\Delta_{10} = \Delta_3 + \Delta_4$. To prevent that $E_{1100} < E_{\mathrm{GSM}}$, we have blockades between 7 and 10 and between 8 and 10. Then again the states (1000) and (0100) are ground states which must not happen for $L_{\texttt{FMU}}$.

- We now exclude fig. 6.3f. The argumentation is similar to the one above. Because $(1110), (1101)$ and (1011) are ground states, we can conclude that $\Delta_2 = \Delta_8$, $\Delta_3 = \Delta_8$ and $\Delta_4 = \Delta_{11}$. At first consider, that ancilla 11 is not in blockade with ancilla 9. Then, because (1010) is a ground state, there can be no blockade between 8 and 11, and, with the same argument, there is no blockade between 8 and 9. Then however $E_{1000} = E_{1111} = E_{\mathrm{GSM}}$, so (1000) is a ground state, which must not be.
  The case where ancilla 9 is in blockade with ancilla 11 remains. But then ancilla 9 and 11 cannot be both excited, so to realize (1100) as ground state, we must have $\Delta_{10} = \Delta_3 + \Delta_4$. But then

$$E_{1100} = -\Delta_1 - \Delta_2 - \Delta_9 - \Delta_{10} < -\Delta_1 - \Delta_2 - \Delta_3 - \Delta_4 = E_{1111} = E_{\mathrm{GSM}}. \tag{6.18}$$

  So (1100) is not a ground state, although for $L_{\texttt{FMU}}$ it must be.
- We now exclude fig. 6.3e. Again we can conclude, that $\Delta_3 = \Delta_6$, $\Delta_1 = \Delta_5$ and $\Delta_2 = \Delta_9$. To exclude (1000) from being a ground state, there must be at least one blockade between either 5 and 6, or between 6 and 9, or between 9 and 5. If 5 is in blockade with 6, we can not realize (0101) kinematically. So these blockades must be between 5 and 9 or between 6 and 9. Lets assume there is a blockade between 5 and 9. To realize 0011 as ground state, we must have $\Delta_7 = \Delta_1$ or $\Delta_7 = \Delta_2$. To exclude (0001) from being a ground state, there has to be a blockade between either 7 and 6, or alternatively between 5 and 6. The second case restores the situation above, which is already excluded. So let there be a blockade is between 7 and 6. To realize (0000) as ground state,ports 1, 2 and 3 must be not excited, for this however Δ_8 then must be excited. So $\Delta_8 = \Delta_3$ or $\Delta_8 = \Delta_2$. But switching port 4 back on we again realize (0001) as ground state. so this class is excluded.
- We now exclude fig. 6.3g. If one of the free ancilla 9 and 10 are in blockade with two ancillas besides 11, we can immediately exclude the class. To see this lets assume ancilla 9 is in blockade with ancillas 5 and 6. Then to realize (0111) and (1011) to be degenerate with (1111), (as both should be ground states), we find that $\Delta_5 = \Delta_1 + \Delta_9$ and $\Delta_6 = \Delta_2 + \Delta_9$. But then

$$E_{0011} = -\Delta_3 - \Delta_4 - \Delta_5 - \Delta_6 + \epsilon < -\Delta_1 - \Delta_2 - \Delta_3 - \Delta_4 - \Delta_9 + \epsilon = E_{1111}, \tag{6.19}$$

  where ϵ denotes energy contributions from ancilla 10. So (0011) is below the other ground states. The cases where each of the free ancillas is in blockade with only one of the other ancilla (and possibly the center ancilla 11) remains. This however is similar to the case, where we have only one free ancilla.
- The class fig. 6.3b remains. Note, that we excluded this one also numerically with a slightly changed version of the program introduced in section 2.1, by going through all possible ancilla-ancilla blockades of the $N = 7$ ancillas.

  However a analytical proof is given here. Again we see, that $\Delta_1 = \Delta_5$ and $\Delta_2 = \Delta_7$.
  Let us first assume, that the ancillas in blockade with ports 3 and 4 are in blockade pairwise (so 8 is in blockade with 9 and 10 is in blockade with 11). then one of the two ancillas or both of them in blockade with the port must have the same detuning than the port to realize (1110) and (1101). Lets assume only one ancilla has the same detuning, and that this holds for both ports. Then they have to be in blockade with each other. Otherwise either the state (1000) is a ground state, or, to prevent this, we must imply a blockade between the mentioned ancillas of 3 (or port 4) and ancilla 7. Then the state (1001) is inconsistent with this blockade.

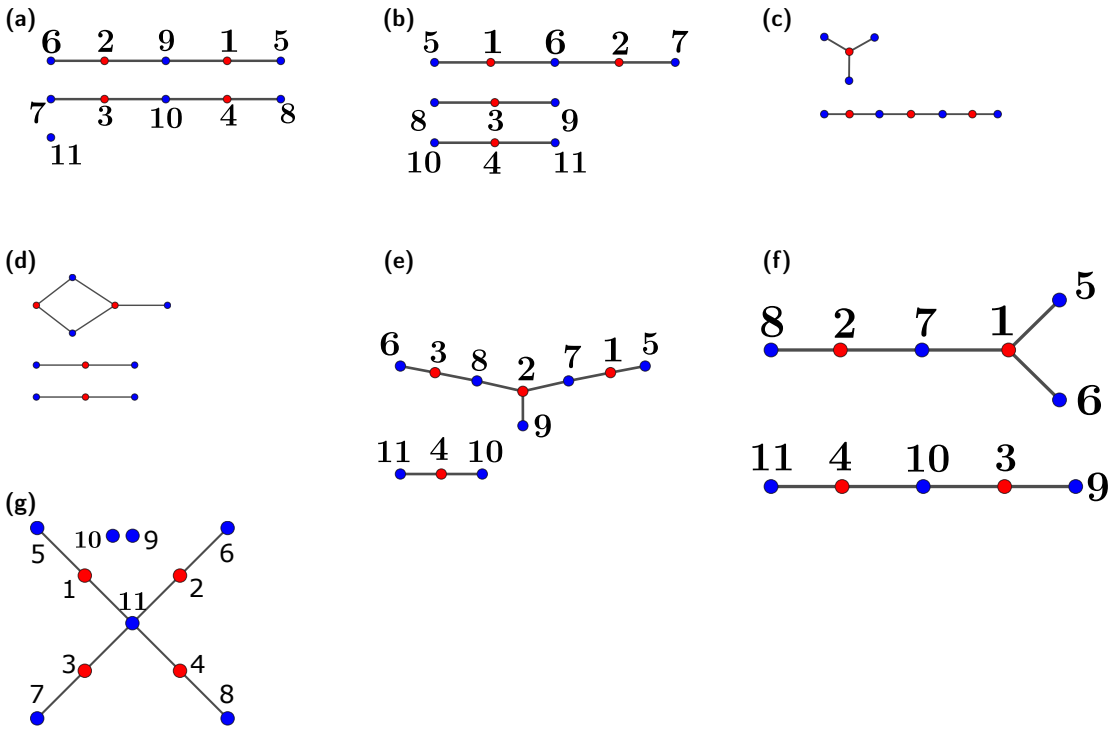

Figure 6.3: The relevant seven classes of blockade graphs for the Fibonacci model vertex complex on eleven atoms with ports of degree 2 and none or one port of degree three. Ports (ancillas) are colored red (blue) and connections between ancillas are omitted.

Lets now assume, that one of the two ports 3 and 4, lets say port 3 has two ancillas in blockade, which have the same detuning as it. Port 4 has still only one ancilla with the same detuning at its own, lets say 10. The same argument as before still holds, only now, both ancillas from port 3 are in blockade with the 10.
Lets assume, that for both ports 3 and 4, both ancillas have the same detuning as the ports. Then there are two degenerate ways to realize (1101) and (1110) as ground states, which is not consistent with $L_{\texttt{FMU}}$.
Lastly we check what happens if the ancilla in blockade with ports 3 and 4 are not in blockade pairwise. To realize (1110) and (1101) as ground states, that are degenerate with (1111), we have $\Delta_8 + \Delta_9 = \Delta_3$ and $\Delta_{10} + \Delta_{11} = \Delta_4$. Then however, none of the states, where only one of the two ancillas in blockade with a ports 3 or 4 is excited, are ground states, because the system would be energetically lower, if instead of this ancilla the adjacent port would be excited. Then the two ancillas in blockade with the same port 3 or 4 are either both excited, or both are not excited. So they act as a single atoms, however we already excluded $N = 9$ atoms from realizing a $L_{\texttt{FMU}}$-complex. This excludes fig. 6.3b from realizing a $L_{\texttt{FMU}}$-complex.

□

Chapter 7

Bibliography

[1] Verresen R, Lukin MD, Vishwanath A. 2021 Prediction of toric code topological order from Rydberg blockade. *Phys. Rev. X* **11**, 031005. (doi:10.1103/PhysRevX.11.031005).

[2] Stastny S, Büchler HP, Lang N. 2023. Functional completeness of planar rydberg structures. (doi:10.48550/ARXIV.2301.01508).

[3] Peng Xinhua Du Jiangfeng SD. 2012 An efficient exact quantum algorithm for the integer square-free decomposition problem. *Scientific Reports* **2**, 2045-2322, 260. (doi:10.1038/srep00260).

[4] Lang N. 2013 *One-Dimensional Topological States of Synthetic Quantum Matter* master thesis, Institute for Theoretical Physics III, University of Stuttgart, p 37-39. https://serv.nl5.de/theses/MSc_Nicolai_Lang_2013_V10.pdf.

[5] Kitaev AY. 2003 Fault-tolerant quantum computation by anyons. *Annal of Physics* **110**, 002030. (doi:10.1016/S0003-4916(02)00018-0).

[6] Bravyi SB, Kitaev AY. 1998 Quantum codes on a lattice with boundary. *arXiv e-prints* quant-ph/9811052.

[7] Levin MA, Wen XG. 2005 String-net condensation: A physical mechanism for topological phases. *Physical Review B* **71**, 045110. (doi:10.1103/PhysRevB.71.045110).

[8] Trebst S, Troyer M, Wang Z, Ludwig AWW. 2008 A short introduction to fibonacci anyon models. *Progress of Theoretical Physics Supplement* **176**.

[9] Schulz MD, Dusuel S, Schmidt KP, Vidal J. 2013 Topological phase transitions in the golden string-net model. *Physical Review Letters* **110**, 14, 147203. (doi:10.1103/physrevlett.110.147203).

[10] Simon SH, Fendley P. 2013 Exactly solvable lattice models with crossing symmetry. *Journal of Physics A: Mathematical and Theoretical* **46**, 10, 105002. (doi:10.1088/1751-8113/46/10/105002).

[11] Gaëtan Alpha Miroshnychenko Yevhen WTCAVMCDPPBAGP. 2009 Observation of collective excitation of two individual atoms in the rydberg blockade regime. *Nature Physics* **5**, 1745-2481, 115–118. (doi:10.1038/nphys1183).

[12] Jaksch D CJIZPRSLCRLMD. 2000 Fast quantum gates for neutral atoms. *Phys. Rev. Lett.* **85**, 2208–2211. (doi:10.1103/PhysRevLett.85.2208).

[13] https://www.itp.uni-hannover.de/fileadmin/itp/ag/weimer/blockade.pdf.

[14] Nguyen MT, Liu JG, Wurtz J, Lukin MD, Wang ST, Pichler H. 2022 Quantum optimization with arbitrary connectivity using Rydberg atom arrays (doi:10.48550/ARXIV.2209.03965).

[15] Barredo D, de Léséleuc S, Lienhard V, Lahaye T, Browaeys A. 2016 An atom-by-atom assembler of defect-free arbitrary two-dimensional atomic arrays. *Science* **354**, 6315, 1021–1023. (doi:10.1126/science.aah3778).

[16] Pichler H, Wang ST, Zhou L, Choi S, Lukin MD. 2018 Quantum optimization for maximum independent set using Rydberg atom arrays (doi:10.48550/arxiv.1808.10816).

[17] Dewdney AK. 1979 Logic circuits in the plane. *ACM SIGACT News* **10**, 3, 38–48. (doi:10.1145/1113654.1113655).

[18] Clark BN, Colbourn CJ, Johnson DS. 1990 Unit disk graphs. *Discrete Mathematics* **86**, 1-3, 165–177. (doi:10.1016/0012-365x(90)90358-o).

[19] Proof that IS is NP hard with 3sat: https://www.cs.umd.edu/class/fall2017/cmsc451-0101/Lects/lect20-np-3sat.pdf.

[20] http://compsci.hunter.cuny.edu/~sweiss/course_materials/csci335/lecture_notes/3sat-indset.pdf.

[21] Breu H, Kirkpatrick DG. 1998 Unit disk graph recognition is np-hard. *Computational Geometry* **9**, 1, 3–24. (doi:https://doi.org/10.1016/S0925-7721(97)00014-X). Special Issue on Geometric Representations of Graphs.

[22] Kochenberger Gary Hao Jin-Kao GFLMLZWHWY. 2014 The unconstrained binary quadratic programming problem: a survey. *Journal of Combinatorical Optimization* **28**, 0925-7721, 58–81. (doi:https://doi.org/10.1007/s10878-014-9734-0).

[23] Stastny S. 2023. Data for master thesis "functional rydberg complexes in the pxp-model. (doi:10.18419/darus-3349).

[24] Virtanen P, Gommers R, Oliphant TE, Haberland M, Reddy T, Cournapeau D, Burovski E, Peterson P, Weckesser W, Bright J, *et al.* 2020 SciPy 1.0: fundamental algorithms for scientific computing in python. *Nature Methods* **17**, 3, 261–272. (doi:10.1038/s41592-019-0686-2).

[25] Nelder JA, Mead R. 1965 A simplex method for function minimization. *The Computer Journal* **7**, 4, 308–313. (doi:10.1093/comjnl/7.4.308).

[26] Gao F, Han L. 2010 Implementing the Nelder-Mead simplex algorithm with adaptive parameters. *Computational Optimization and Applications* **51**, 1, 259–277. (doi:10.1007/s10589-010-9329-3).

[27] Xiang Y, Sun D, Fan W, Gong X. 1997 Generalized simulated annealing algorithm and its application to the thomson model. *Physics Letters A* **233**, 3, 216–220. (doi:10.1016/s0375-9601(97)00474-x).

[28] Xiang Y, Gong XG. 2000 Efficiency of generalized simulated annealing. *Physical Review E* **62**, 3, 4473–4476. (doi:10.1103/physreve.62.4473).

[29] Semeghini G, Levine H, Keesling A, Ebadi S, Wang TT, Bluvstein D, Verresen R, Pichler H, Kalinowski M, Samajdar R, *et al.* 2021 Probing topological spin liquids on a programmable quantum simulator. *Science* **374**, 6572, 1242–1247. (doi:10.1126/science.abi8794).

[30] Laughlin DE. 2019 Magnetic transformations and phase diagrams. *Metallurgical and Materials Transactions A* **50**, 06, 25552569. (doi:10.1007/s11661-019-05214-z).

[31] Lang N, Lecture notes on topological phases,pages 6-8. https://serv.nl5.de/documents/TPM_SS21.pdf.

Acknowledgements

Finally, i want to thank all the people, who made this thesis possible, and who supported me during the time of my studies.

At first i want to thank Prof. Hans Peter Büchler for allowing me to work at the ITP3, and to help publish the results.
Furthermore, i want to thank Prof. Maria Daghofer for her time and the productive discussions we've had.

I want to specially thank Dr. Nicolai Lang. He was a mentor for me and he had the basic idea for the concept this thesis is based upon, so literally, but also figuratively, without him this thesis would not have come together. We had many productive discussions, and his door was always open, when i had questions or wanted to report my progress. In these meetings he always gave advice and a helping hand, and i learned at lot from him, not just about physics, but about a effective workflow in general.

I also want to thank Dr. Sebastian Weber, for sharing his expertise on Qutip, as well as the rest of the team from the institute.

Lastly, but most importantly, i want to thank my parents Robert and Cornelia as well as Jochen and Gabriele for their unconditional support, without which i would not have been able to complete my studies, and be where i am now. Thank you.